

Assessment of the Impact of Sea Level Rise on Salinity Intrusion in Coastal Areas of Bangladesh

by

Abdur Rahman Tazkia

Roll No. 1014042136

In partial fulfillment of the requirements for the Degree of
MASTER OF SCIENCE IN CIVIL ENGINEERING (ENVIRONMENTAL)

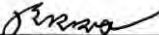


Department of Civil Engineering
BANGLADESH UNIVERSITY OF ENGINEERING AND
TECHNOLOGY, DHAKA


December, 2018

This thesis titled “**Assessment of the Impact of Sea Level Rise on Salinity Intrusion in Coastal Areas of Bangladesh**”, submitted by Abdur Rahman Tazkia, Roll No. 1014042136F, Session: October 2014, has been accepted as satisfactory in partial fulfillment of the requirement for the degree of **Master of Science in Civil Engineering (Environmental)** on 1st December 2018.


BOARD OF EXAMINERS


Dr. Muhammad Ashraf Ali
Professor
Department of Civil Engineering,
BUET, Dhaka

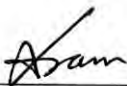
Chairman
(Supervisor)


Dr. Ahsanul Kabir
Professor and Head
Department of Civil Engineering,
BUET, Dhaka

Member
(Ex-officio)


Dr. A. B. M. Badruzzaman
Professor
Department of Civil Engineering,
BUET, Dhaka

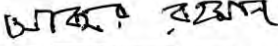
Member


Dr. Md. Akramul Alam
Professor
Department of Civil Engineering,
DUET, Gazipur - 1700, Bangladesh.

Member (External)

DECLARATION

It is hereby declared that this thesis or any part of it has not been submitted elsewhere for the award of any degree or diploma.


(Abdur Rahman Tazkia)
Roll No: 1014042136

Dedicated to

My Parents

ACKNOWLEDGEMENT

Thanks to Almighty Allah for His graciousness and unlimited kindness. I am indebted to many people, who directly or indirectly helped me in completing this research. I wish to express my gratitude to my supervisor Professor Dr. Muhammad Ashraf Ali, Professor, Department of Civil Engineering, BUET for his guidance and encouragement throughout the course of this study. I also wish to thank Dr. Ahsanul Kabir, Professor and Head, Department of Civil Engineering, BUET for his valuable comments and suggestions. I am grateful to Dr. A.B.M. Badruzzaman, Professor, Department of Civil Engineering, BUET for his comments and suggestions to improve this work. Finally, I wish to thank to Dr. Md. Akramul Alam, Professor, Department of Civil Engineering, DUET for his valuable advice and comments.

ABSTRACT

Salinity intrusion has become a major problem in the south west coastal region of Bangladesh over the past few decades. Together with sea level rise, the reduction of upstream flow of major rivers of Bangladesh has potential negative effect on salinity intrusion. Salinity intrusion will have devastating effects on coastal life, particularly on agriculture, water supply and ecosystem. The main objective of this research was to assess the effect of sea level rise on salinity intrusion in the coastal areas of Bangladesh. A widely used flow simulation model Delft3D has been set up and validated for the coastal part of Ganges, Brahmaputra and Meghna (GBM) delta; the hydrodynamic module Delft3D-FLOW has been used in this study. Using the model, salinity pattern of Bangladesh coastal zone has been assessed for 0.5m, 1m and 1.5m sea level rise (SLR) along with one additional scenario in which 20 percent decrease in Brahmaputra discharge has been considered with 1m SLR.

This model has been calibrated with different versions of bathymetry starting from the General Bathymetric Chart of the Oceans (GEBCO) data. Model performance has been observed by comparing output to observed data in the form of tidal constituents. The model has been run to assess its performance on salinity by comparing model output with observed salinity at different BWDB monitoring stations. The Delft3D model has been able to capture the tidal phenomenon of the complex coastal Bengal Delta with a moderate level of success. Bathymetric data appears to have a significant influence on model performance. Use of improved bathymetric data improved model output appreciably. Comparison of predicted salinity and water level with available data at different stations suggests that the model performance for salinity is comparatively poor than it is for water level.

Model predictions suggest that stations (river reaches) located in the Meghna and the Tentuli river systems would experience increase in salinity in response to increase in sea level. But all other stations located in the small distributories of Ganges, Meghna and Tentulia would undergo a decrease in salinity in response to sea level rise. It appears that under extra pressure of tide from sea (due to sea level rise), the fresh water would face difficulty to flow downstream through Meghna. So, it is likely that a part of the upstream flow would find their way into the distributories of Ganges, Padma, Meghna and Tentulia. So, fresh water availability in Meghna and Tentulia should decrease, while all other small distributories would get higher fresh water compared to existing condition. Therefore, salinity in Meghna and Tentulia would increase with sea level rise, while salinity in smaller rivers would decrease. This result was explained by model simulation by comparing seasonal variation of mean water level for different scenarios at different stations, with the understanding that the seasonal variation of water level is representative of fresh water availability at different times of a year. The model simulated mean water levels at different scenarios show that fresh water would decrease in estuary of Meghna and Tentulia and increase in all other small distributories with increase in sea level rise; this explains why salinity would increase in estuary of Meghna and Tentulia and decrease in other places. Finally, spatial pattern of salinity has been prepared based on observed data and model output for different sea-level rise scenarios. These results could be utilized in devising management strategies for mitigation of adverse impacts of sea level rise in coastal areas of Bangladesh.

Table of Contents

ACKNOWLEDGEMENT	vii
ABSTRACT	viii
TABLE OF CONTENTS	ix
LIST OF FIGURES	x
LIST OF TABLES	xii
LIST OF ABBREVIATIONS	xiii
Chapter 1: Introduction	
1.1 General	1
1.2 Objectives	2
1.3 Outline of Methodology	2
1.4 Organisation Of the Thesis	3
Chapter 2: Literature Review	
2.1 Introduction	4
2.2 Sea level Rise	4
2.2.1 Concept of Sea Level Rise	4
2.2.2 Causes of Sea Level Rise	5
2.2.3 Sea Level Rise in Bangladesh	5
2.3 Projections of Sea Level Rise	6
2.4 Regional sea level changes	7
2.5 Explanation of Some Terms Used in This work	8
2.6 Numerical hydrodynamic modeling	9
Chapter 3: Methodology	
3.1 Introduction	13
3.2 Model Setup	13
3.2.1 Study area	13
3.2.2 Delft3D model	14
3.2.3 Grid and Bathymetry	16
3.2.4 Model calibration	17
Chapter 4: Results and Discussion	
4.1 Introduction	35
4.2 Model Performance in Describing Salinity	35
4.3 Effect of Sea Level Rise on Salinity	47

Chapter 5: Conclusions and Recommendations	
5.1 Conclusions	74
5.2 Recommendations	76
References	77

List of Figures

Figure 2.1	Future sea level rise scenario for the Bay of Bengal	8
Figure 3.1	Study Area	16
Figure 3.2	Morphological mesh	22
Figure 3.3	Bathymetry	22
Figure 3.4	All stations	23
Figure 3.5	Comparison of water level: a at station Hiron Point, (b) at station CharChanga	24
Figure 3.6	Comparison of water level: a.at station Cox's Bazar. b. at station Chandpur	25
Figure 3.7	Comparison of water level: a.at station Mongla. b. at station Betagi	26
Figure 3.8	Comparison of water level at station Hiron Point for month January and February	27
Figure 3.9	Comparison of water level at station Hiron Point for month March and April	27
Figure 3.10	Comparison of water level at station Hiron Point for month May and June	28
Figure 3.11	Comparison of water level at station Hiron Point for month July and August	28
Figure 3.12	Comparison of water level at station Hiron Point for month September and October	29
Figure 3.13	Comparison of water level at station Hiron Point for month November and December	29
Figure 3.14	Comparison of water level at station Char Changa for month January and February	30
Figure 3.15	Comparison of water level at station Char Changa for month March and April	30
Figure 3.16	Comparison of water level at station Char Changa for month May and June	31
Figure 3.17	Comparison of water level at station Char Changa for month July and August	31
Figure 3.18	Comparison of water level at station Char Changa for month September and October	32
Figure 3.19	Comparison of water level at station Char Changa for month November and December	32
Figure 3.20	Comparison of amplitudes and phases of tidal constituents obtained by different version of bathymetry for Hiron Point	34
Figure 3.21	Comparison of amplitudes and phases of tidal constituents obtained by different version of bathymetry for station Charchanga	34
Figure 3.22	Comparison of amplitudes and phases of tidal constituents obtained by different version of bathymetry for station Cox's bazar	35
Figure 3.23	Comparison of complex error of tidal constituents obtained by different Model for station Hiron Point ,Char Changa and Cox's bazar	36
Figure 4.1	Map of Salinity stations where observed and model predicted data is compared	38
Figure 4.2	Comparison of Salinity at station Mongla	39
Figure 4.3	Comparison of Salinity at station Khulna	40
Figure 4.4	Comparison of Salinity at station Gazirhat	40
Figure 4.5	Comparison of Salinity at station Patuakhali	41
Figure 4.6	Comparison of Salinity at station Barisal	42
Figure 4.7	Comparison of Salinity at station Tajimuddin	43
Figure 4.8	Comparison of Salinity at station Daulatkhan	43
Figure 4.9	Comparison of Salinity at station Char Fession	44
Figure 4.10	Comparison of Salinity at station Dasmunia	45
Figure 4.11	Comparison of Salinity at station Dhulia.	46

Figure 4.12	Comparison of Salinity at station Bamna	46
Figure 4.13	Comparison of Salinity at station Jhalokati	47
Figure 4.14	Comparison of Salinity at station Patgati	48
Figure 4.15	Comparison of Salinity at station Pirojpur	48
Figure 4.16	Comparison of Salinity with different scenario at station Char Fession	50
Figure 4.17	Comparison of Salinity with different scenario at station Daulatkhan	51
Figure 4.18	Comparison of Salinity with different scenario at station Tajimuddin	52
Figure 4.19	Comparison of Salinity with different scenario at station Dasmonia	52
Figure 4.20	Comparison of Salinity with different scenario at station Dhulia	53
Figure 4.21	Comparison of Salinity with different scenario at station Patuakhali	54
Figure 4.22	Comparison of Salinity with different scenario at station Betagi	55
Figure 4.23	Comparison of Salinity with different scenario at station Chalna	55
Figure 4.24	Comparison of Salinity with different scenario at station Mongla	56
Figure 4.25	Comparison of Salinity with different scenario at station Khulna	57
Figure 4.26	Comparison of Salinity with different scenario at station Bamna	57
Figure 4.27	Comparison of Salinity with different scenario at station Jhalokati	58
Figure 4.28	Comparison of Salinity with different scenario at station Patharghata	59
Figure 4.29	Comparison of Salinity with different scenario at station Hiron Point	59
Figure 4.30	Map Showing Stations where Salinity Increases with SLR (Red Squares)	61
Figure 4.31	Comparison of Mean Water Level with different scenario at station Char Fession	63
Figure 4.30	Comparison of Mean Water Level with different scenario at station Daulatkhan	63
Figure 4.31	Comparison of Mean Water Level with different scenario at station Tajimuddin	64
Figure 4.32	Comparison of Mean Water Level with different scenario at station Dasmonia	64
Figure 4.33	Comparison of Mean Water Level with different scenario at station Dhulia	65
Figure 4.34	Comparison of Mean Water Level with different scenario at station Patuakhali	66
Figure 4.35	Comparison of Mean Water Level with different scenario at station Chalna	67
Figure 4.36	Comparison of Mean Water Level with different scenario at station Mongla	67
Figure 4.37	Comparison of Mean Water Level with different scenario at station Bamna	68
Figure 4.38	Comparison of Mean Water Level with different scenario at station Hiron Point	68
Figure 4.39	Comparison of Mean Water Level with different scenario at station Patgati	68
Figure 4.40	Comparison of Mean Water Level with different scenario at station Pirojpur	69
Figure 4.41	Map Showing Spatial Pattern of Salinity Distribution over Bangladesh Coastal zone prepared from observed data	69
Figure 4.42	Map Showing Spatial Pattern of Salinity Distribution over Bangladesh Coastal zone prepared from model output of existing condition	72
Figure 4.43	Map Showing Spatial Pattern of Salinity Distribution over Bangladesh Coastal zone prepared from Model Simulation with 0.5m SLR	73
Figure 4.44	Map Showing Spatial Pattern of Salinity Distribution over Bangladesh Coastal zone prepared from Model Simulation with 1m SLR	74
Figure 4.45	Map Showing Spatial Pattern of Salinity Distribution over Bangladesh Coastal zone prepared from Model Simulation with 1.5m SLR	75

List of Tables

Table 2.1	Probable Sea level Rise with different Emissions Scenario	6
Table 2.2	Global-mean sea level rise (m) projected by semi-empirical models and compared with the IPCC AR4 and AR5 projections	8
Table 3.1	Name and locations of all stations, data from which were used in this work	20

List of Abbreviations

AR	Assessment Report
BBS	Bangladesh Bureau of Statistics
BIWTA	Bangladesh Inland Water Transport Authority
BWDB	Bangladesh Water Development Board
CZPo	Coastal Zone Policy
EEZ	Exclusive Economic Zone
FAR	First IPCC Assessment Report FAR
FES	Finite Element Solution
GBM	Ganges Brahmaputra Meghna
GEBCO	General Bathymetric Chart of Ocean
GHGs	Green House Gases
GIS	Global Information System
GMSL	Global Mean Sea Level
GSL	Geocentric Sea Level
IPCC	Intergovernmental Panel on Climate Change
MSL	Mean Sea Level
ONR	Office of Naval Research
RCP	Representative Concentration Pathway
RSL	Relative Sea Level
SEMs	Semi-Empirical Models
SLR	Sea Level Rise
SRES	Special Report on Emissions Scenarios
TUD	Delft University of Technology

CHAPTER 1

INTRODUCTION

1.1 General

Bangladesh is a low-lying, revering country located in South Asia with a coastline of 580 km (360 mi) on the northern littoral of the Bay of Bengal. Bangladesh has been formed as a delta plain at the confluence of the Ganges (Padma), Brahmaputra (Jamuna), and Meghna Rivers and their tributaries. The soft sediments of the delta are very mobile, and the positions and hypsometry of river channels is subject to change year on year with net gains of 14.8 km² between 1972 and 1840, and of 4.4 km² between 1840 and 1984 (Allison, 1998). Along with altering the morphology of the river channel, erosion can cause the position of the channels to change as islands accrete and erode (Rahman et al., 2011). Due to this changing nature it is necessary to update bathymetry data time to time for predicting tides accurately.

The majority of Bangladesh is comprised of extensive low-lying flood plains (Yu et al., 2010), and this area has been recognized as being highly vulnerable to sea-level rise (Nicholls et al. (1999). The Brahmaputra-Ganges-Meghna (BGM) river delta is part of the lowland Bangladesh Plain; here most land elevations are less than 10 meters above sea level, and close to mean sea level (MSL) at the south of the delta. So, coastal flooding can be damaging to crops bringing saline water inland, while river flooding brings freshwater to leach dangerous salts out of the soil (Clarke et al., 2015). Tides, particularly the overall tidal range are important to the growth of mangrove trees which will not survive if their roots are submerged for long periods (Auerbach et al., 2015; Gopal and Chauhan, 2006; Barbier, 2012). Again Salinity intrusion is a growing problem in the coastal areas around the globe, especially in the low-lying developing countries (Nicholls et al., 2007). The problem becomes exacerbated particularly in the dry season when rainfall is inadequate and incapable of lowering the concentration of salinity of surface water. Climate change associated hazards like sea level rise, cyclone and storm surge have been contributing to aggravate the problem. Already huge areas in south western part of Bangladesh have become unsuitable for normal agricultural purpose. Besides, the Sundarbans is under increasing threat of salinity intrusion. Already, the effect of salinity intrusion is visually observed on Sundry trees of Sundarbans. Sundry tree, which is one of the major trees of Sundarbans, is suffering from agamora (top leaf dying) disease.

IPCC AR4 (2007) predicts that the sea level rise is likely to persist for centuries, resulting from the process and feedback of climate, even though the concentration of Green House Gases (GHGs) is to become steady. Regional variation is expected to be the dominating factor over natural variability in sea level change by the end of 21st century (IPCC, 2013). Some regions are expected to experience very high levels of sea level rise compared to the global mean (IPCC, 2013). The IPCC for the Bay of Bengal predicts SLR between 0.2 m to 1 m for low to high emission scenarios in 2100. Another recent work (Jevrejeva et al., 2014) estimates 1.8 m as the upper limit of global mean sea level rise by 2100. Considering these predictions, it is important to investigate the salinity intrusion problem with probable sea level rise situation. Together with sea level rise, the reduction of upstream flow of major rivers of Bangladesh for implementing water diversion structures outside the border of the country has potential negative effect on salinity intrusion. Salinity intrusion will have devastating effects on coastal life, particularly in the context of agriculture, water supply and ecosystem. Considering all these risks, it is very important to understand the probable salinity pattern in the coastal zone of Bangladesh with sea level rise in near future.

1.2 Objectives

The overall objective of this research was to assess effect of sea level rise on salinity intrusion in the coastal areas of Bangladesh. The approach to fulfill the objectives involved:

- a) Setting up the open source morphological model Delft3D for Bangladesh coastal area, and validating the model using available data.
- b) Preparation of present spatial map of salinity in coastal zone of Bangladesh.
- c) Preparation of future spatial salinity maps considering probable Sea Level Rise, and
- d) Comparing predicted salinity patterns at different measuring stations for different SRL scenarios.

1.3 Outline of Methodology

In order to predict salinity situation accurately by modeling, a coastal model must be set up and validated for the coastal region. This research work involved setting up and validation of Delft3D model (open source version, 2008) for the coastal part of GBM delta. In particular, the hydrodynamic module Delft3D-FLOW was used in this study. In this research, evaluation of salinity pattern of Bangladesh coastal zone was assessed for 0.5m, 1m and 1.5m sea level

rise (SLR) along with one extra scenario in which 20 percent decrease in Brahmaputra discharge is considered with 1m SLR.

The model was calibrated and validated using BIWTA tide gauge data at three locations (Hiron point, Char Changa and Cox's Bazar). The validated model was used for salinity calculation. The processes considered included: (i) tide from southern boundary; (ii) fresh water flow from major river system (upstream); and (iii) molecular dispersion. The southern boundary was raised by 0.5m, 1m and 1.5m to mimic 0.5m, 1m and 1.5m sea level rise, respectively. The upstream flow of Brahmaputra was reduced to simulate the future reduction in upstream flow. The time series of salinity data at different stations were compared with model output to check the model performance. The model output was processed in Arc GIS software to produce spatial map of salinity for base condition and different sea level rise scenarios.

1.4 Organization of the Thesis

The thesis is presented in five Chapters. Chapter 1 presents the background and objectives of the research. Chapter two presents literature review, particularly focusing on sea level rise, projection of sea level rise, and regional sea level rise. Chapter 3 presents the methodology used in this research; including details of the numerical model used, and model setup. Chapter 4 presents the results and discussion, including calibration and validation of the model, prediction of salinity under different scenarios considered in this study and their implications. Finally, Chapter 5 presents the major conclusions drawn from the study and recommendations for future work.

CHAPTER 2

LITERATURE REVIEW

2.1 Introduction

Bangladesh, a low-lying deltaic land, is particularly vulnerable to sea level rise and its associated hazards. The overall objective of this research was to assess effect of sea level rise on salinity intrusion in the coastal areas of Bangladesh. This Chapter presents an overview of sea level rise, including causes of sea level rise, predictions of sea level rise, and regional sea level changes. It also provides an overview of hydrodynamic models available for analyzing coastal hydrodynamic problems

2.2 Sea Level Rise

Some features related to sea level rise is discussed below to clarify the objectives and methodology of this work.

2.2.1 Concept of sea level rise

The level of the sea observed along the coast changes in response to a wide variety of geological, astronomical, meteorological, climatological, geophysical, and oceanographic forcing mechanisms. From the highest frequency wind waves and sea swell to tsunamis and local seiches, to the daily tides, to monthly, seasonal, and annual variations, to decadal and multi-decadal variations, and finally, to changes over hundreds of millions of years, sea level is constantly changing at any given location.

Sea level is the level of the ocean's surface. Sea level at a particular location changes regularly with the tides and irregularly due to conditions such as wind and currents. Other factors that contribute to such fluctuation include water temperature and salinity, air pressure, seasonal changes, the amount of stream runoff, and the amount of water that is stored as ice or snow. The reference point used as a standard for determining terrestrial and atmospheric elevation or ocean depths is called the mean sea level and is calculated as the average of hourly tide levels measured by mechanical tide gauges over extended periods of time.

In addition, there is a subtle, but significant distinction to make when discussing sea level change and the context for which estimation of the change is required. This distinction is one between global sea level change and relative sea level change (Williams et al., 2009).

Relative Sea Level (RSL) is measured with respect to the surface of the solid earth, whereas Geocentric Sea Level (GSL) is measured with respect to a geocentric reference such as the reference ellipsoid (IPCC, 2013). Mean Sea Level (MSL) is defined as the temporal average for a given location and Global Mean Sea Level (GMSL) is the spatial average of all the MSL (IPCC, 2013).

2.2.2 Causes of Sea level rise

The notion that sea level is changing was recognized in the First IPCC Assessment Report (FAR), where the change from the year 1990 to 2001 was addressed (Warrick and Oerlemans, 1990). Two major causes of sea level rise were identified. First one is the expansion of ocean water due to global warming induced thermal expansion and the second is the addition of ice water on the ocean from the land through the melting of glacier ice sheets (Church et al., 2011). The first IPCC report also expressed that SLR rate will be higher in the 21st century than the 20th and will continue to rise even if reduction in the GHG emissions is achieved.

Processes that contribute to global and regional sea level changes encompass the ocean, atmosphere, land ice, and hydrological cycle. So, the two main factors that are critical to sea level rise are: Thermal expansion and Cryospheric contribution. However, a local perturbation in sea level is influenced by Local atmospheric circulation; Local tectonic movement; Local subsidence / soil compaction; Sediment contributions; and Anthropogenic contributions.

2.2.3 Sea level rise in Bangladesh

Bangladesh is vulnerable to current coastal hazards and anticipated SLR because of its low elevation. Drainage congestion and water logging are already an alarming problem in Bangladesh and likely to be exacerbated by SLR and increased river flooding. Large uncertainties are associated with regional to district level estimates of inundation which is due to the compounding effects of the variable rates of uplift and sedimentation, river flooding and erosion. Siltation is gradually increasing due to SLR. As a result of reduced upstream flow, the silt flocculate/deposit in the riverbed which restricts removal of excess water from the countryside and causes drainage congestion.

The Northern Indian Ocean, which includes the Bay of Bengal, has also been reported to experience a relatively high rate of SLR compared to other oceans globally (Han et al., 2010; Unnikrishnan, 2007). Based on global sea level data and modeling, Ericsson et al. (2006) have estimated that the SLR of the Bay of Bengal is the world's highest, at 10 mm/yr.

The study of SMRC (2003) found that the tidal level in Hiron Point, Char Changa and Cox's Bazar rose by 4.0 mm/yr, 6.0 mm/yr and 7.8 mm/yr, respectively. The rate of the tidal trend is almost double in the eastern coast than that of the western coast. This difference could be due to subsidence and uplifting of land.

2.3 Projections of sea level rise

Evidence for global mean SLR has been documented in assessments of the IPCC. The IPCC continuously revises its projections of global mean SLR, drawing on the knowledge and data of the international science community. The projections of global-mean sea level rise and its contributions have been generated for four RCP and SRES scenarios.

RCP means representative concentration pathways which have considered time series of emissions and concentrations of the full suite of greenhouse gases and aerosols and chemically active gases, as well as land-use/land cover (Moss et al., 2008). Each RCP is the representative value out of many possible scenarios that would lead to the specific radiative forcing characteristics. The term pathway emphasizes that not only the long-term concentration levels are of interest, but also the trajectory taken overtime to reach that outcome. (Moss et al.2010).

The sea level rise estimations include global as well as local scenarios. For the global mean sea level (GMSL), contribution from thermal expansion and cryospheric contributions have been considered. The global SLR scenarios projected by IPCC are given in Table 2.1. The results include projections for each decade from the year 2010 till2100 under low, medium and high emission scenarios of climate change.

Table2.1: Probable Sea level Rise with different Emissions Scenario

Year	Value	RCP2.6/Low Emission (m)	RCP4.5/Medium Emission (m)	RCP6.0/Medium Emission (m)	RCP8.5/High Emission (m)
	Range	[0.24 0.48]	[0.28 0.54]	[0.28 0.53]	[0.37 0.67]
2090	Mean	0.4	0.47	0.47	0.62
	Range	[0.26 0.54]	[0.32 0.62]	[0.33 0.63]	[0.45 0.81]
2100	Mean	0.44	0.53	0.55	0.74
	Range	[0.28 0.61]	[0.36 0.71]	[0.38 0.73]	[0.53 0.98]

Source: IPCC, 2013

The semi-empirical models were used in the IPCC 5th Assessment Report. Semi-Empirical Models (SEMs) project sea level assuming that statistical relationships between observed GMSL and global mean temperature (Rahmstorf, 2007a; Vermeer and Rahmstorf, 2009; Grinsted et al., 2010) or total radiative forcing will continue in the future (Jevrejeva et al.,

2008; Jevrejeva et al., 2009). Table 2.2 shows the global-mean sea level rise (m) projected by semi-empirical models and compared with the IPCC AR4 and AR5 projections. In each case the results have a probability distribution, whose 5-, 50- and 95-percentiles are shown in the columns as indicated. The AR5 5–95% process-based model range is interpreted as a likely range (medium confidence).

Table 2.2: Global-mean sea level rise (m) projected by semi-empirical models and compared with the IPCC AR4 and AR5 projections

Scenario SRES A1B	From	To	5%	50%	95%
IPCC AR4a	1990	2100	0.22	0.37	0.50
IPCC AR4a,b	1990	2100	0.22	0.43	0.65
IPCC AR5	1996	2100	0.40	0.58	0.78

(Source: IPCC, 2013)

For very high emissions, IPCC AR5 predicts a global rise of 520 to 980 mm (52-98 cm) by the year 2100, while even with aggressive emission reduction; a rise of 280 to 610 mm (28-61 cm) is predicted

2.4 Regional Sea Level Changes

Regional variation is expected to be the dominating factor over natural variability in sea level change by the end of 21st century (IPCC, 2013). Melting of land ice mass will be the main contributing factor. Some of the regions are expected to experience changes in sea level extensively different than the global mean as revealed from the ensemble mean regional relative sea level change between 1986-2005 and 2081-2100 under the RCP scenario of 4.5. In the IPCC AR5, projections of sea level rise for nine representative coastal regions including the Bay of Bengal have been given for all the emission scenarios as shown below in Figure 2.1. The IPCC for the Bay of Bengal predicts SLR between 0.2 to 1m for low to high emission scenarios in 2100. For the future, the IPCC projections for very high emissions (red, RCP8.5 scenario) and very low emissions (blue, RCP2.6 scenario) are shown (IPCC, 2013).

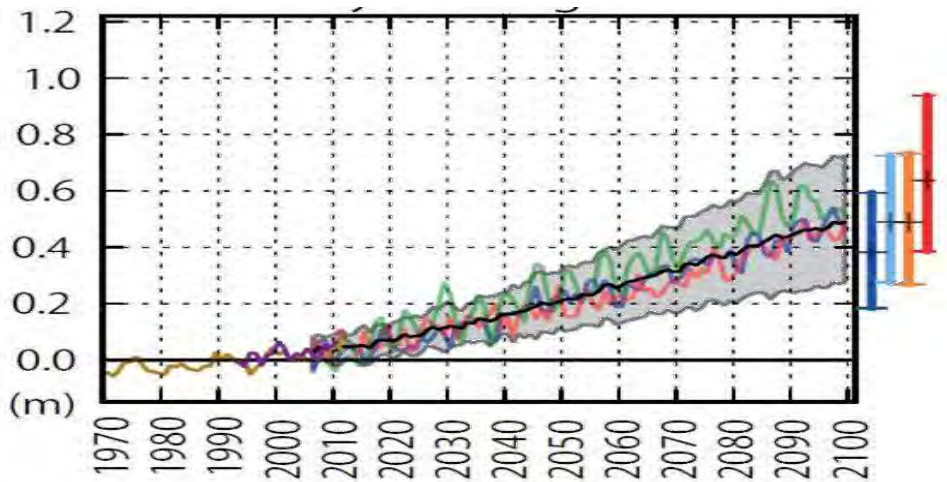


Figure 2.1 Future sea level rise scenario for the Bay of Bengal (IPCC, 2013)

AR5 notes that a collapse of the marine-based sectors of the Antarctic ice sheet, if initiated, could potentially add up to a further several tenths of a meter of sea level rise, independent of scenario; Levermann et al. (2014) estimate that this could be around 0.5 m. This additional amount, when combined with the upper limit of the AR5 highest-emission-scenario (RCP8.5) likely range, gives a value of sea level rise by 2100 of around 1.5 m, not including potential local variations or subsidence. Another recent work (Jevrejeva et al., 2014) estimates 1.8 m as the upper limit of global mean sea level rise by 2100. Considering all these prediction, in this work model has been run for 0.5m, 1m and 1.5m sea level rise to evaluate probable inundated areas.

2.5 Explanation of Some Terms Used in This work

FES 2012

FES2012 is the last version of the FES (Finite Element Solution) tide model developed in 2012. It is a fully revised version of the global hydrodynamic tide solutions initiated by the works of Christian Le Provost in the early nineties. The new model has been developed, implemented and validated by the LEGOS, NOVELTIS and CLS, within a CNES funded project.

FES2012 takes advantage of longer altimeter time series, improved modelling and data assimilation techniques, and more accurate ocean bathymetry. Special efforts have been dedicated to address the major non-linear tides issue and to the determination of accurate tidal currents.

FES 2012 is based on the resolution of the tidal barotropic equations (T-UGO model) in a spectral configuration.

A new original high resolution global bathymetry was built, and a new global finite element grid (~1.5 million nodes) is used leading to a twice more accurate 'free' solution (independent of in situ and remote-sensing data) than the FES2004 version. Then the accuracy of this 'free' solution was improved by assimilating long-term altimetry data (Topex/ Poseidon, Jason-1, Jason-2, ERS-1, ERS-2 and ENVISAT) through an improved representer assimilation method. Final FES2012 solution shows strong improvement compared to FES2004 and GOT4V8, particularly in coastal and shelf regions.

FES 2014

FES2014 is the last version of the FES (Finite Element Solution) tide model developed in 2014-2016. It is an improved version of the FES2012 model. This new FES2014 model has been developed, implemented and validated by the LEGOS, NOVELTIS and CLS, within a CNES funded project.

TPXO7.2

TPXO is a series of fully-global models of ocean tides, which best-fits, in a least-squares sense, the Laplace Tidal Equations and altimetry data. Each next model in TPXO series is based on updated bathymetry and assimilates more data compared to previous versions. We support only current and previous versions. The tides are provided as complex amplitudes of earth-relative sea-surface elevation for eight primary (M2, S2, N2, K2, K1, O1, P1, Q1), two long periods (Mf, Mm) and 3non-linear (M4,MS4,MN4)harmonic constituents. TPXO solutions are provided in binary and netcdf formats. The binary format can be read using OTPS (Fortran) or TMD (Matlab) packages. The southern boundary data has been extracted from TPXO7.2 using TMD (Matlab) packages. TMD is a Matlab toolbox to extract TPXO7.2 global model output.

2.6 Numerical Hydrodynamic Modeling

The rapid development of computing technology has furnished a large number of models to be employed in coastal hydrodynamic problems. A variety of coastal models are available and the modeling techniques have become quite mature. The numerical technique can be based on the finite element method, finite difference method, boundary element method, finite volume method and Eulerian-Lagrangian method. The time-stepping algorithm can be

implicit, semi-implicit, explicit, or characteristic-based. The shape function can be of the first order, second order, or a higher order. The modeling can be simplified into different spatial dimensions, i.e., a one-dimensional (1D) model, two-dimensional (2D) depth-integrated model, 2D lateral-integrated model, 2D layered model and 3D model.

An analysis of coastal hydraulics and water quality often demands the application of heuristics and empirical experience, and is accomplished through some simplifications and modeling techniques according to the experience of specialists. However, the accuracy of the prediction is to a great extent dependent on open boundary conditions, model parameters, and the numerical scheme. The adoption of a proper numerical model for a practical coastal problem is a highly specialized task. These predictive tools inevitably involve certain assumptions and/or limitations, and can be applied only by experienced engineers who possess a comprehensive understanding of the problem domain. This leads to severe constraints on the use of models and large gaps in understanding and expectations between the developers and practitioners of a model.

Hydrodynamic modeling is the study of fluids in motion. Fluid motion can be generated by many forces acting alone or in combination. These include forces generated by tide, wind and waves (i.e. metocean) as well as gradient (e.g. river flow, weirs and dams), turbines (e.g. tidal lagoons and tidal farms) and masses of fluid meeting (e.g. oceans, rivers, wastewater or cooling water discharges). Hydrodynamic movement generates forces that act on solid bodies immersed in fluid (e.g. structures, seabed features and land boundaries), which in turn affects the behavior of the fluid. Understanding and quantifying this complex interaction is essential for effective and responsible development of offshore infrastructure and assets.

Open source models

Recent models often include the interactions of wave fields with currents and bathymetry, the input of wave energy by the wind, and wave breaking. For example, Holthuijsen et al. (1993) introduced the SWAN model, which predicts directional spectra, significant wave height, mean period, average wave direction, radiation stresses, and bottom motions over the model domain. The model includes nonlinear wave interactions, current blocking, refraction and shoaling, and white capping and depth-induced breaking.

Numerical modeling of the nearshore circulation system (including rip and longshore currents) permits the study of both onshore and offshore motions as well as longshore motions and can in fact include the influence of rip currents. A variety of models has been developed, for example, Noda (1974), Birkemeier and Dalrymple (1975), Vemulakonda et al. (1982), Kawahara and Kashiya (1984), Wu and Liu (1985) and Van Dongeren et al. (1994) . These depth-averaged models in general solve the nearshore circulation field forced by bottom variations, although Ebersole and Dalrymple (1980) examined the case of intersecting wave trains and Wind and Vreugdenhil (1986) addressed the circulation induced between two barriers, pointing out the importance of correctly modeling the lateral shear stresses. The last model by Van Dongeren et al. (1994) is quasi-three-dimensional, adding the influence of the undertow on the longshore current, as pointed out by Putrevu and Svendsen (1992). Madsen, Sorensen, and Schaffer (1997) have shown that an extended Boussinesq wave model can predict surf zone hydrodynamics quite well when a wave-breaking algorithm is included. Averaging the numerical model currents over a wave period yields the “mean” flows of the nearshore circulation system. Chen et al. (1999) compared Boussinesq model results with a physical model of the nearshore circulation on a barred shoreline with rip channels. The numerical model predicts the instabilities in the rip currents as seen in the physical model by Haller et al. (1997).

Most of these nearshore circulation models were developed by finite difference methods, although Wu and Liu (1985) used finite element techniques. Some of these models are being used for engineering work, although it should be pointed out that most of them are very computer intensive and require very small time steps (on the order of seconds) to reach steady-state solutions. This often causes problems when trying to determine the effect of several days’ worth of wave conditions or to predict 1 or 50 years of coastal conditions. Models typically have been developed only for monochromatic (single frequency) wave trains rather than for directional spectra. Several open source codes (Delft3D, ossdeltares.nl/web/opendelft3d, TELEMAC, opentelemac.org among others) have been developed recently for modeling coastal hydrodynamics and coastal processes in general.

The Delft3D suite consists of various components to model the particular physics of the water system, such as the hydrodynamics, morphology and water quality. Delft3D allows you to simulate the interaction of water, sediment, ecology and water quality in time and space. The suite is mostly used for the modeling of natural environments like coastal, river and estuarine

areas, but it is equally suitable for more artificial environments like harbors, locks, etc. Delft3D consists of a number of well-tested and validated programs, which are linked to and integrated with one-another. These programs are: D-Flow, D-Morphology, D-Waves, D-Water Quality, D-Ecology, D-Particle Tracking. The Delft3D Wave component can be used to simulate the propagation and transformation of random, short-crested, wind generated waves in coastal waters which may extend to estuaries, tidal inlets, barrier islands with tidal flats, channels etc.

The Delft3D-Wave module consists of a slightly adapted version of the open source model SWAN and a shell allowing for interaction with Delft3D modules like Delft3D-FLOW and providing additional options for model input like "spiderweb windfields". SWAN was developed by Delft University of Technology (TUD) with support of the Office of Naval Research (ONR). It is managed and maintained by TUD with funding of the Dutch Ministry of Public Works. TUD releases authorized versions of SWAN in the public domain as open source code under the GNU GPL license. The SWAN model is applicable in deep, intermediate and shallow waters and the spatial model grid may cover any model surface area of up to more than 50 km by 50 km.

The added value of Delft3D Wave is the capability of Delft3D Hydrodynamics, Morphology and Waves to perform a so-called online calculation, in which information is transferred from Flow and Morphology to Wave and back again. This online coupling allows for the simulation of complex water systems in which flow-wave (wave currents interaction as well as wave setup) or flow-wave-morphology (effect of radiation stress on sediment transport and seabed changes) are important.

SWAN is a phase-averaged wave model which is less or not applicable in regions where complex phenomena occur within relatively short distances, e.g. near coastal structures or steep sloping beaches, and within harbors. For those areas phase-resolving models are required to obtain more accurate wave predictions. Examples of these models are Boussinesq-type models and Multi-layer models.

In practice Delft3D-Wave (in combination with other modules) is used to transform offshore information such as wind speed statistics to nearshore wave conditions, or more concrete, hydraulic loads on revetments, dune retreat, resulting ship motion, etc. Several models and techniques are required for this transfer, that are coupled in a so-called coastal engineering platform.

CHAPTER 3

METHODOLOGY

3.1 Introduction

The overall objective of this research was to assess effect of sea level rise on salinity intrusion in the coastal areas of Bangladesh. This research work involved setting up and validation of Delft3D model for the coastal part of GBM delta; the hydrodynamic module Delft3D-FLOW was used in this study. In this research, evaluation of salinity pattern of Bangladesh coastal zone was assessed for 0.5m, 1m and 1.5m sea level rise (SLR) along with one extra scenario in which 20 percent decrease in Brahmaputra discharge is considered with 1m SLR. This Chapter describes the model set up to accomplish the objectives of the study. This Chapter also describes the calibration and validation of the model; the model was calibrated and validated using three BIWTA tide gauge data at locations (Hiron point, Char Changa and Cox's Bazar) and two BWDB stations Mongla and Betagi. The validated model was subsequently used for salinity calculation.

3.2 Model Setup

This article includes discussion about study area, Delft3D software and detail about grid and bathymetry used as input in model.

3.2.1 Study area

The domain to be covered by the model has been selected such that it can capture a good portion of Bay of Bengal and a major portion of complex river network of Bangladesh. The mesh used for this model covers 20.717°N to 23.972°N and on an average 87°E to 92°E. Bangladesh, a flood plain delta, is a land of rivers and canals. The country slopes gently from north to south, comprising about 710 km coastline. According to the Coastal Zone Policy (CZPo, 2005) of the Government of Bangladesh, 19 districts out of 64 are in the coastal zone covering a total of 147 upazilas. Out of these 19 districts, 12 districts are contiguous with the sea or lower estuary directly.

The coastal zone covers 47,201 sq km land area, which is 32 % of the total land mass of the country (Islam, 2004, p. xvii). Water area covers 370.4 km from the coastline (UNCLOS, 1982, Article 57), estuaries and the internal river water. The Exclusive Economic Zone (EEZ)

is also treated as a coastal zone of its own. The southern part of Bangladesh falls under the coastal zone that receives the discharge of numerous rivers, including the Ganges-Brahmaputra-Meghna (GBM) river systems, one of the most productive ecosystems of the world. Except Chittagong and Cox's Bazar, all parts of the coastal zone are plain land with extensive river networks and accreted land. The map (Figure 3.1) shows all districts which are considered under coastal area of Bangladesh.

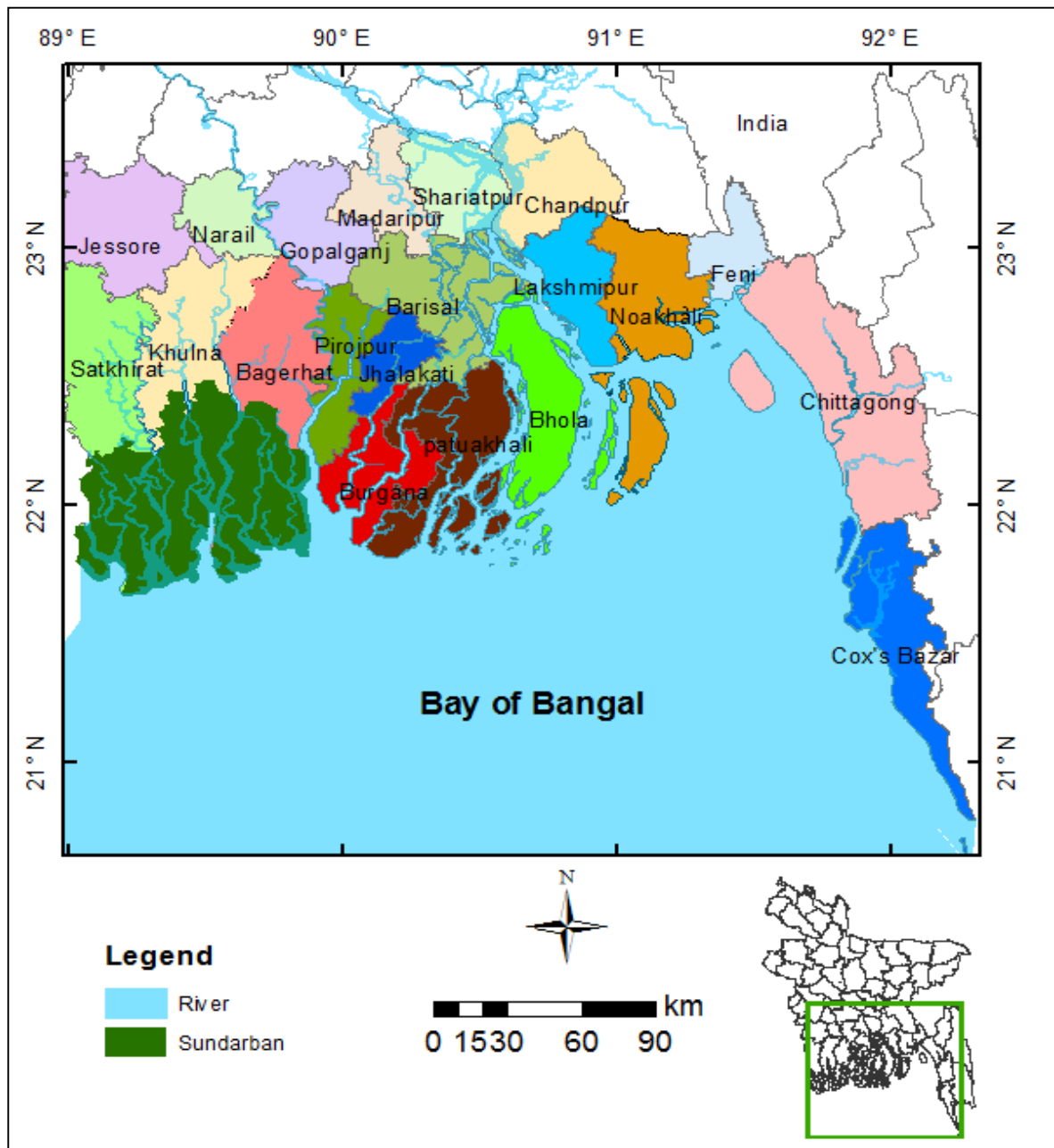


Figure 3.1: A map showing coastal districts of Bangladesh

The total population living in the coastal zone is 35.1 million, i.e. 28 % of the total population of the country (BBS, 2003). Population density in the exposed coast is 482 persons per sq km as opposed to 1,012 for the interior coast. Average population density of the zone is 743 per sq km, compared with the national average of 839. Population density of the interior coast is much higher than that of the exterior coast and the country's average. There are about 6.8 million households in the zone, 52 % of which are absolute poor according to Islam (2004). Fishing, agriculture, shrimp farming and salt farming are the main economic activities in the coastal area. The Sundarbans is a major source of subsistence for almost 10 million people (Islam and Haque, 2004). Main activities in the Sundarbans area are fishing, wood and honey collection. Almost ten thousand households in the area have neither homestead land nor cultivable land while more than a million households in the area have only homestead but no cultivable land (Islam, 2004, p. 136). Moreover, Sundarbans being the largest mangrove forest in the world has very important role for ecological balance of southern coastal environment of Bangladesh.

3.2.2 Delft3D model

In this research, simulations have been carried out by means of the Delft3D model (open source version, 2008). In particular, the hydrodynamic module Delft3D-FLOW has been used. Delft3D-FLOW is a multi-dimensional (2D or 3D) hydrodynamic (and transport) simulation program which calculates unsteady flow and transport phenomena that result from tidal and meteorological forcing on a rectilinear or a curvilinear boundary-fitted grid. In 3D simulations, the vertical grid is defined following the σ co-ordinate approach. The Delft3D-FLOW model solves the Navier Stokes equations for an incompressible fluid, under the shallow water and the Boussinesq assumptions. In the vertical momentum equation, the vertical accelerations are neglected, which leads to the hydrostatic pressure equation. In 3D models, the vertical velocities are computed from the continuity equation. The set of partial differential equations in combination with an appropriate set of initial and boundary conditions is solved on a finite difference grid. The time step for the hydrodynamic computation has been selected equal to 5. The computational time step has been fixed to optimize the total computational time for one-year simulation. The higher computational time step reduce precision and make the model vulnerable to instability. On the other hand, very small computational time step makes total simulation time exceedingly large. Considering these limitation, the time step has been fixed to 5min. Turbulence effects are computed by

means of the K-epsilon model.

3.2.3 Grid and Bathymetry

There are publicly available topographic data from The General Bathymetric Chart of the Oceans (GEBCO, 2014), and ETOPO (NGDC, 2011). These data sets are suitable in deeper water offshore, but fail to capture the near shore and inland bathymetry within the delta. River and tidal flows are critically dependent on good representation of coastline and bottom bathymetry. So, a more accurate bathymetry data has been collected from Bangladesh Water Development Board (BWDB) and bathymetric survey conducted by the Institute of Water and Flood Management (IWFM) of Bangladesh University of Engineering and Technology (BUET) under the ESPA Deltas Project. This bathymetry has been generated performing new surveys along with considering existing surveys. In this bathymetry, the ocean part is from GEBCO data but inland river bathymetry has been produced by interpolating cross sections data collected by new surveys. But in the shallow area near coast GEBCO data is not satisfactory for representing the real topography of land. So, a further improvement has been performed using tidal chart of Bangladesh Navy (digitizing the hardcopy of the map) in the shallow region of the coast. This improvement has been done by a group of IRD (Institute de Recherche pour le Développement) scientists of France. Moreover, elevation information of the 139 coastal polders was also incorporated in this final version of the bathymetry. In this research, along with GEBCO bathymetry, both versions of improved bathymetries have been used to simulate tide level in order to observe the effect of bathymetry on the simulation.

The final version of bathymetry of the coastal areas of Bangladesh and Bay of Bengal used in this work has been prepared merging the following data sets:

- 1) GEBCO 30 arc-second global grid of elevations, GEBCO_2014 Grid, was published in 2014
- 2) Land elevation (DEM) is a merged product of FAP 19 rectilinear grid 300mx300m, datum PWD and FINNMAP data topographic data, datum PWD.
- 3) River bathymetry survey data from BWDB, datum PWD.
- 4) River bathymetry survey data from IWFM, BUET, datum PWD (by various projects of IWFM including ESPA deltas).
- 5) Coastal Polders boundary and elevation from CEIP-1 project of BWDB.
- 6) Coastlines of Bangladesh from LANDSAT 8 imagery from February 2015.

This bathymetry data currently in geographic coordinates using WGS84 ellipsoid and vertical datum is mean sea level (MSL).

Though Delft3D model is capable of working with both structured and unstructured mesh, unstructured grid version is not yet “open source”. So, in this work structured rectangular grid has been used. Primarily, a mesh for the domain (discussed above) has been produced using Delft Dashboard with a constant grid spacing 0.006° (nearly 666m) both in M and N direction. Then this mesh is edited in Delft3D RFGRID grid generator. Bathymetry data has been interpolated for this mesh with Delft3d QUICKIN tool.

The open boundary conditions in the Bay of Bengal are time series water level. These data have been generated from TPXO 7.2 global inverse tidal model. To simulate freshwater effect open boundaries have been defined at three upstream points of GBM delta: (i) Near Hardinge Bridge for Ganges flow, (ii) near Bahadurabad for Brahmaputra flow, and (iii) near Bhairab Bazar for Meghna flow. The boundary condition of these three points is discharge data collected from the Bangladesh Water Development Board.

3.2.4 Model Calibration

The simulation period for calibration of model has been considered from 1st January, 2009 to 30th December, 2009. The simulation period for validation of model has been considered from 1st November, 2009 to 30th December, 2010. The first two months of simulation output have not been considered for validation to nullify the effect of initial condition. The tidal gauge stations at Hiron point, Char Changa and Cox's Bazar of Bangladesh Inland Water Transport Authority (BIWTA), and the Chandpur, Mongla and Betagi gauge station of Bangladesh Water Development Board (BWDB) have been considered for tidal validation of the model. To assess model performance in describing salinity, data from 18 BWDB salinity stations have been used. Table 3.1 shows the names and location of all the stations for both salinity and tide, data from which were used in this study.

Table 3.1: Name and locations of all stations, data from which were used in this work

Sl. No.	Station Name	Longitude	Latitude
1	Bamna	90.0926	22.3444
2	Barisal	90.3804	22.7002
3	Betagi	90.1825	22.4362
4	Bhatiapara	89.6988	23.2141
5	Chalna	89.5298	22.6021
6	Char Fession	90.8331	22.1913
7	Dasmunia	90.6101	22.2889
8	Daulatkhan	90.8183	22.6110
9	Dhulia	90.5429	22.5656
10	Gazirhat	89.5614	22.9611
11	Gournadi	90.2351	22.9762
12	Jhalokati	90.1831	22.6300
13	Khulna	89.5764	22.8195
14	Mongla	89.5976	22.4642
15	Patgati	89.9182	22.8761
16	Patuakhali	90.3596	22.3617
17	Pirojpur	89.9664	22.5816
18	Tajumuddin	90.8542	22.4688
19	Chandpur	90.6400	23.2309
20	Hiron Point	89.5300	21.7400
21	Char Changa	90.9500	22.100
22	Cox's Bazar	91.9500	21.4300

Figure 3.2 shows “morphological mesh” and Figure 3.3 shows updated bathymetry for mesh of study area. Figure 3.4 and Table 3.1 show the names and coordinates of all the validation stations. The model was calibrated for the year 2009 for tide, and the calibration parameter used for tide validation was Manning roughness coefficient “n”. To calibrate the model, at first a single value of n was used over the whole area. This value of n was changed over the typical range of 0.015 to 0.025 in order to get the best-fit results (by comparison with observed water level data). The best-fit was obtained for n value of 0.02. However, it was observed that while this n value provided overall best fit, the model fit was not good for a number of monitoring stations. Effort was then made to improve the result by assigning different n value for river reaches for which relatively poor fit was obtained. While this resulted in improvement of fit for certain monitoring stations in that reach, it deteriorated fit for other stations. For example, at Mongla station the amplitude was significantly underestimated (see Figure 3.6) by the model run with a global n value of 0.02. So to improve the fit at Mongla, n value was changed (decreased) for Gorai-Modhumoti-Pussur River

system. It was observed that while it improved the fit for Mongla, it worsened the fit for other points of this river system such as Hiron Point. It may be possible that changing n values over shorter reaches could improve model fit in overall study area; but it would be difficult to justify such changes in n values, and the possible combination of such changes (to improve model fit) could become very large. It became apparent that this approach would not be practical for improving the model fit. Therefore, the uniform n value that provided best fit was chosen. The value of “ n ” finally used is 0.02 over the whole study area.

For salinity, the calibration parameter used is the “coefficient of diffusivity”, which has been discussed in Chapter 4. Salinity of southern boundary is set to a constant value 34ppt over the whole simulation period. Salinity varies a little with temperature. But since temperature has not been included in the model as a parameter, the average salinity found (according to National Institute of Oceanography of India) in northern Bay of Bengal is used as boundary condition. Salinity at northern Boundary condition is set to 0 ppt as the discharge of Ganges, Brahmaputra and Upper Meghna is fresh water with no traceable salinity.

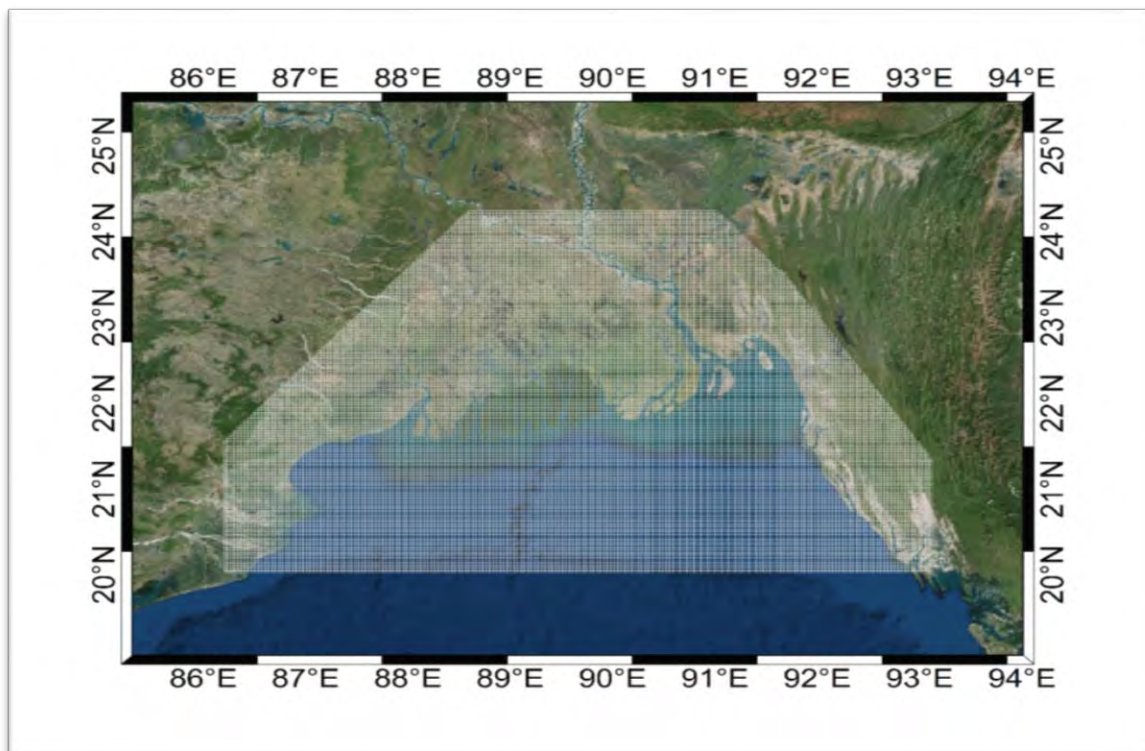


Figure 3.2: Morphological mesh

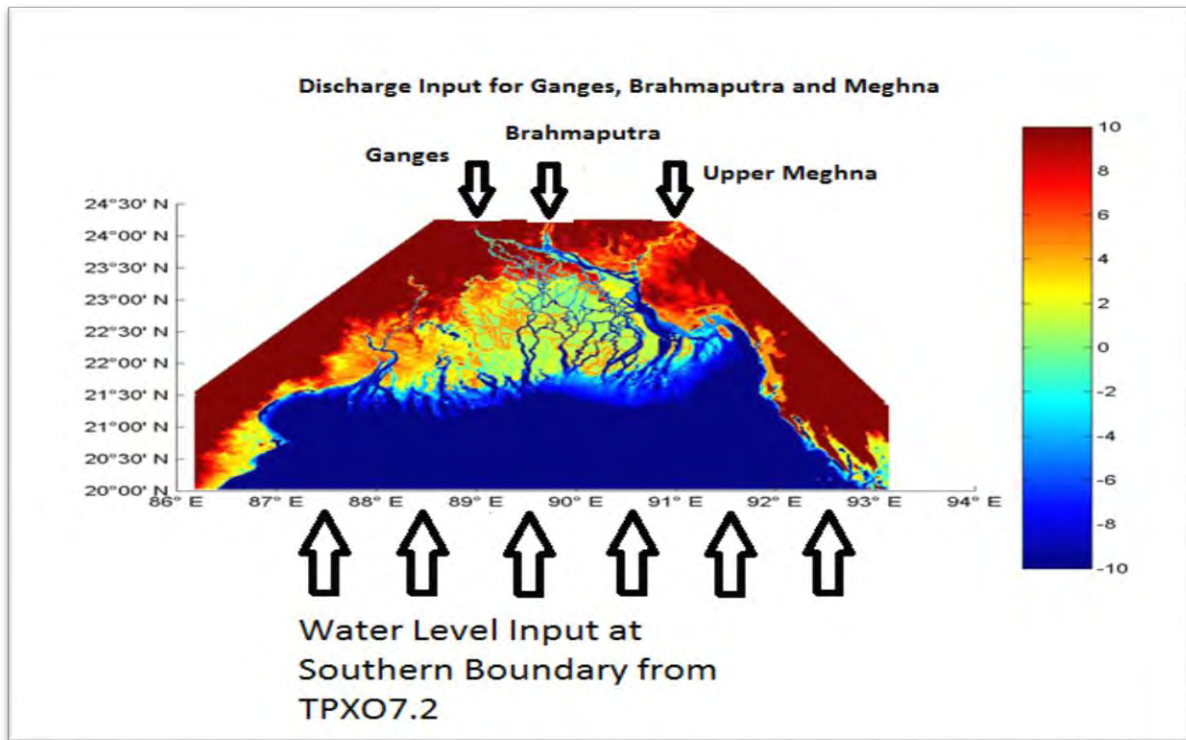


Figure 3.3: Initial bed level at the simulation starting date (Upgraded Bathymetry)

Figure 3.5 depicts the water level from 1st January 2010 to 30th December 2010 at the tidal gauge station Hiron Point and Char Changa for both observed data and model predicted data. The Hiron Point is located at the estuary of Pussur River very close to Bay of Bengal. Char Changa is located at the mouth of Meghna River where it meets the Bay of Bengal. Both of these stations are highly influenced by strong tidal effect.

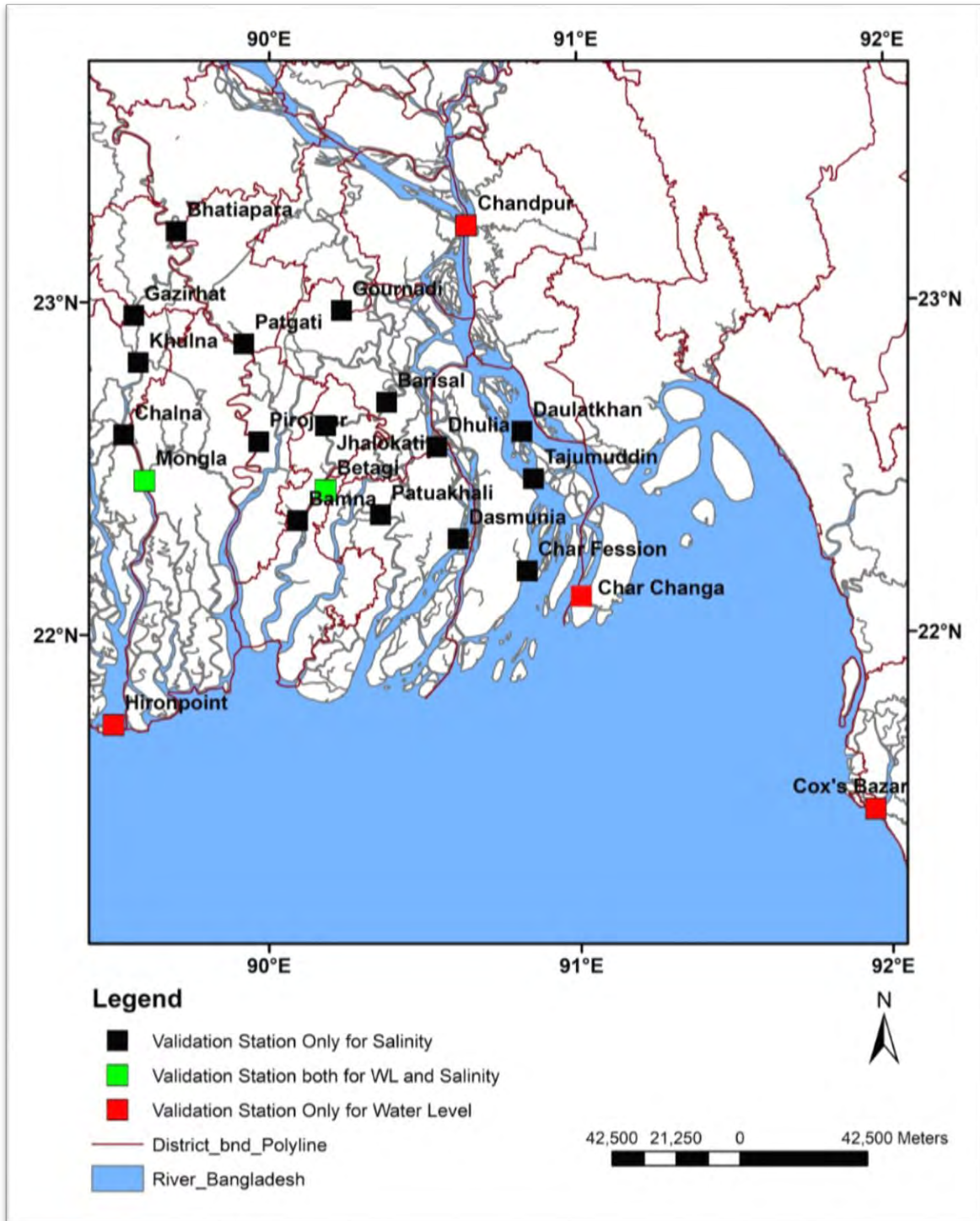


Figure 3.4: Location of all gauge stations, data from which were used for validation of the model

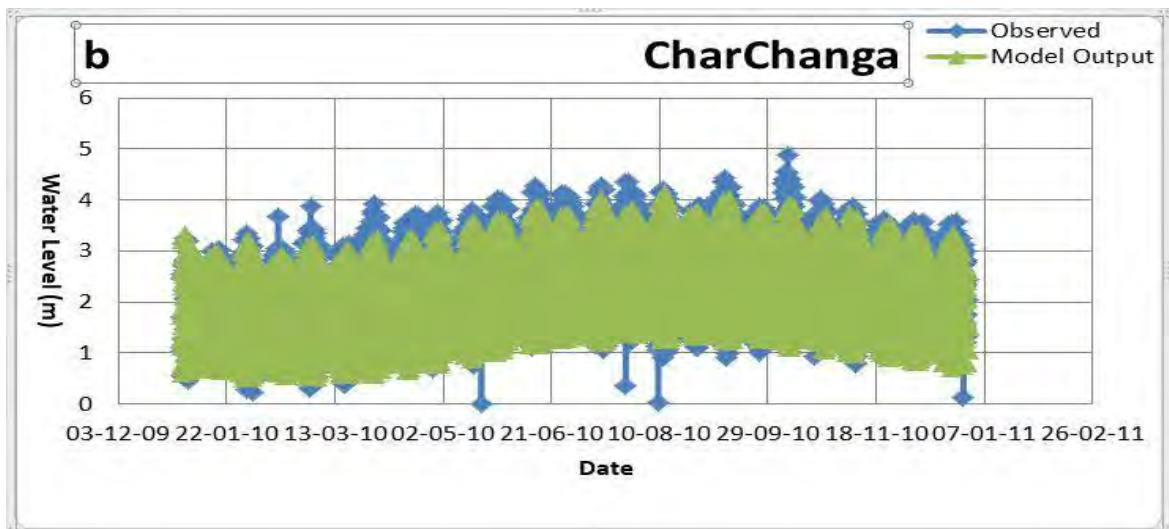
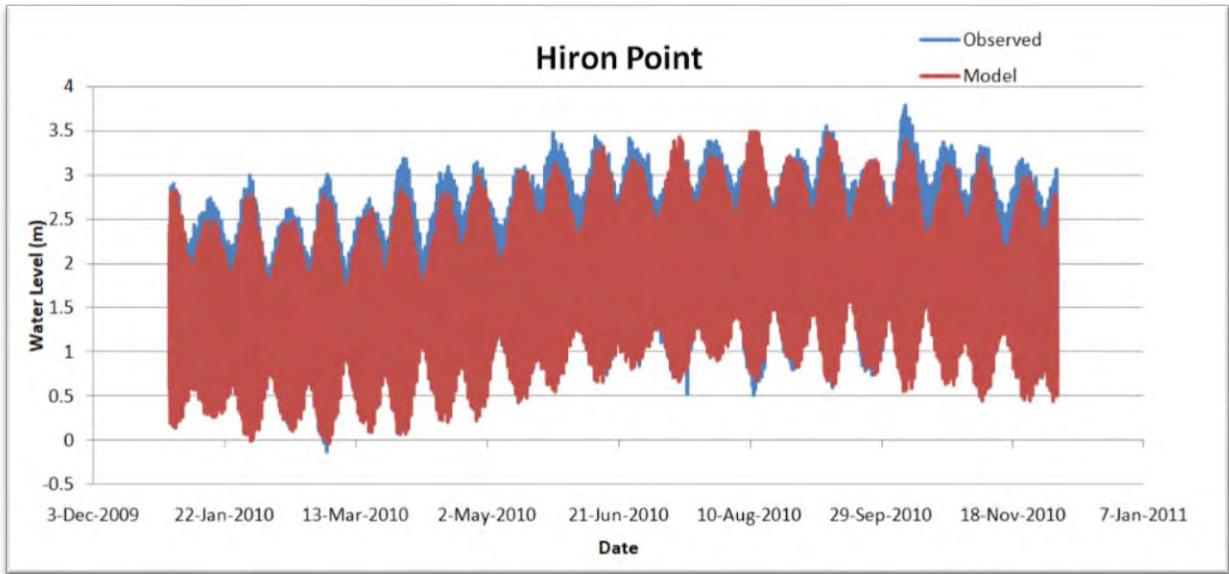


Figure 3.5: Comparison of observed and model predicted water level: (a) at Hiron Point; (b) at Char Changa

Figure 3.6 shows the water level from 1st January 2010 to 30th December 2010 at the tidal gauge station Cox’s Bazar and Chandpur for both observed data and model predicted data. The Cox’s Bazar station is strongly influenced by tide; but as Chandpur station is located in the Meghna River far inland from the Bay of Bengal, it is much less influenced by tide. In Chandpur, the water level is influenced significantly by fresh water discharge from Padma, Jamuna and upper Meghna. As observed in Fig. 3.6(b), the tidal range in Chandpur is much less than other three stations [see Fig. 3.5(a), 3.5(b) and 3.6(a)], but the seasonal variation of water level is high.

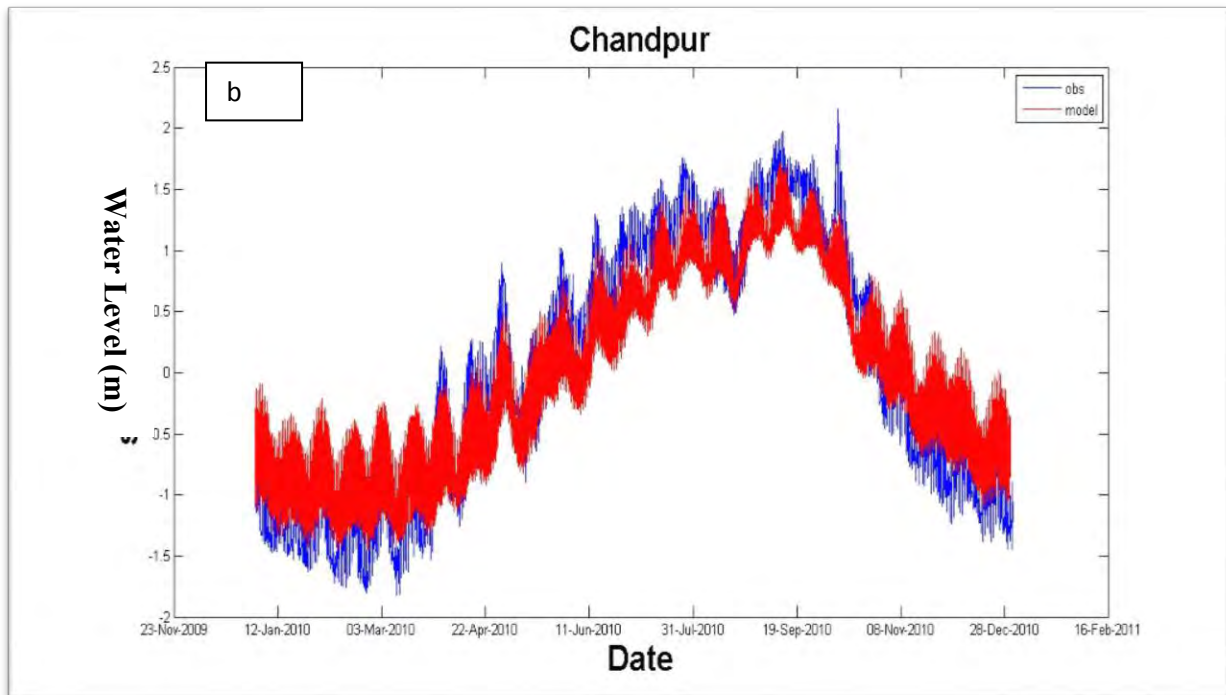
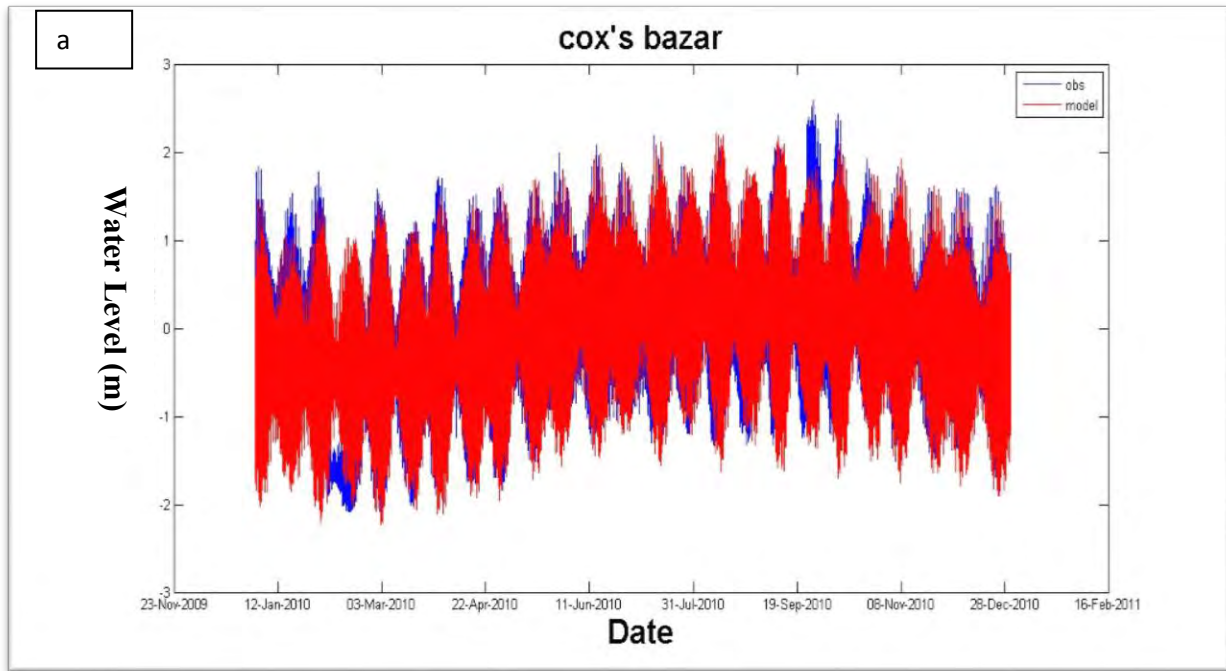


Figure 3.6: Comparison of observed and model predicted water level: (a) at Cox’s Bazar, (b) at Chandpur

Figure 3.7 shows the water level from 1st January 2010 to 30th December 2010 at the tidal gauge station Mongla and Betagi for both observed data and model predicted data. Mongla is located in the Pussur River not far from the Bay of Bengal. The water level of this station is governed by tidal effect. From Fig. 3.7, it can be observed that at this point the model prediction fits poorly with observed data. It possibly indicates that the bathymetry used in the

model for this area does not match with the actual situation. Betagi is located in the Bishkhali River where water level is also governed by tide effect.

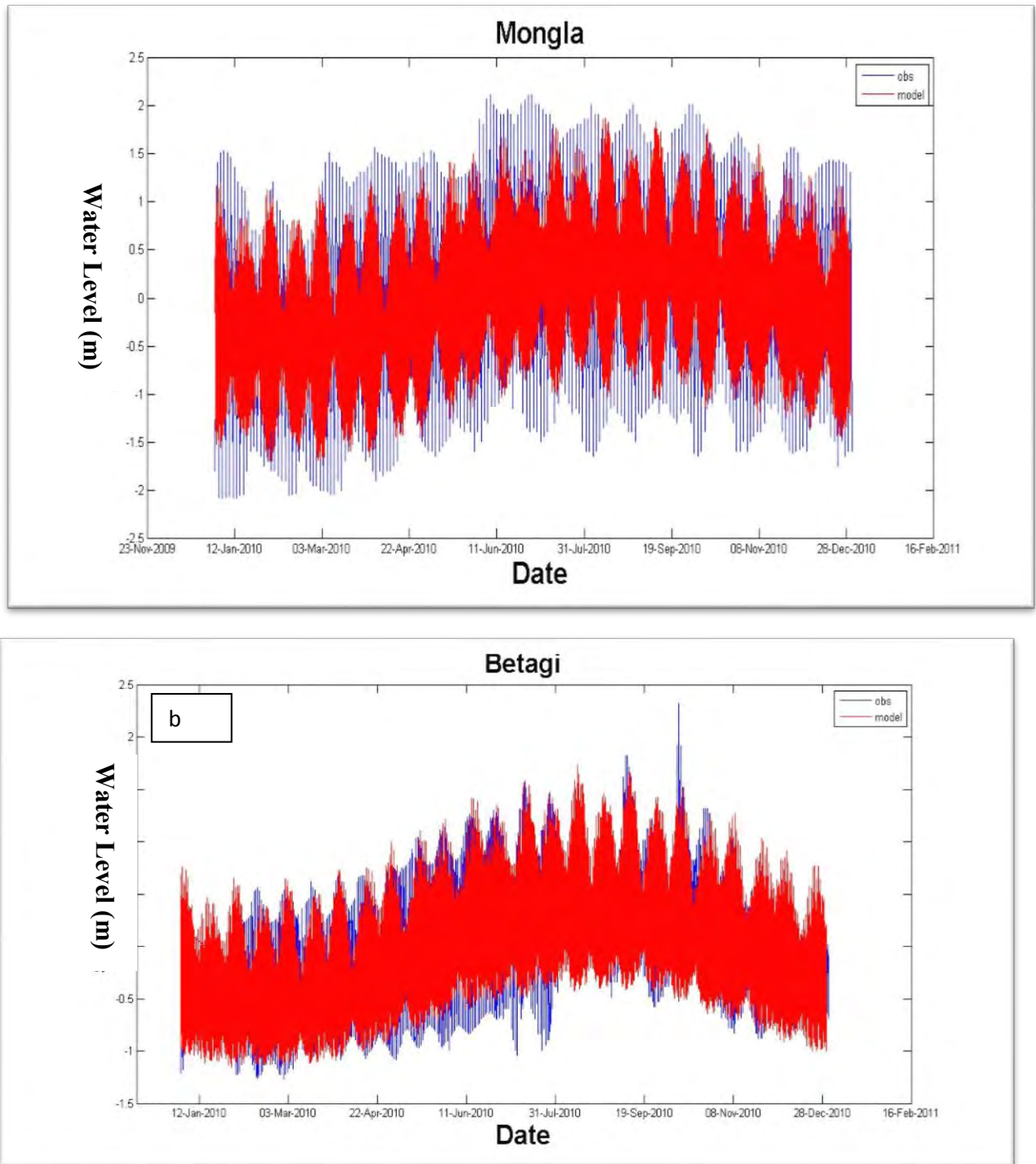


Figure 3.7: Comparison of observed and model predicted water level: (a) at Mongla, (b) at Betagi

Figure 3.5 to 3.7 helps to understand the overall yearly pattern of water level in different Locations. But, it does not help much to distinguish daily variation of observed data and

model predicted data. Figure 3.8 to 3.19 depicts six hourly water level data for two months window at stations Hiron Point and Char Changa to realize match between observed and model predicted data better.

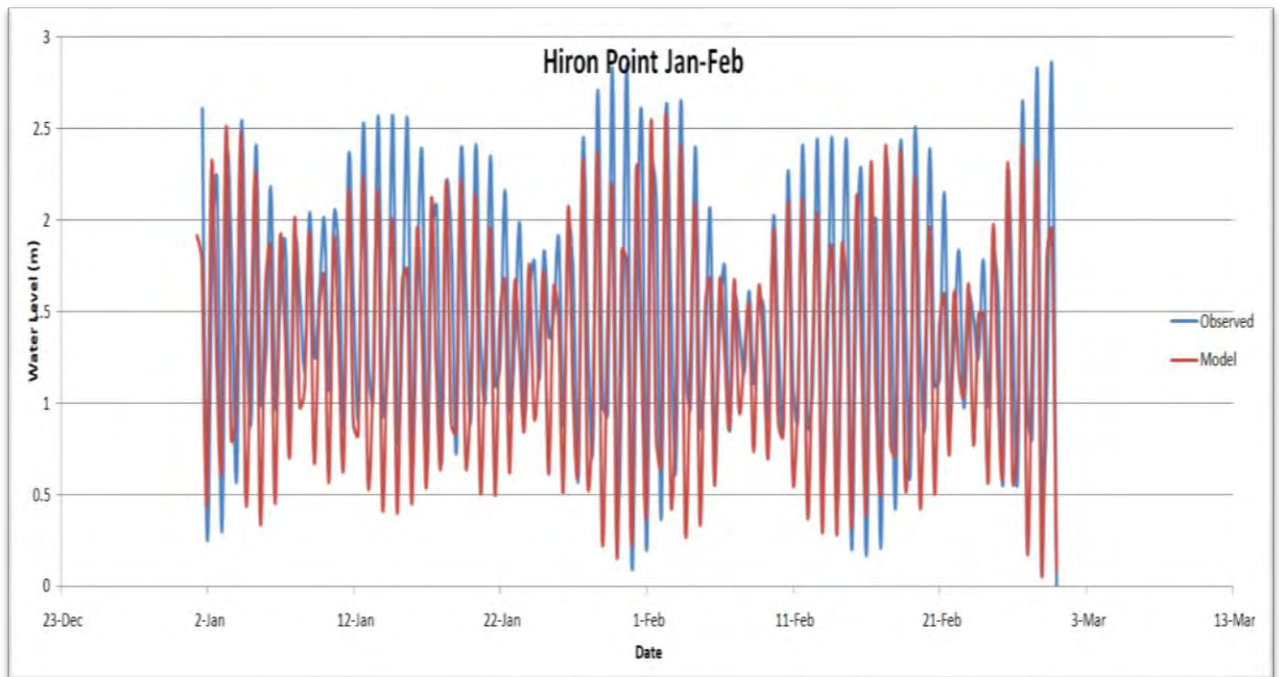


Figure 3.8: Comparison of observed and model predicted water level: at Hiron Point for month January-February

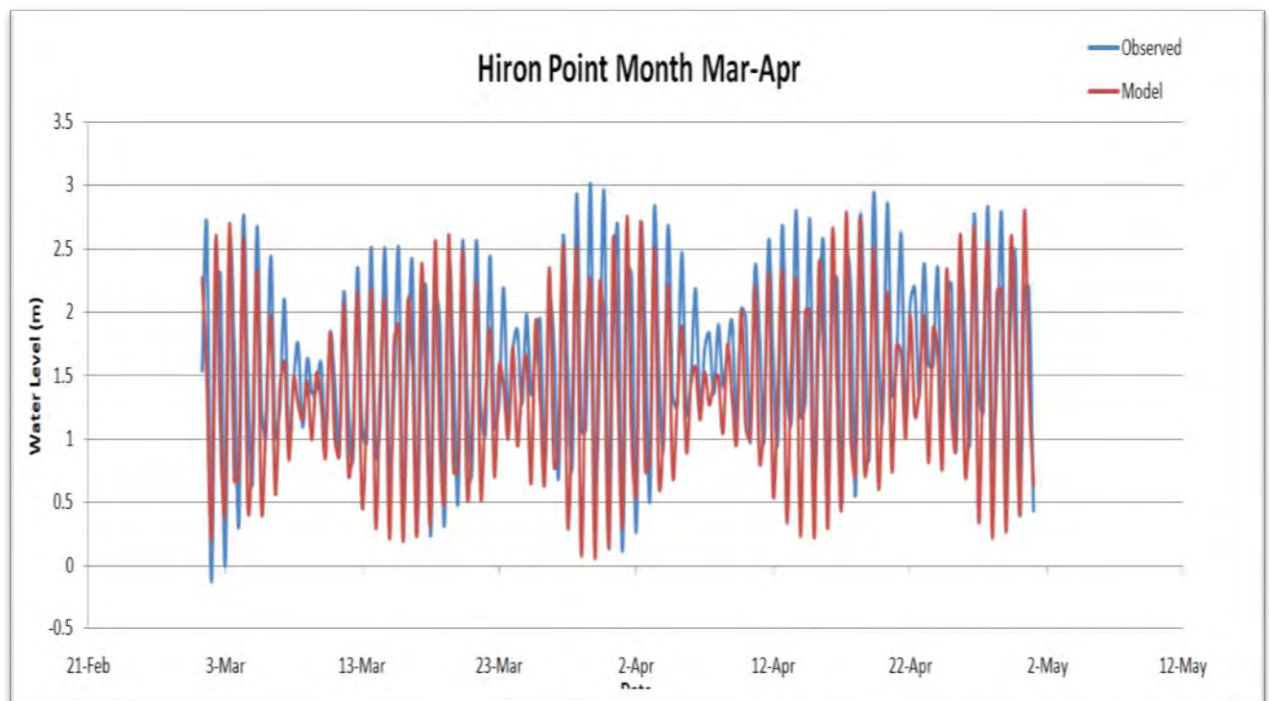


Figure 3.9: Comparison of observed and model predicted water level: at Hiron Point for month March-April

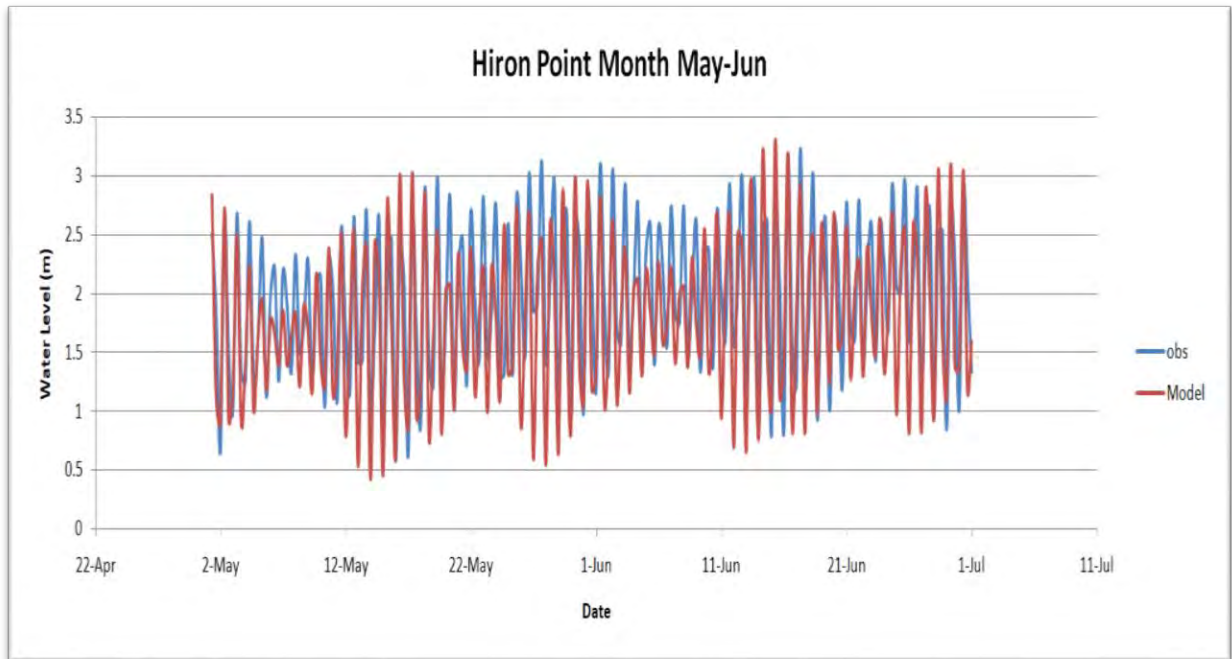


Figure 3.10: Comparison of observed and model predicted water level: at Hiron Point for month May-June

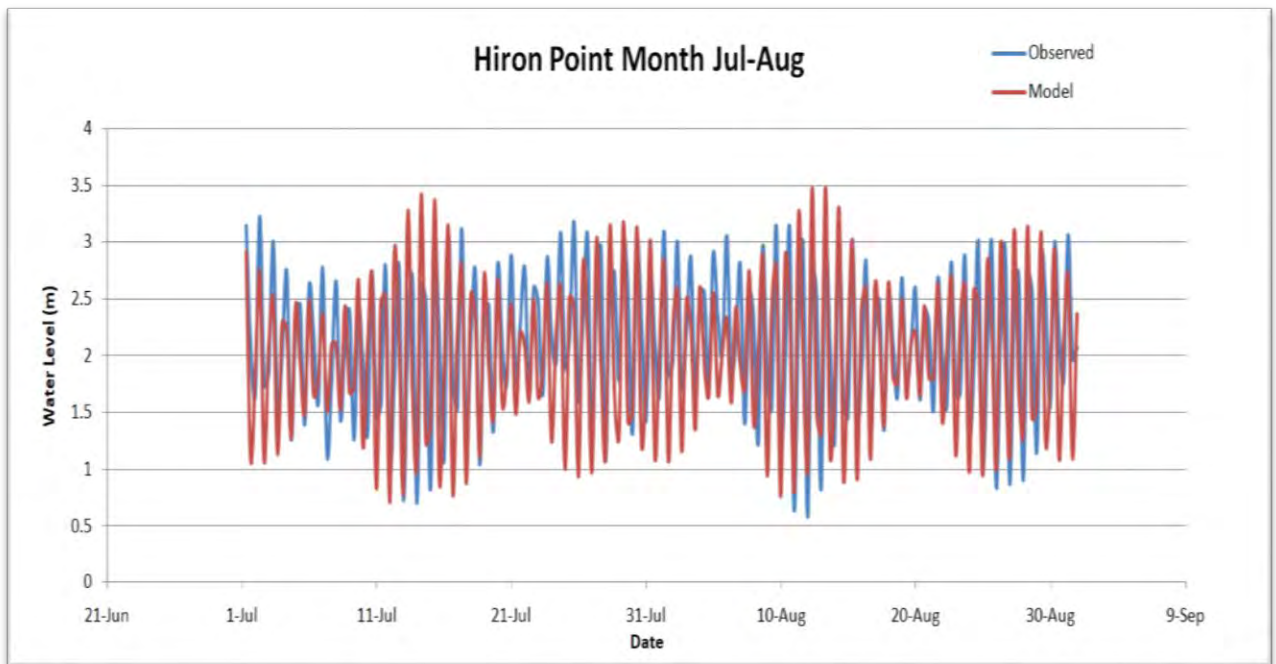


Figure 3.11: Comparison of observed and model predicted water level: at Hiron Point for month July-August

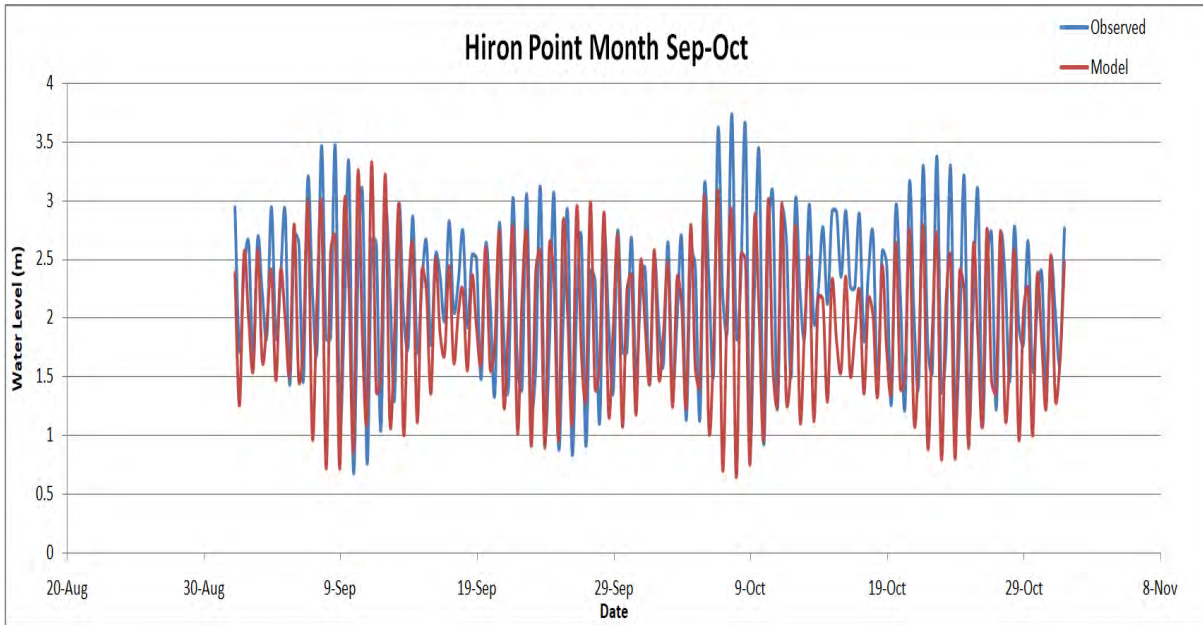


Figure 3.12: Comparison of observed and model predicted water level: at Hiron Point for month September-October

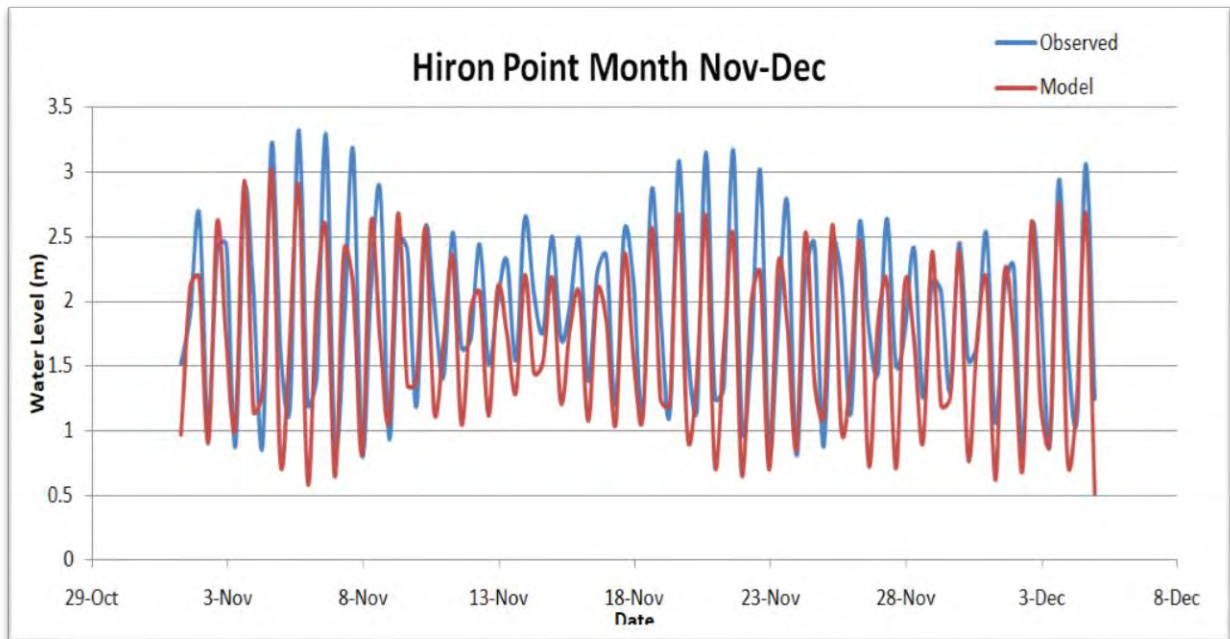


Figure 3.13: Comparison of observed and model predicted water level: at Hiron Point for month November-December

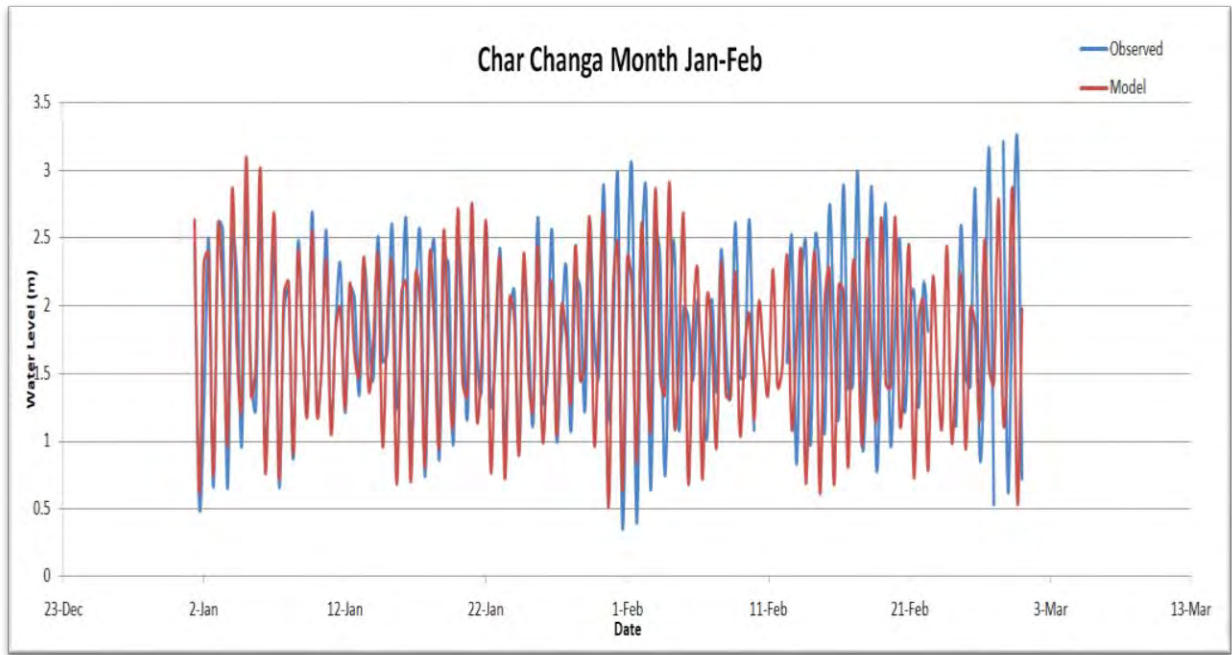


Figure 3.14: Comparison of observed and model predicted water level: at Char-Changa for month January-February

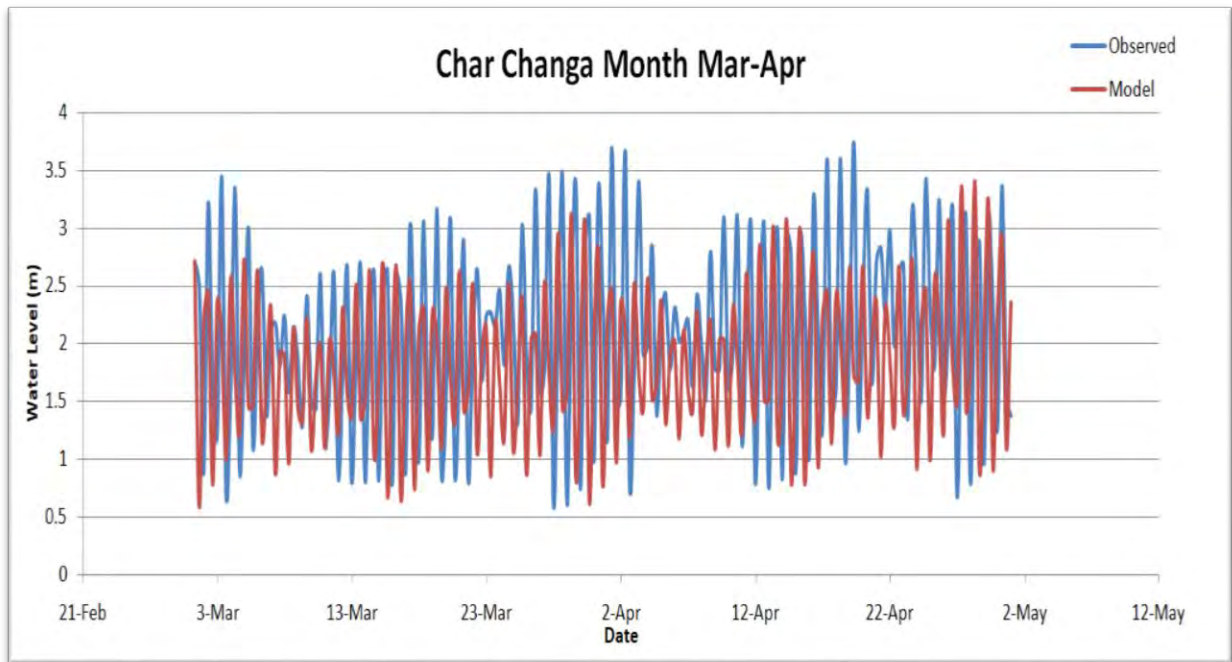


Figure 3.15: Comparison of observed and model predicted water level: at Char Changa for month March-April

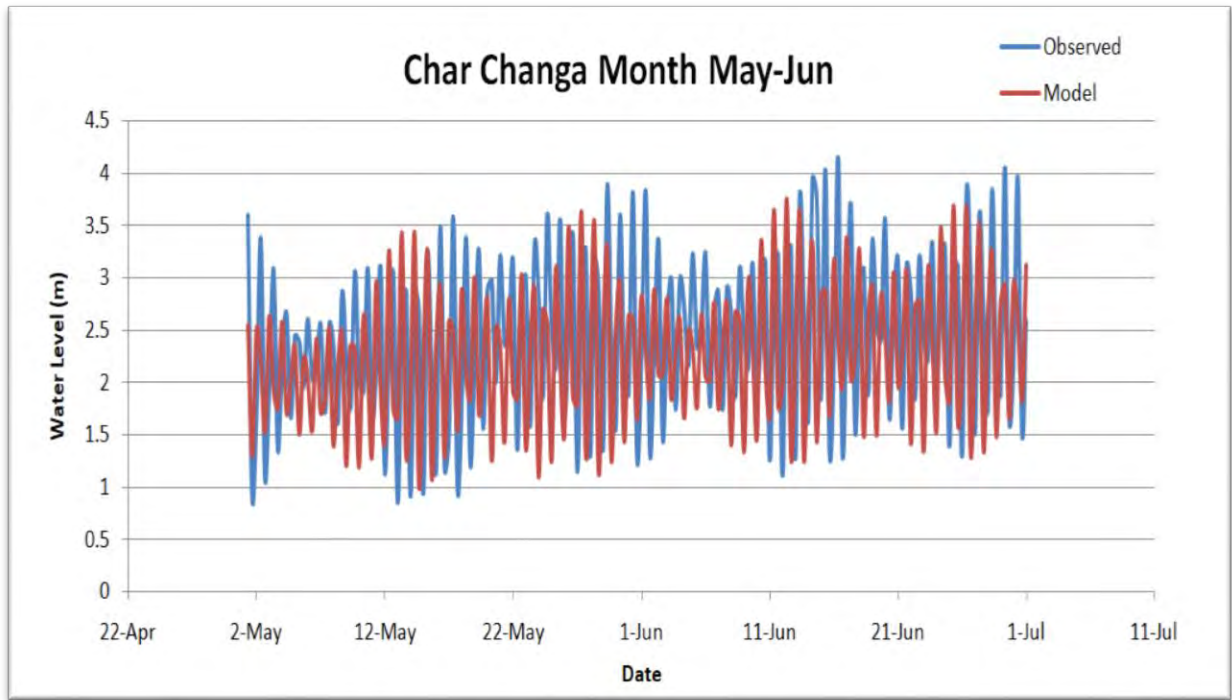


Figure 3.16: Comparison of observed and model predicted water level: at Char Changa for month May-June

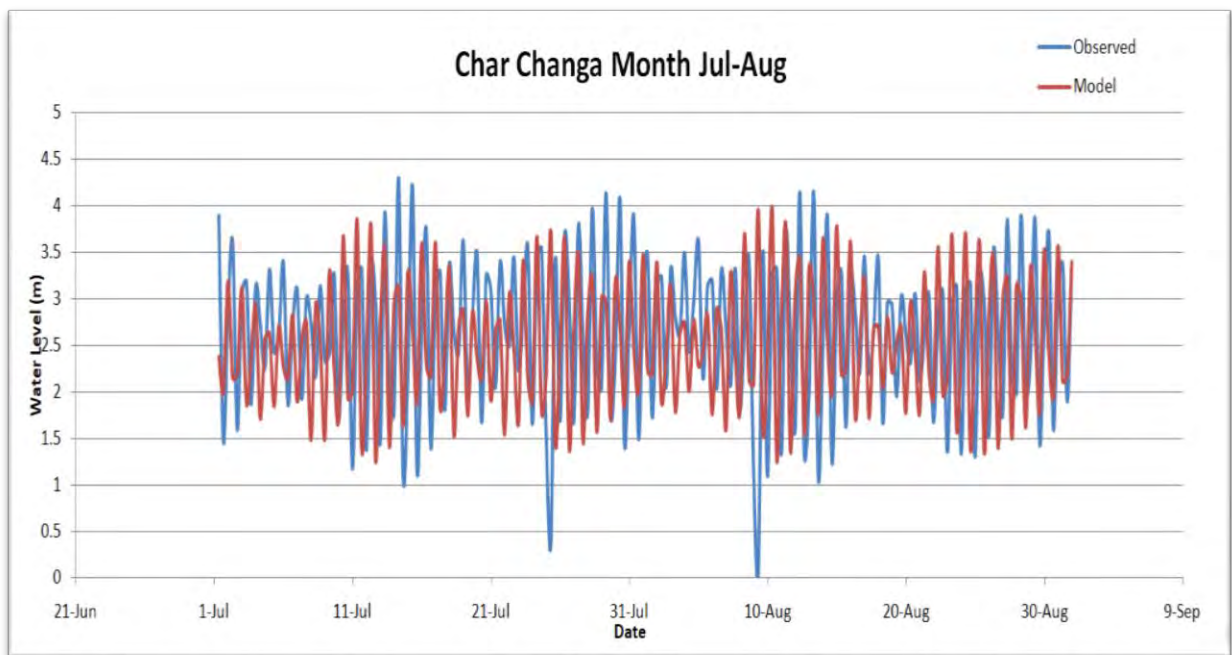


Figure 3.17: Comparison of observed and model predicted water level: at Char Changa for month July-August

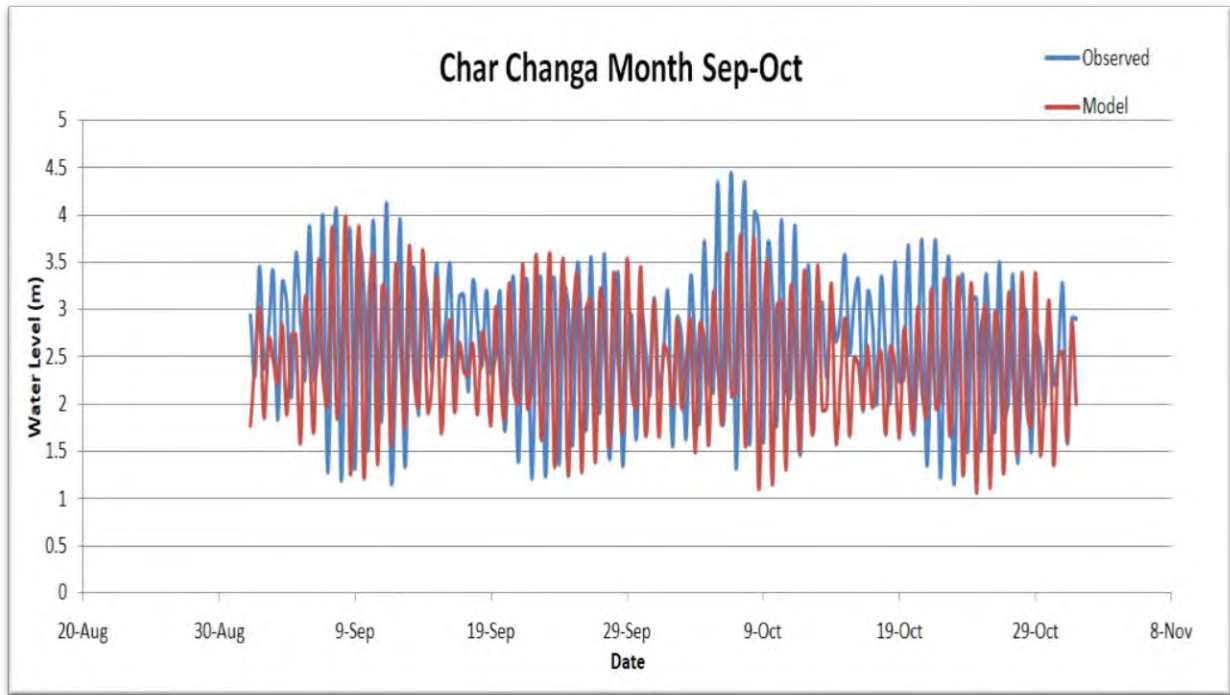


Figure 3.18: Comparison of observed and model predicted water level: at Char Changa for month September-October

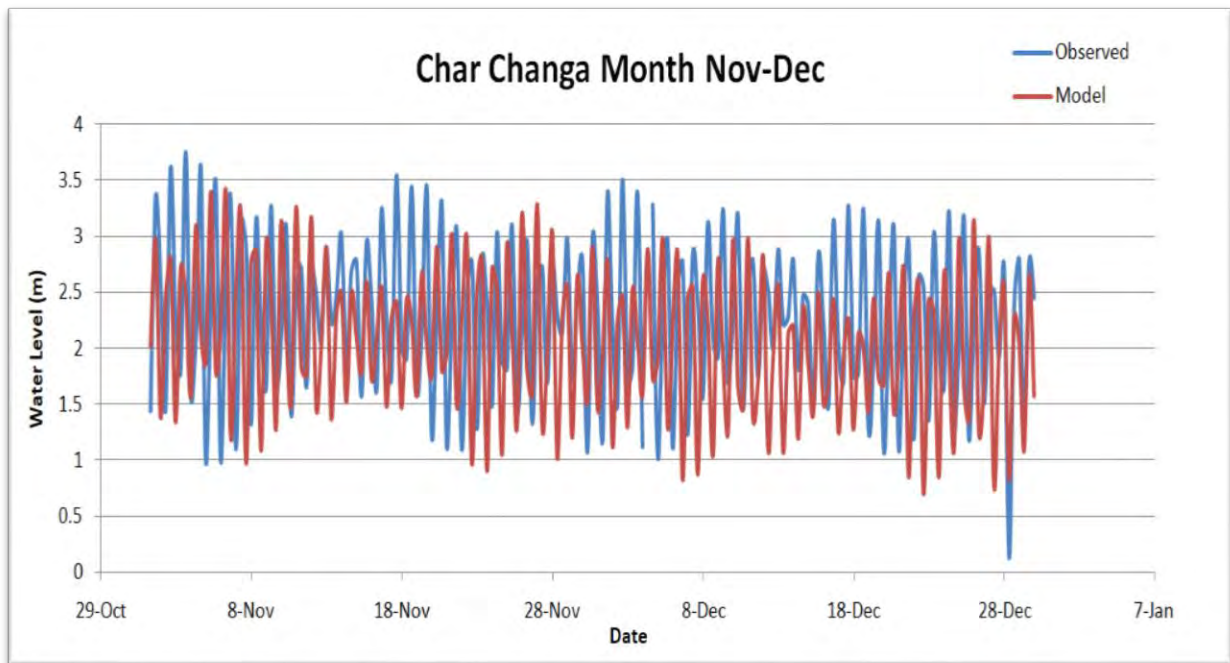


Figure 3.19: Comparison of observed and model predicted water level: at Char Changa for month November-December

To analyze the model performance more precisely the amplitude and phase of major tidal constituents are calculated both from observed and predicted data. The tides at sea are a sequence of sinusoidal, tidal harmonic components which are known as tidal constituents that are different for every location. These constituents are calculated by harmonic analysis theory. It is a complex procedure though the fundamentals are simple. The basic Equation is:

$$\eta = a_0 + \sum_{i=1}^n (a_i * \cos(\omega t - \phi_i)) \dots \dots \dots (i)$$

Where, η = tidal level, a_0 = amplitude at mean water level, a_i = amplitude at i-constituent, ϕ_i = phase angle at i- constituent, t = time. If water level of a location and a period according to different tidal constituents are input to a wave equation, amplitude and phase of that tidal wave can be calculated from that equation. Practically there is Matlab toolbox (and other software) which take input in a form of time series of tidal water level of a particular location and provide amplitude and phase of required tidal constituents. The dominant tidal constituents are the diurnal constituents, K1, O1, P1, Q1, and S1, with periods of 23.93, 25.82, 24.07, 26.87, and 24.00 h, respectively, and the semidiurnal constituents M2, S2, N2, and S2, with periods of 12.42, 12.00, 12.66, and 11.97 h, respectively. The sum of these sinusoidal curves with slightly different periods yields a spring-neap tide cycle, whereby the tidal range fluctuates from a maximum (spring tide) to a minimum (neap tide) and back to the maximum over a 28-day cycle. Amplitude and phase of major tidal constituents were calculated for different version of bathymetry for the station Hiron Point, Charchanga and Cox's Bazar.

Figure 3.20 shows comparison of four sets of tidal constituents from different bathymetry for Hiron Point. From Figure 3.20, it is noticed that model outputs using every bathymetry (GEBCO, ESPA-DELTA and Improved) are in good agreement with observed constituents. Error (here error is defined as the difference with amplitude calculated from observed data) in amplitude for the major influential constituent M2 using GEBCO bathymetry is nearly 8cm. For ESPA-Deltas bathymetry, error in amplitude is also 8cm. It is convenient because in ocean part ESPA Deltas bathymetry is same as GEBCO bathymetry. It is seen from the Figure 3.20 that the error in amplitude for improved version of bathymetry is only 1cm for M2. The error in other constituents is negligible for outputs using all versions of bathymetry. The predicted phases are also in good agreement, except for S2.

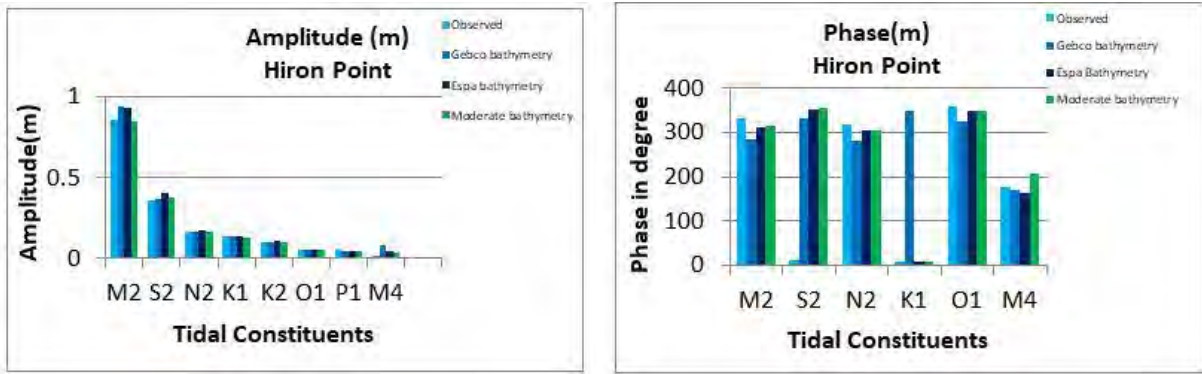


Figure 3.20: Comparison of amplitudes and phases of tidal constituents obtained by different version of bathymetry for Hiron Point station.

As shown in Fig. 3.21, at tide gauge station Char Changa, the error in amplitude for all constituents is quite significant for the outputs using GEBCO and ESPA Deltas bathymetry. For M2, error from GEBCO data output is nearly 25cm, and error from ESPA deltas output is 19cm. But in this station error of output from improved recent version of bathymetry is nearly 6cm. So, it is clear that the region improved bathymetry can eliminate a major portion of error from the output of GEBCO data. As Char Changa is located at the mouth of Meghna, which carries sediment load from a combined flow of Ganges, Brahmaputra and upper Meghna rivers, it is possible that the variation of bathymetry in this region cannot be represented by GEBCO data.

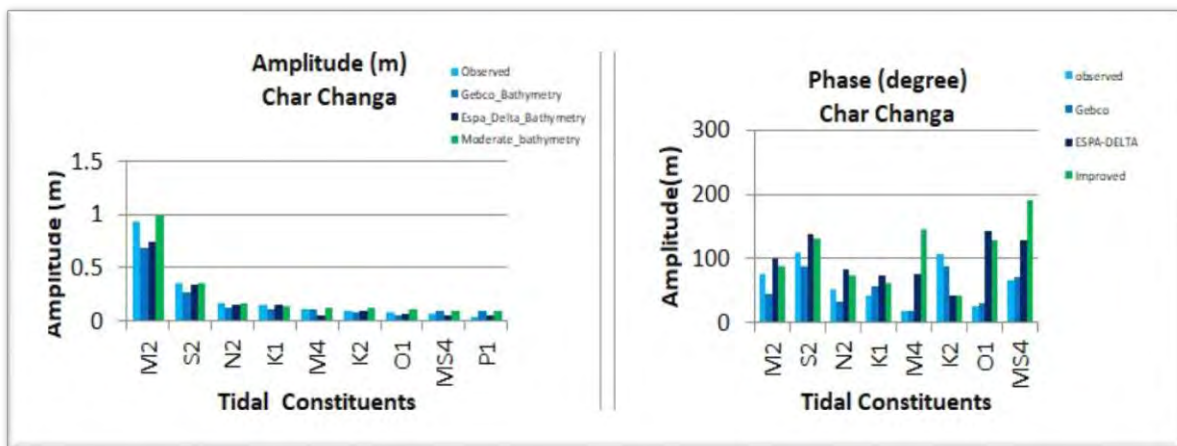


Figure 3.21: Comparison of amplitudes and phases of tidal constituents obtained by different version of bathymetry for Char Changa station

The model output using all versions of bathymetry is in good agreement at station Cox's Bazar, as shown in Fig. 3.22. Error in amplitude for GEBCO bathymetry output is nearly

19cm for constituent M2, and error in amplitude for ESPA Deltas data output is nearly 14cm for same constituent. But error is only 9cm for M2 for improved bathymetry. Thus, performance of latest bathymetry is satisfactory and better than older versions of bathymetry in every station.

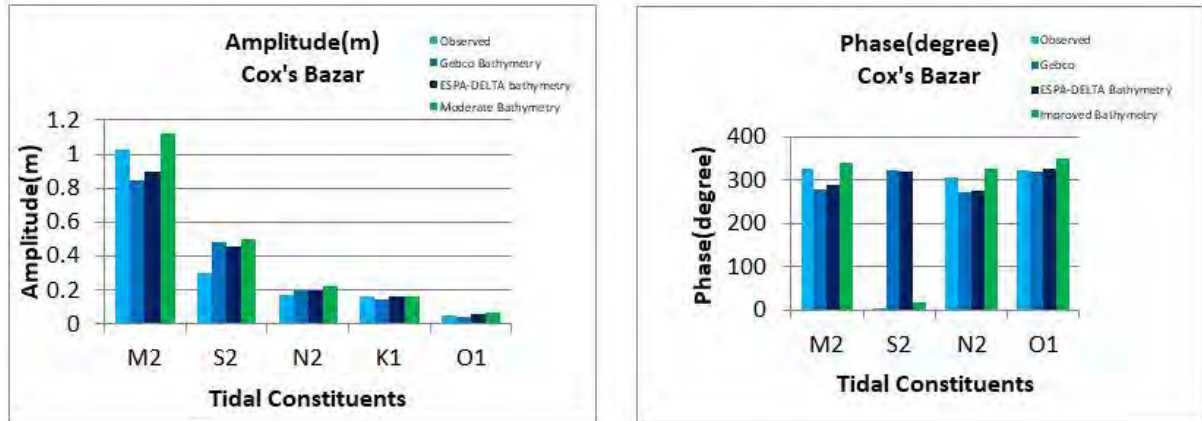


Figure 3.22: Comparison of amplitudes and phases of tidal constituents obtained by different version of bathymetry for Cox's Bazar station

To assess the performance of the model, its output has also been compared with output of global model FES2012 and FES2014. The comparison has been made between the complex errors of each constituents of each station and between summations of errors of all constituents of each stations. Complex error is a simple way to take into account both the amplitude and phase error. The idea is simply to build a complex number where amplitude is the real part and phase is the imaginary part. Then the complex difference (equation below) Δz is proportional to the RMS difference, and one can build RSS (Root Sum Square error) by combining the errors in difference constituents and site.

$$\sigma = \sqrt{0.5}|\Delta z|^2 \dots \dots \dots (ii)$$

Here, $\Delta z = |A_{obs}e^{i\phi_{obs}} - A_{mod}e^{i\phi_{mod}}|$

$$\sigma_{site} = \sqrt{0.5 \sum_{Constituents} |\Delta z|^2} \dots \dots \dots (iii)$$

- In the equation,
- Aobs = Amplitude of observed Harmonic Constituents.
 - Øobs = Phase of observed Harmonic Constituents.
 - Amod = Amplitude of model Harmonic Constituents.
 - Ømod = Phase of model Harmonic Constituents.

Figure 3.23 shows the comparison of complex errors of different constituents at different stations. At Hiron Point, the accumulated complex error for four influential constituents (M2, S2, K1, O1) from Delft3D output is 17.5 cm. But, for global model FES2012 and FES2014 this error is 40 cm and 41.9 cm, respectively. At Charchanga this error for Delft3D is 44.8 cm and for FES2012 and FES2014 is 54.5 cm and 52.6 cm, respectively. For Cox's Bazar, Delft3D performance is slightly worse than global models.

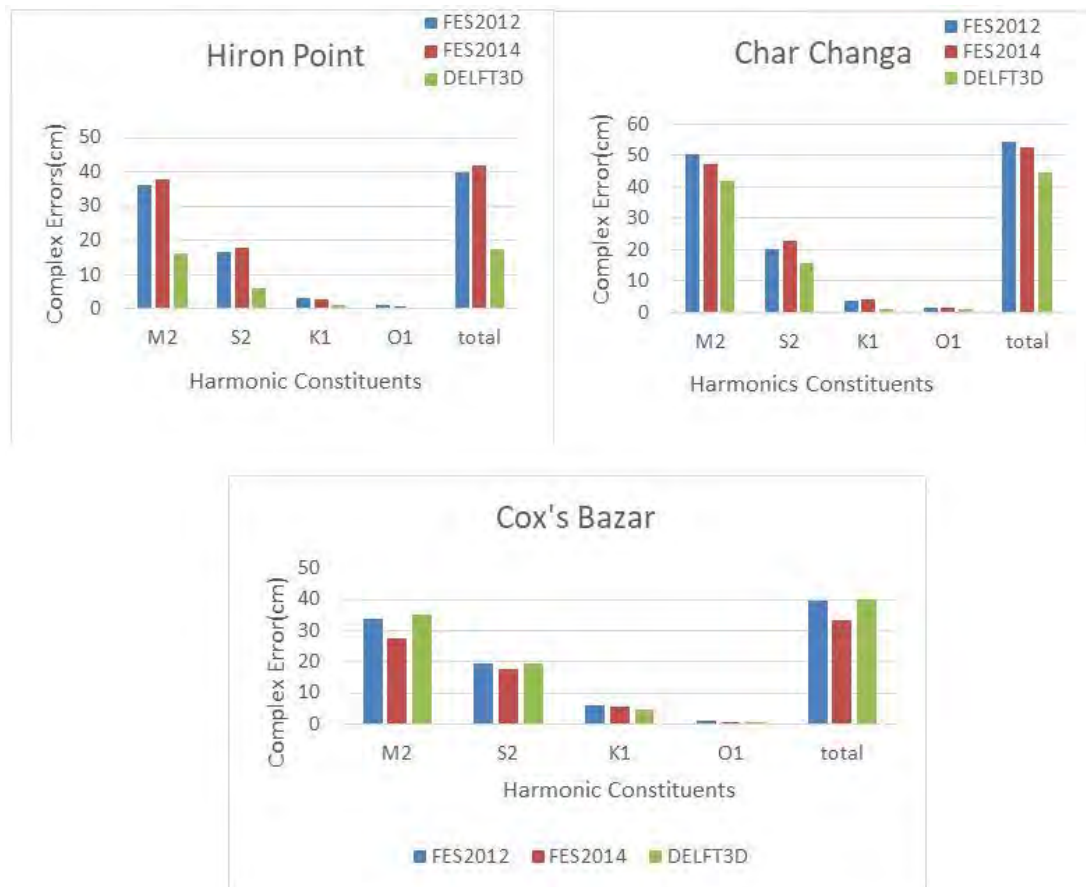


Figure 3.23: Comparison of complex error of tidal constituents obtained by different Model for station Hiron Point, Char Changa and Cox's bazar.

CHAPTER 4

RESULTS AND DISCUSSION

4.1 Introduction

The main objective of this research was to assess effect of sea level rise on salinity intrusion in the coastal areas of Bangladesh. This research work involved setting up and validation of Delft3D model for the coastal part of GBM delta; the hydrodynamic module Delft3D-FLOW was used in this study. In this research, evaluation of salinity pattern of Bangladesh coastal zone was assessed for 0.5m, 1m and 1.5m sea level rise (SLR) along with one additional scenario in which 20 percent decrease in Brahmaputra discharge is considered with 1m SLR. Chapter 3 describes the model set up, calibration and validation of the model. This Chapter first presents the performance of the model in describing salinity in the coastal areas of Bangladesh. This Chapter then presents the predicted salinity patterns at different monitoring stations in response to different sea level rise (SLR) scenarios, and discusses implications of these predictions.

4.2 Model Performance in Describing Salinity

Unlike water level which is governed at most of the locations of this study area by tidal influence, salinity of study area is dominated by the fresh water flows from upstreamsources. The calibrated model (Delft3D-FLOW, as described in Chapter 3) was used to predict salinity for the year 2010. The predicted salinity has been compared with data recorded at 14 BWDB salinity stations. Figure 4.1 shows the location of the 14 monitoring stations for which salinity has been compared. Based on these comparisons, performance of the calibrated model in predicting salinity was assessed.

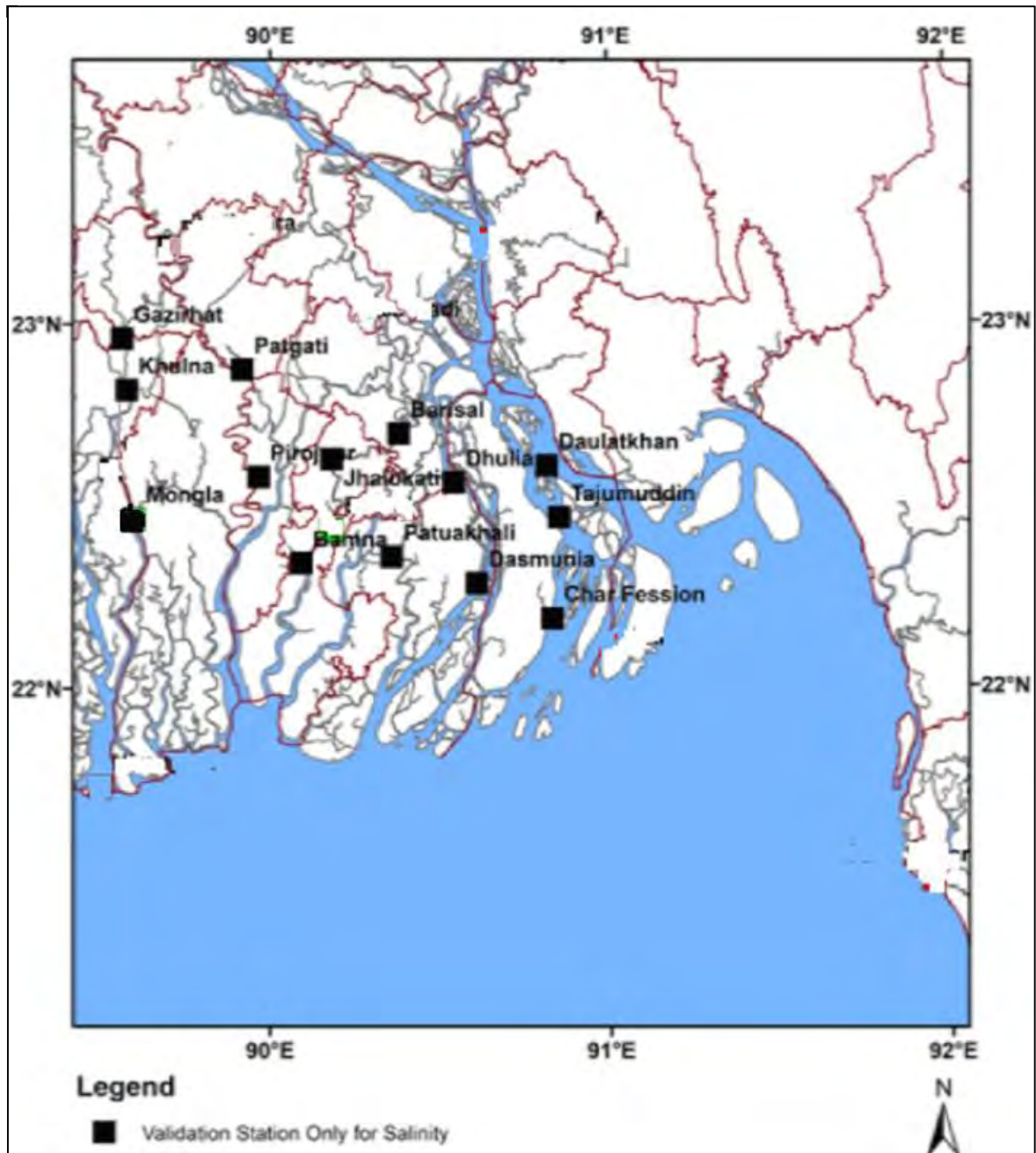


Figure 4.1: Location of 14 BWDB monitoring stations for which salinity was compared for the year 2010 using the calibrated model predicted data and observed data

Figure 4.2 shows the comparison between observed salinity and model output at the Mongla station. This location is fed by the distributary of Ganges, mainly by the Gorai River and some other small channels. Fig. 4.2 shows that the model could reasonably capture the variation of salinity at Mongla station.

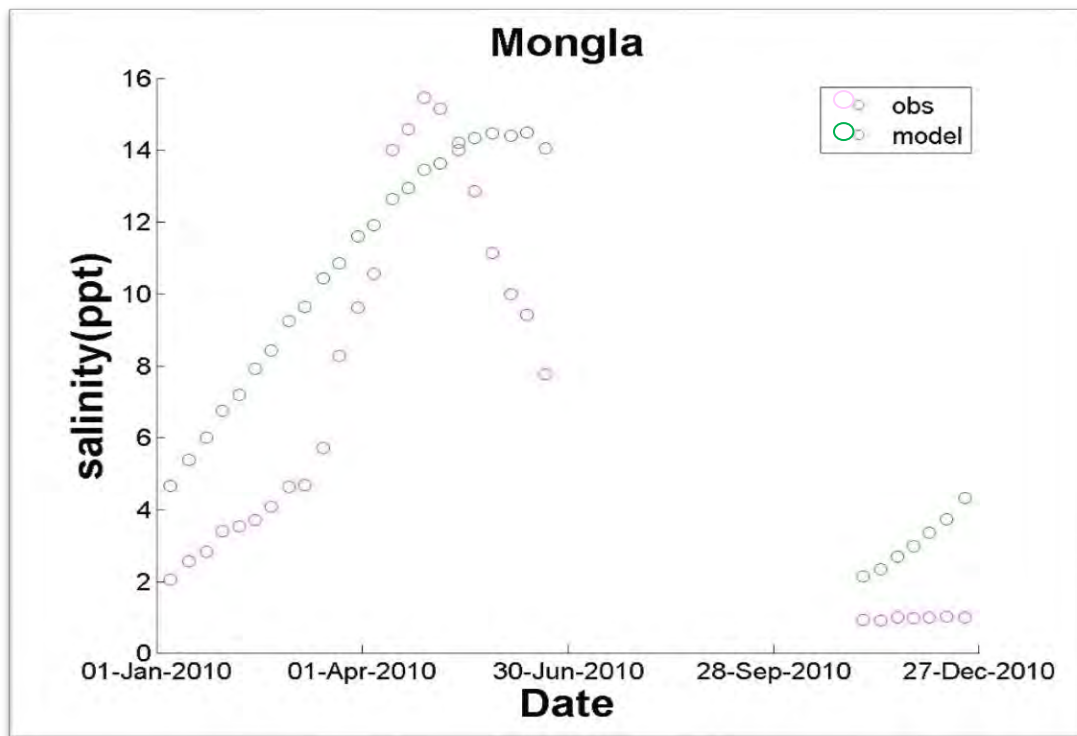


Figure 4.2: Comparison of predicted and observed salinity at Mongla station

Figure 4.3 and Fig. 4.4 show the comparison of observed salinity and model predicted salinity at the Khulna and Gazirhat, respectively. These two locations are also fed by the distributary of Ganges, mainly the Gorai River. The bathymetry used in this model has been updated after 2010. In 2010 the mouth of Gorai river was dredged by Bangladesh Water Development Board (BWDB), which increased the Gorai discharge significantly and reduced the salinity of the area fed by Gorai River. Figure 4.3 and 4.4 show that the model underestimated the salinity value significantly at Khulna and Gazirhat. This is probably because the salinity data in 2010 were recorded prior to the occurrence of increased discharge resulting from dredging Gorai mouth.

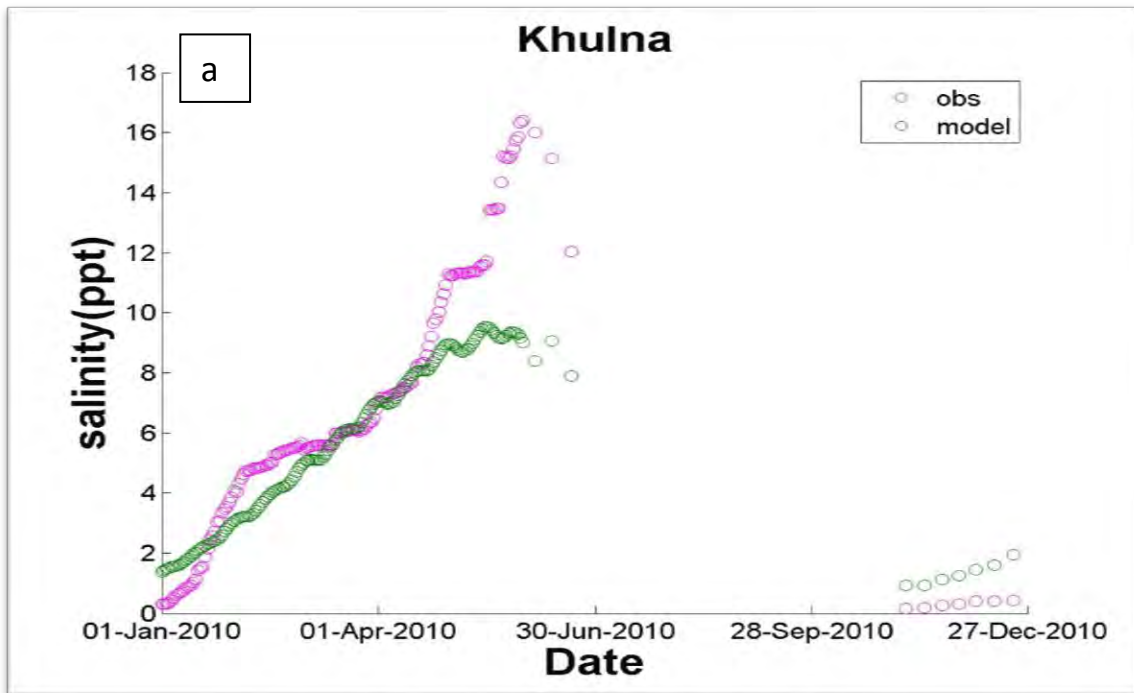


Figure 4.3: Comparison of predicted and observed salinity at Khulna station

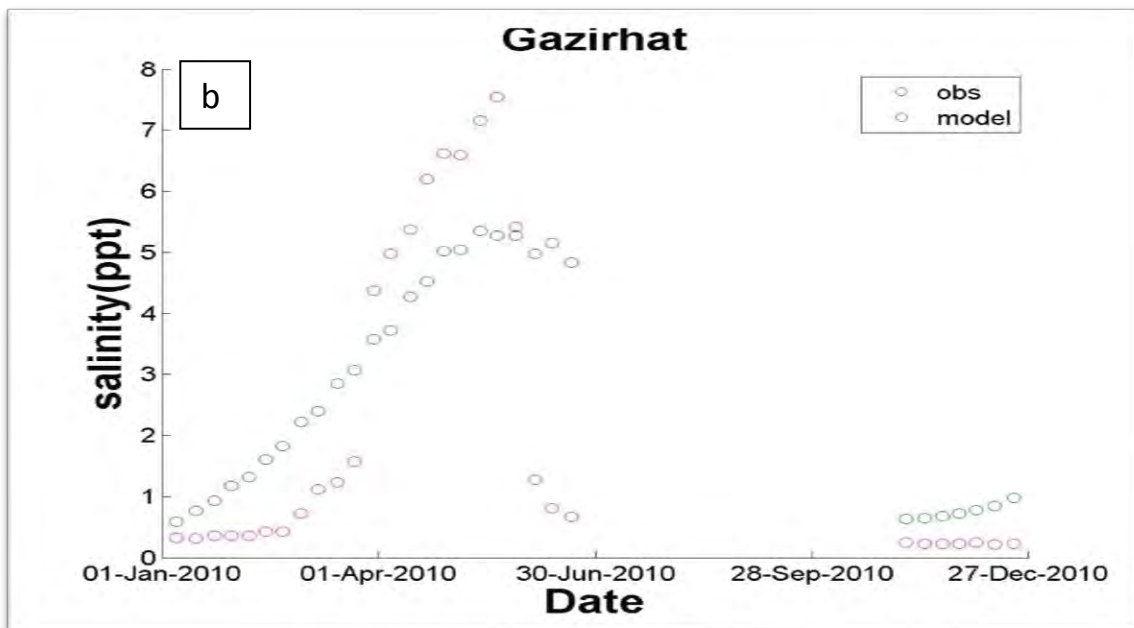


Figure 4.4: Comparison of predicted and observed salinity at Gazirhat station

Figure 4.5 and Fig. 4.6 show the comparison of observed salinity data and model output at the Patuakhali station and Barisal station, respectively. The gauge station at Patuakhali is located in the Galachipa river, which is fed by sufficient fresh water from Tentulia river. This (Tentulia) river is the second major channel after Meghna through which most of the fresh water discharge of GBM basin flows into Bay of Bengal. In Fig. 4.5 it is observed that the maximum value of observed salinity is close to only 0.6 ppt but the model predicted a value of nearly 2 ppt. It indicates the connectivity of river Galachipa with river Tentulia in this model is poor than the connectivity in reality.

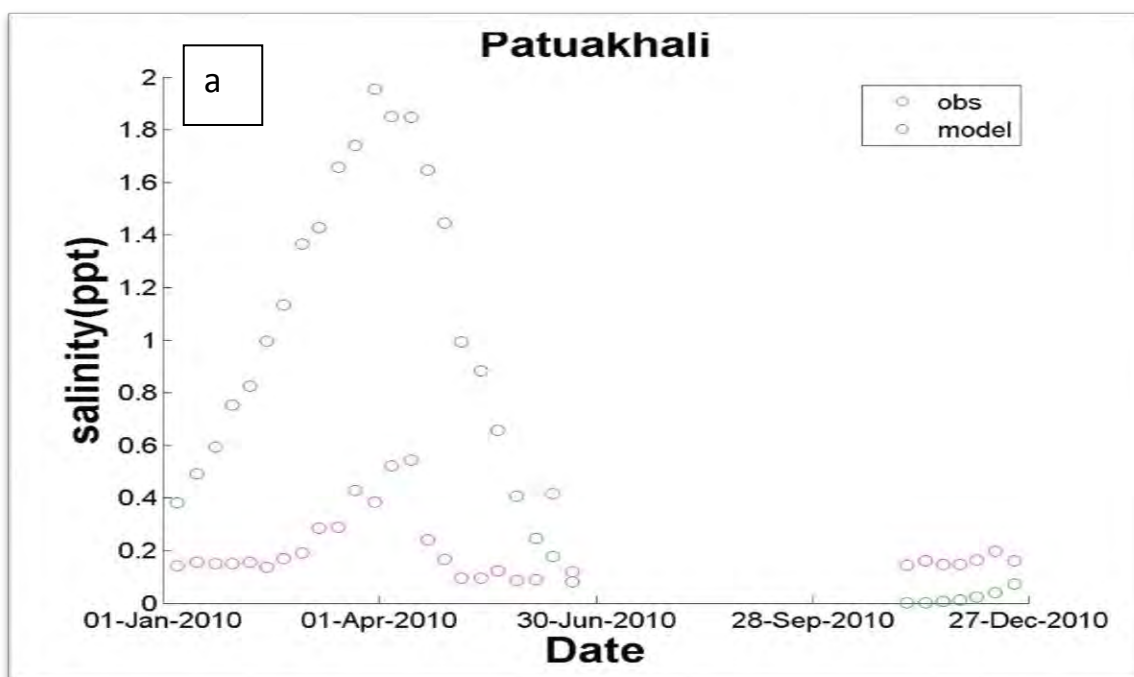


Figure 4.5: Comparison of predicted and observed salinity at Patuakhali station

The gauge station Barisal is located in the Bishkhali river which is also fed with sufficient fresh water from Tentulia river. In Fig. 4.6, it can be seen that the observed salinity in this station apparently does not change with season. Throughout the whole year, value of observed salinity is close to only 0.2 ppt; but the model predicted value has a seasonal variation from 0 to 0.5 ppt. It is most likely due to poor connectivity in the model between Bishkhali river and Tentulariver.

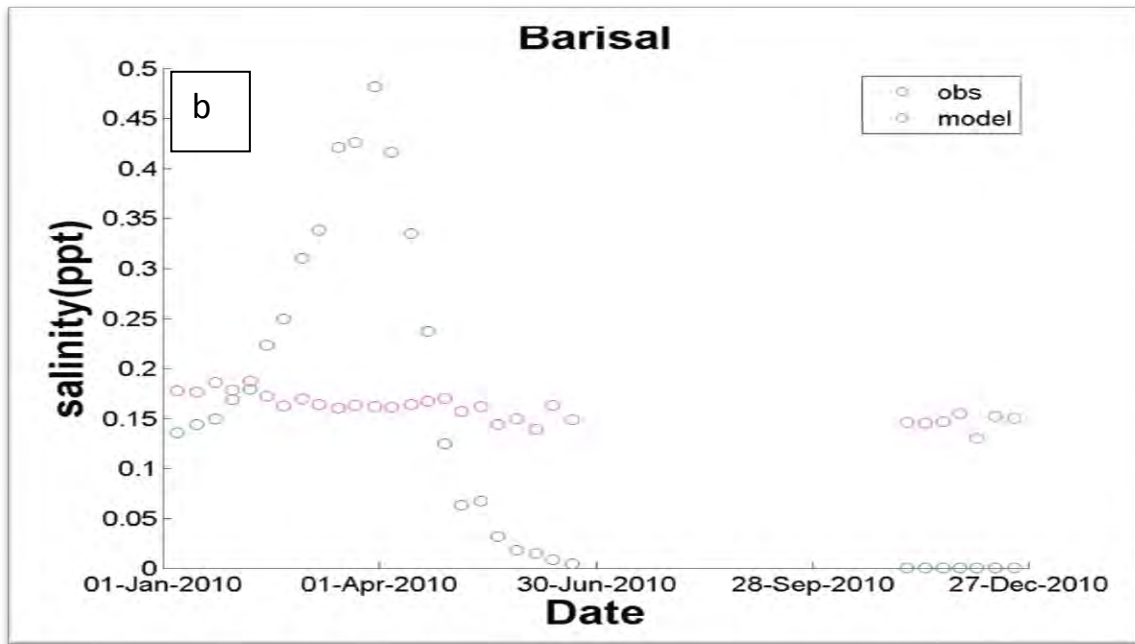


Figure 4.6: Comparison of predicted and observed salinity at Barisal station

Figure 4.7 and Fig. 4.8 show the comparison of observed salinity data and model output at the Tajimuddin station and Daulatkhan station, respectively. The gauge stations at Tajimuddin and Daulatkhan are located in the estuary of Meghna river which is the single most major channel through which most of the fresh water discharge of GBM basin flows into Bay of Bengal. So, these two stations experience a huge amount of fresh water flow; as these stations are located very close to Bay of Bengal they also experience vigorous tidal effect.

The match between observed and model predicted data is poor for these (Tajimuddin and Daulatkhan) two stations. The pattern of observed data seems erratic though model output shows a clear curve with peak at April and lowest from June to December. The observed salinity pattern is difficult to explain. Though erratic, for both stations observed data show the peak salinity in December, whereas model shows peak at April. The reason of this disparity is perhaps the model bathymetric data failed to capture the real average slope of Ganges, Jamuna and Meghna river system.

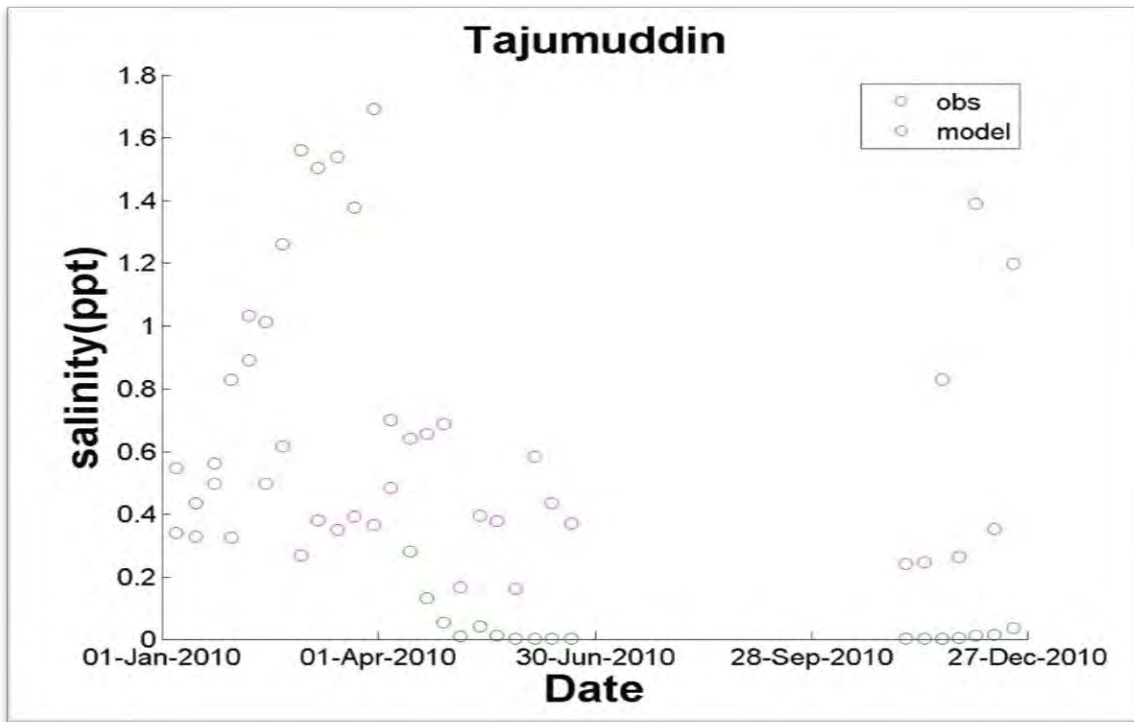


Figure 4.7: Comparison of predicted and observed salinity at Tajumuddin station

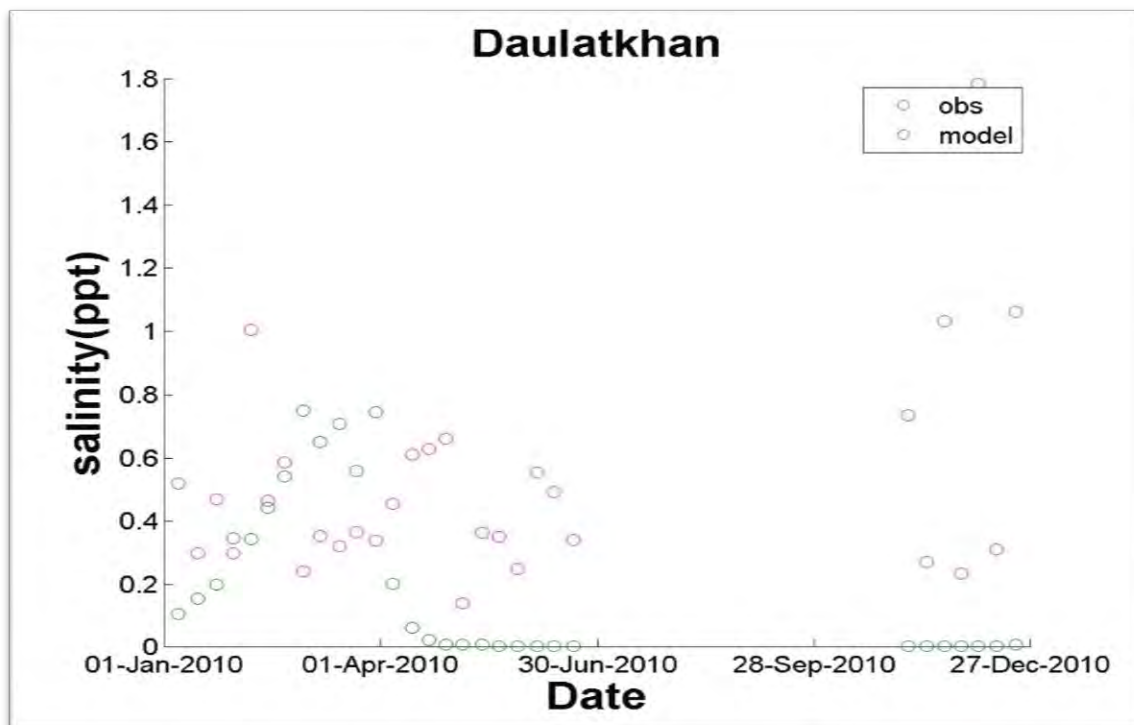


Figure 4.8: Comparison of predicted and observed salinity at Daulatkhan station

Figure 4.9 and Fig. 4.10 show the comparison of observed salinity data and model output at the Char Fession station and Dasmonia station, respectively. The guage station at Char Fession is also located at the estuary of Meghna river. So, this station experiene a huge amount of fresh water flow and vigourous tidal effect as well. Comparison between observed and model predicted data for this station reveal similar situation as was observed for Tajumuddin and Daulatkhan stations. The station Dasmonia is located in the Tentulia River which is a vital distributory of Meghna. Actualy nearly all fresh water from GBM basin passes through Meghna and Tentulia river together. So, Dasmonia is also influenced by abundant fresh water flow. Observed data of Dasmonia shows no significant seasonal variation which is something contradictory to common sense and it is difficult to find reasons for this observation.

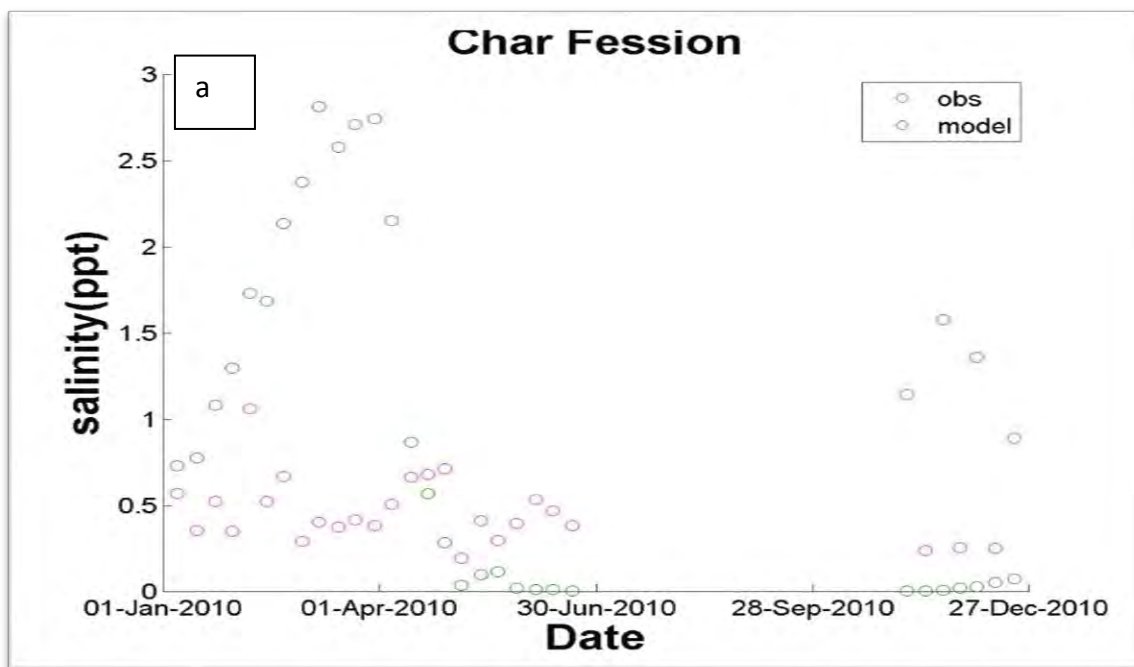


Figure 4.9: Comparison of predicted and observed salinity at Char Fession station

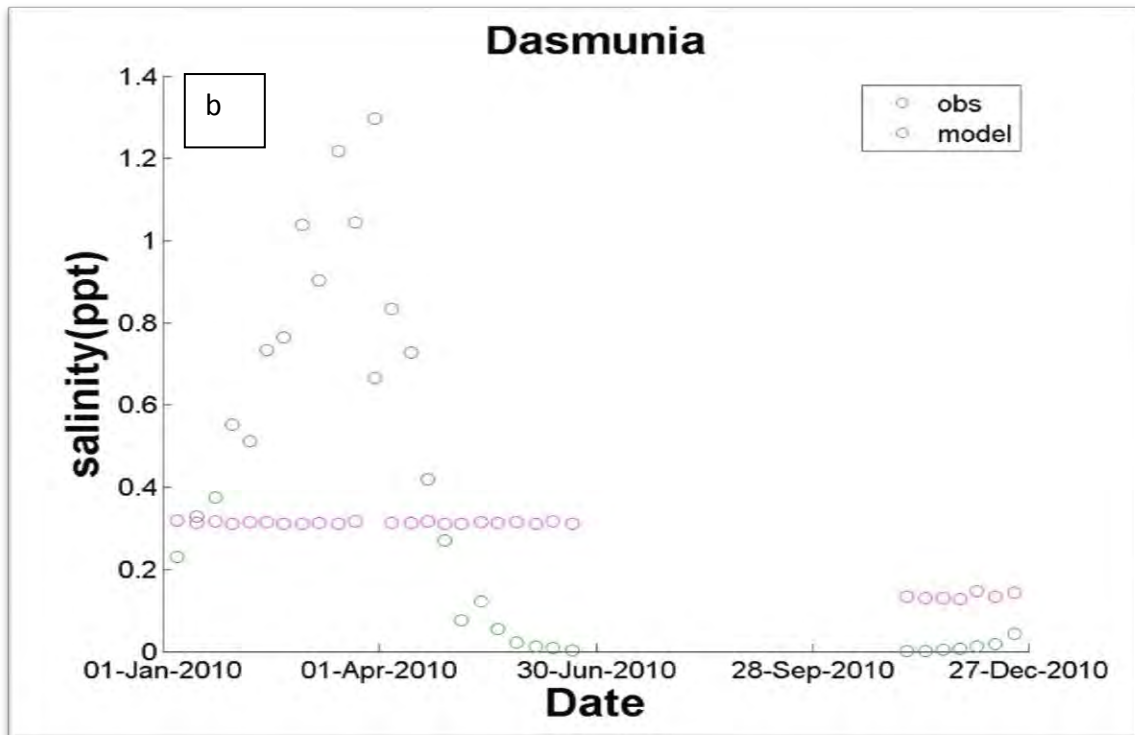


Figure 4.10: Comparison of predicted and observed salinity at Dasmunia station

Figure 4.11 and Fig. 4.12 show the comparison of observed salinity and model output at the Dhulia station and Bamna station, respectively. Dhulia gauge station is located in Tentulia river further inland than Dasmonia. Interestingly, model output at Dasmonia is higher than the observed value but at Dhulia which is located further inland of Dasmonia in same river, the model output is lower than observed values. It indicates Dhulia gets more fresh water in model than it gets in reality. On the other hand, somewhere downstream of the same river Dasmonia gets less fresh water. It appears that the morphology of the Tentulia river from Dhulia to Dasmonia in model failed to capture reality. The Bamna station is located in the Bishkhali river. Bishkhali river is a distributory of Tentulia river. Bishkhali river is fed by abundant fresh water.

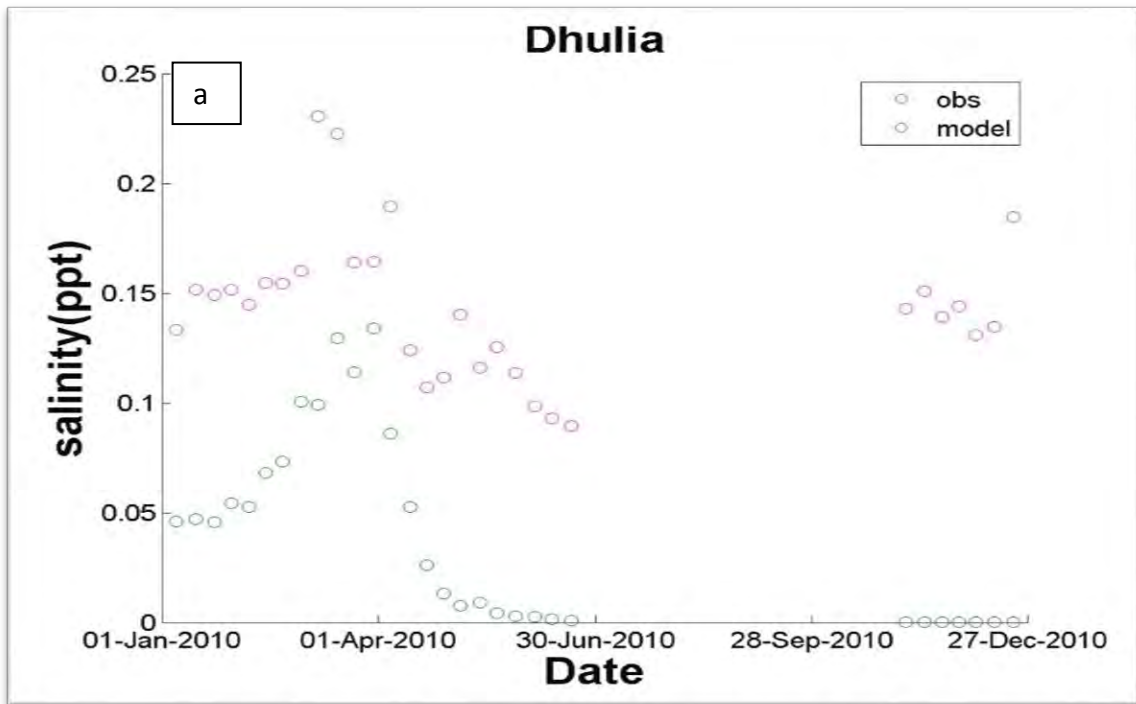


Figure 4.11: Comparison of predicted and observed salinity at Dasmunia station

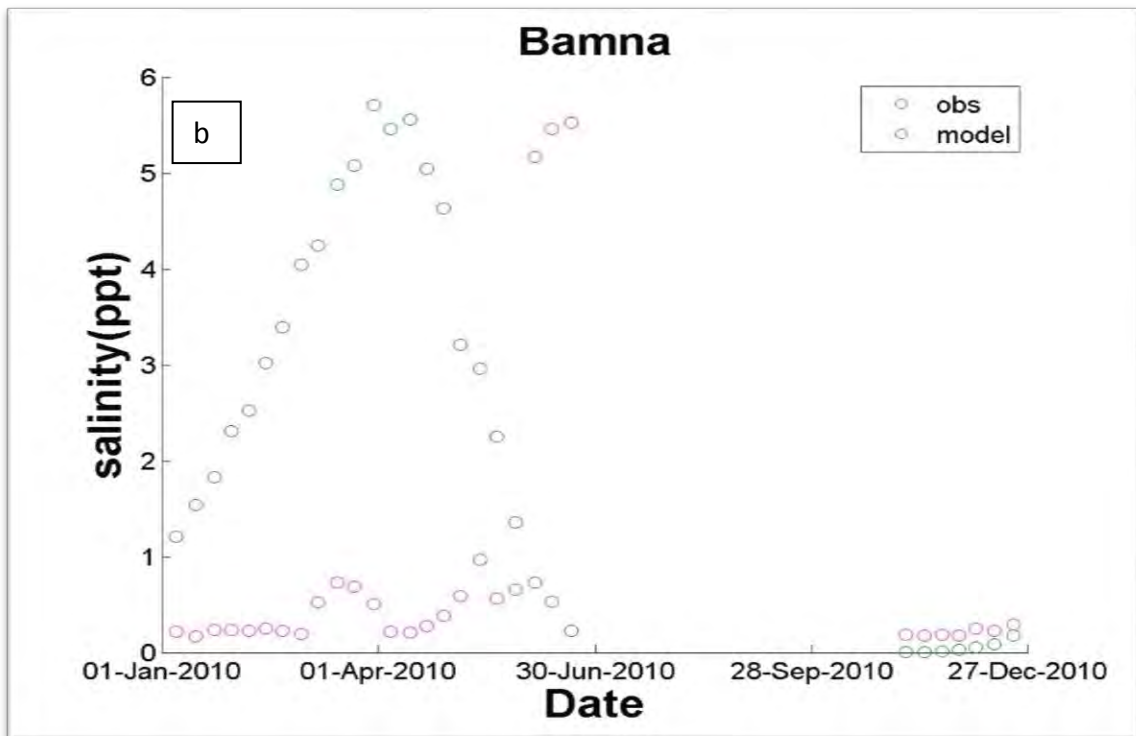


Figure 4.12: Comparison of predicted and observed salinity at Dasmunia station

Figure 4.13 and Fig. 4.14 show the comparison of observed salinity and model output at the Jhalokati station and Patgati station, respectively. Jhalokati station is located in Bishkhali River. The observed data of Jhalokati shows the salinity is more or less 0.25 ppt throughout the whole year. This lack of seasonal variation is hard to explain. Patgati is located in Kaliganga River which is connected to Madhumati river. Figure 4.15 shows the comparison of observed salinity and model output at the Pirojpurstation, located in Bishkhali River.

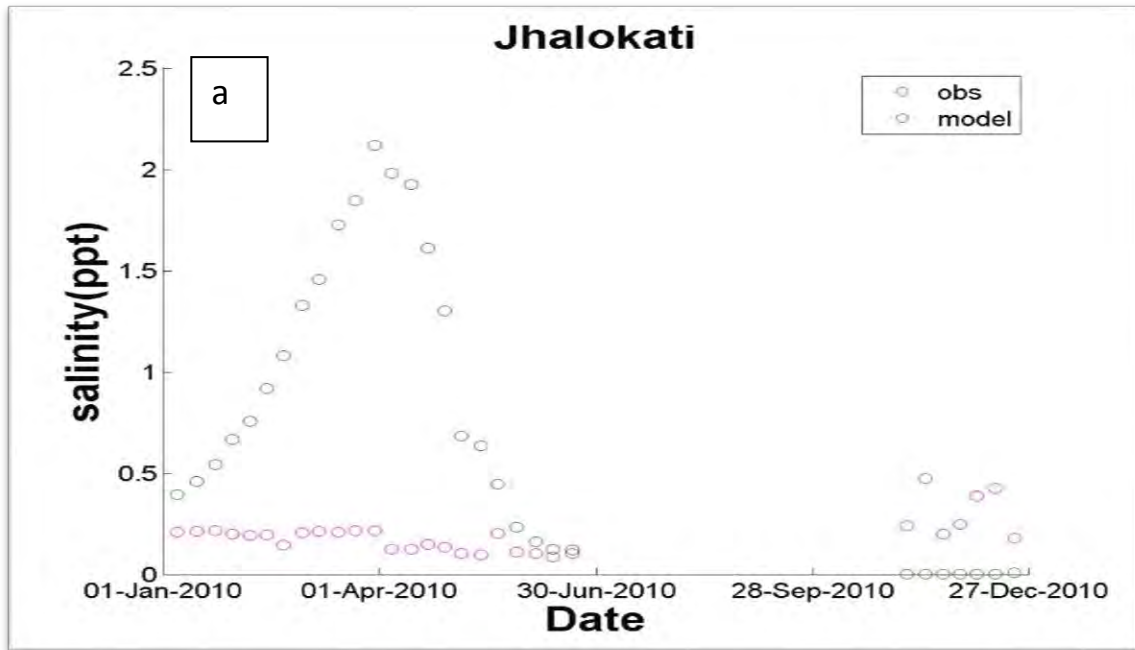


Figure 4.13: Comparison of predicted and observed salinity at Jhalokati station

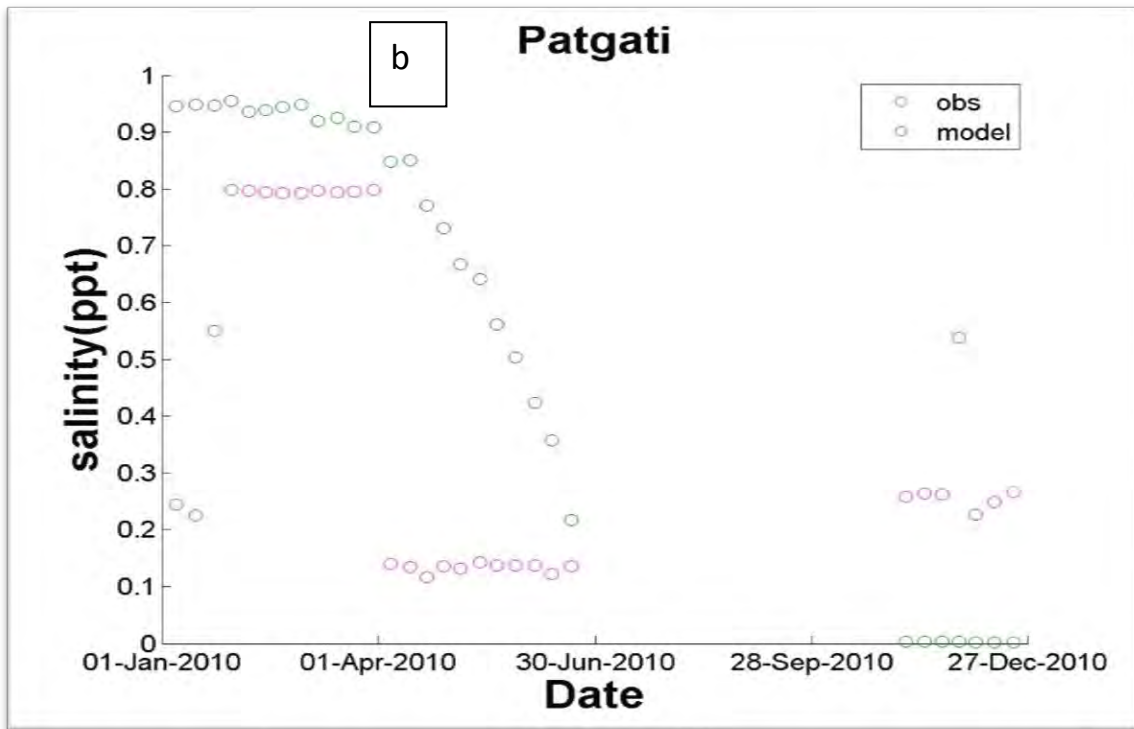


Figure 4.14: Comparison of predicted and observed salinity at Patgati station

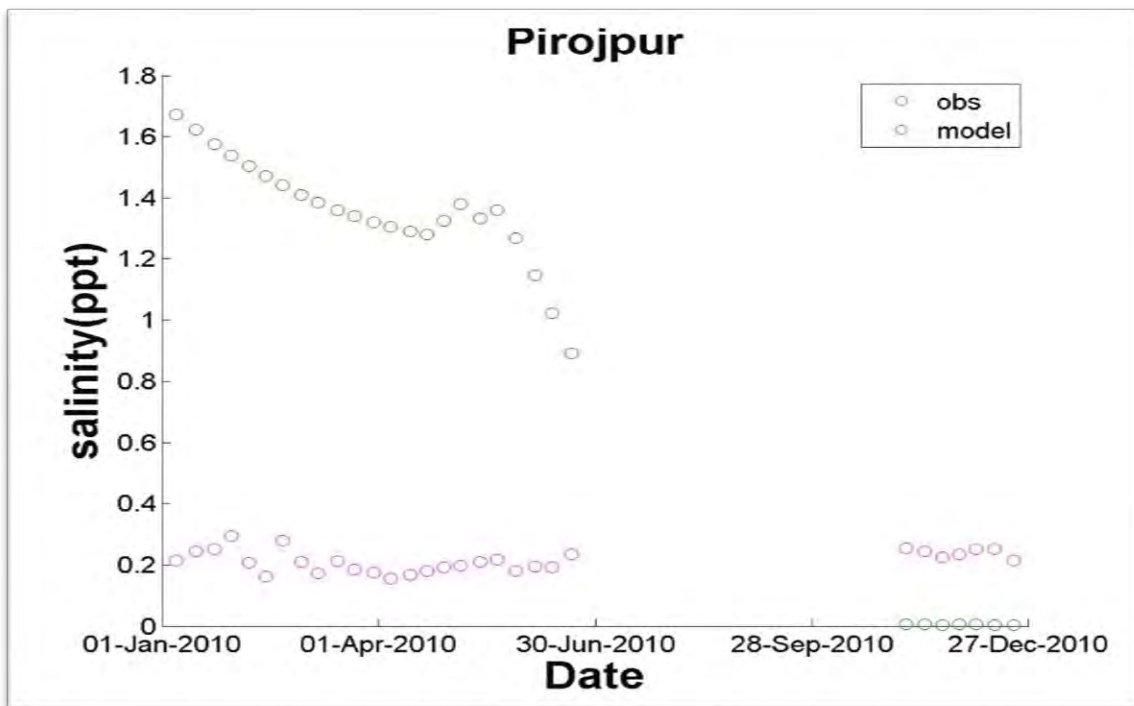


Figure 4.15: Comparison of predicted and observed salinity at Pirojpur station

From the analysis of salinity data and model predictions, it appears that for the gauge stations located in rivers fed by Gorai river system (e.g., Mongla, Khulna and Gazipur), the observed salinity data show a regular pattern; lower values of salinity when fresh water is in abundance and higher values of salinity when fresh water supply is limited. The model predictions also show similar trends.

But this is not the case for gauge station located in rivers fed by Meghna and Tentulia rivers (and their distributaries), e.g., Char Fession, Tazimuddin, Daulatkhan, Dasmonia, Dhulia, Bamna, Jhalokati, Barisal, and Patuakhali. It should be noted that BWDB gauge stations located in Meghna and Tentulia rivers and their distributaries are influenced by higher fresh water flow from upstream. In these stations the observed data show random and haphazard pattern. Even some stations shows no variation of salinity with season at all. This is difficult to explain.

Under this situation, the model output under existing condition has been taken as the existing situation, and effect of sea level rises (SLR) on salinity has been assessed through model simulations. In addition, effect of decreased upstream flow on salinity has also been assessed through model simulations.

4.3 Effect of Sea Level Rise on Salinity

The calibrated model has been used to assess effect of sea level rise (SLR) on salinity. For the model simulations, the fresh water discharge at upstream has been kept fixed at value used for validation of the model for the year 2010. The southern boundary data has also used for the year 2010, but raised by 0.5 m, 1m and 1.5m respectively to simulate 0.5m, 1m and 1.5m SLR respectively. Other than three SLR scenario one extra scenario has been considered, in which the upstream fresh water discharge of Brahmaputra has been reduced by 20 percent and the sea level has been raised by 1m simultaneously, to observe the corresponding change in salinity pattern.

Figure 4.16 and Fig. 4.17 shows predicted salinity at Char Fession and Daulatkhan for the four SLR scenarios considered in this study. At both stations, salinity increases with increasing sea level rise. Higher increase of salinity is observed during the dry period (February to April) of the year, when upstream flows are at their lowest levels. Under existing condition, peak salinity at Char Fession is predicted to be 2.8 ppt in April; peak

salinity has been predicted to increase to 3.5 ppt, 4.6 ppt and 6.1ppt as sea level increases by 0.5 m, 1.0 m and 1.5 m, respectively. Salinity dramatically increases as upstream discharge is reduced. At Char Fession, peak salinity is predicted to reach 4.6 ppt for a sea level rise of 1.0 m (from a baseline/existing value of 2.8 ppt). If upstream flow is decreased by 20%, then the predicted peak salinity reaches 9.5 ppt. This suggests that upstream flow has a more profound effect on salinity compared to sea level rise.

A similar trend is also observed for the Daulatkhan station. Predicted peak salinity at this station increases from existing 0.8 ppt to 1.9 ppt in responses to a 1.0 m sea level rise; if upstream flow of Brahmaputra is reduced by 20%, the peak salinity in response to a 1.0 sea level rise reaches 5.8 ppt. It is important to note here that both of these stations (i.e. Char Fession and Daulatkhan) are located in the Meghna river and close to the Bay of Bengal.

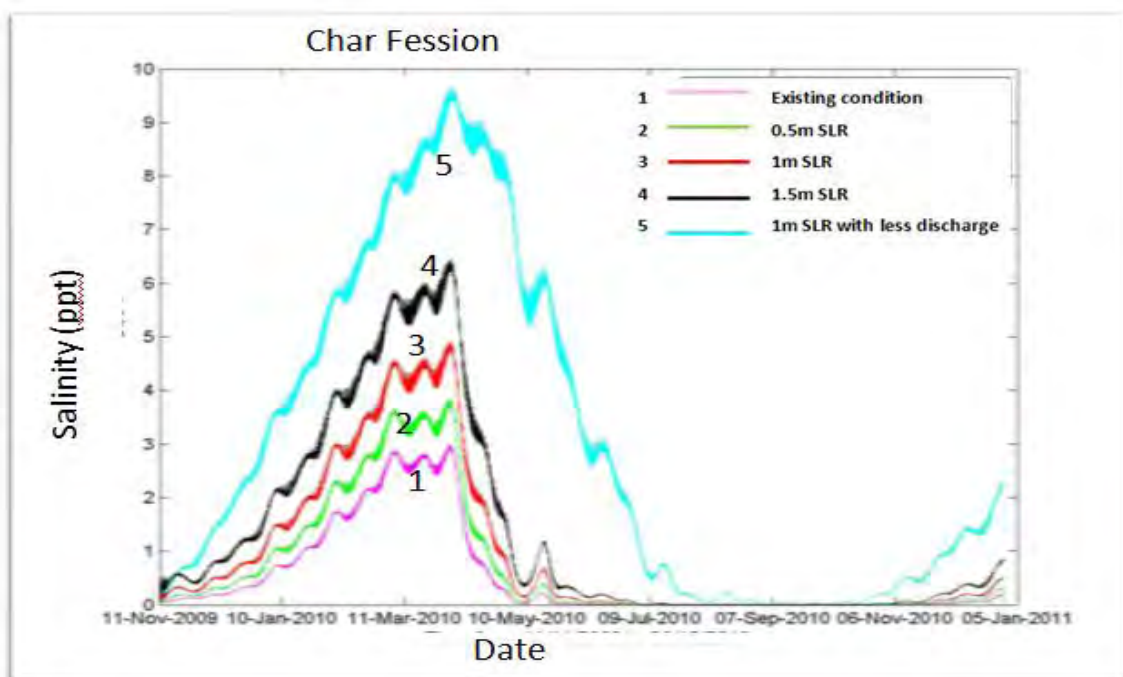


Figure 4.16: Predicted salinity at Char Fession station for different SLR scenarios

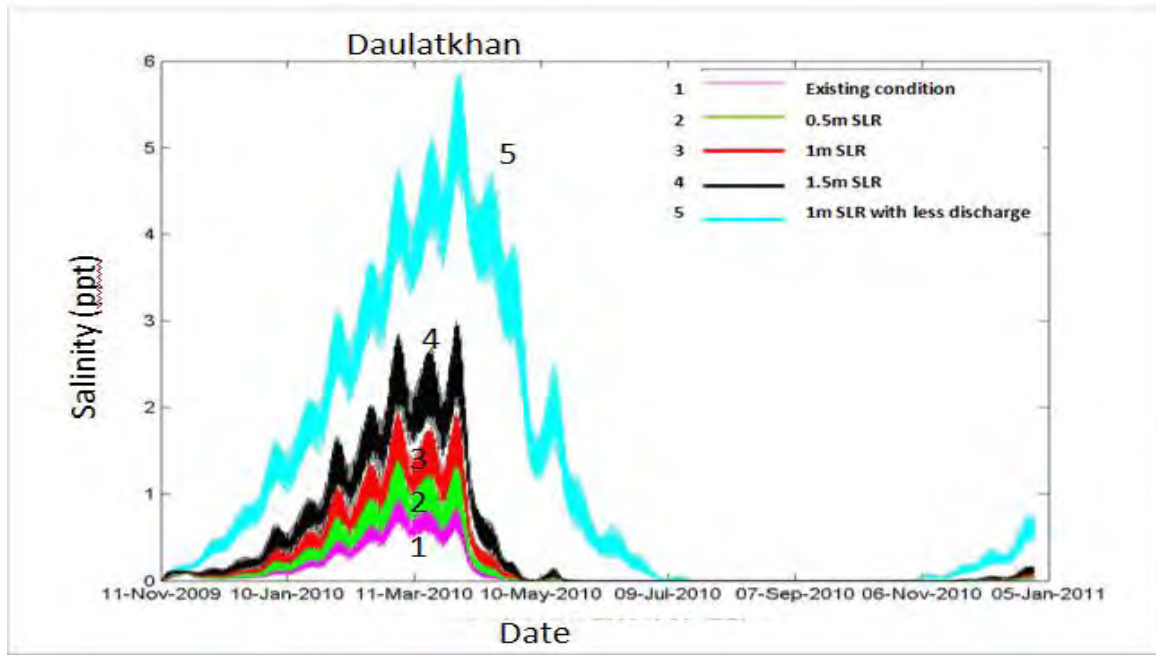


Figure 4.17: Predicted salinity at Daulatkhan station for different SLR scenarios

Figure 4.18, Fig. 4.19 and Fig. 4.20 show predicted salinity for the different SLR scenarios for Tajimuddin, Dasmonia and Dhulia. At all three locations, the predicted changes in salinity show similar pattern; salinity increases as sea level rise increases. The effect becomes more profound as upstream flow is decreased. Predicted peak salinity at Tajimuddin station increases from existing 1.9 ppt to 3.2 ppt, at Dasmonia from 1.25 to 1.75 ppt, and at Dhulia from 0.2 to 0.4 ppt in responses to a 1.0 m sea level rise; if upstream flow of Brahmaputra is reduced by 20%, the peak salinity in response to a 1.0 sea level rise reaches 7.9 , 4.5 and 1.5 ppt respectively at Tajimuddin, Dasmonia and Dhulia.

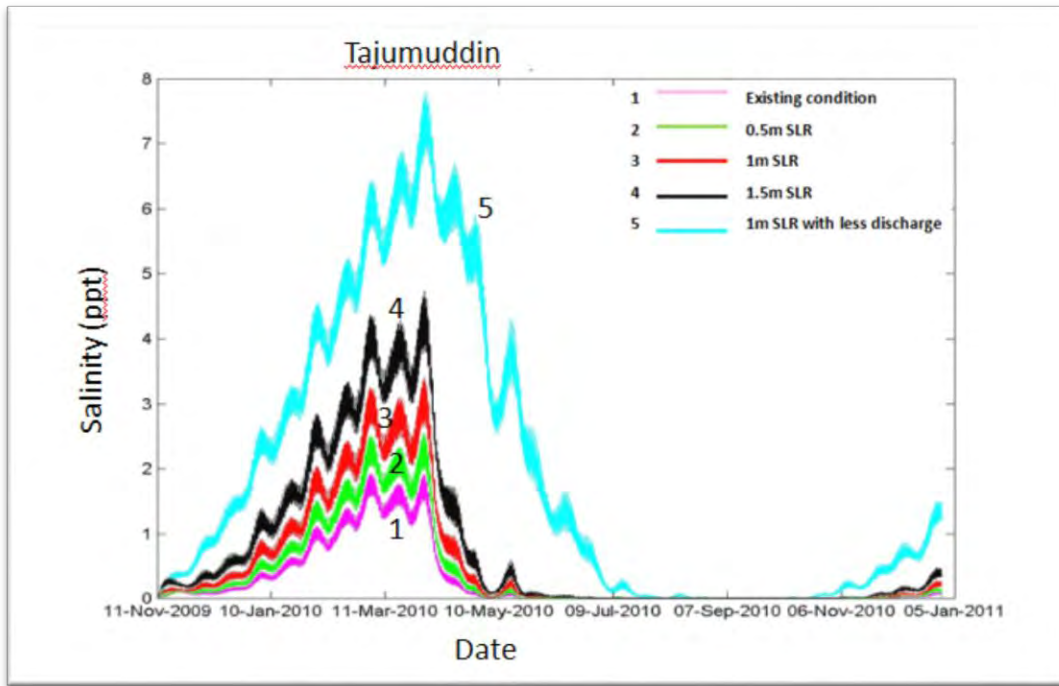


Figure 4.18: Predicted salinity at Tajumuddin station for different SLR scenarios

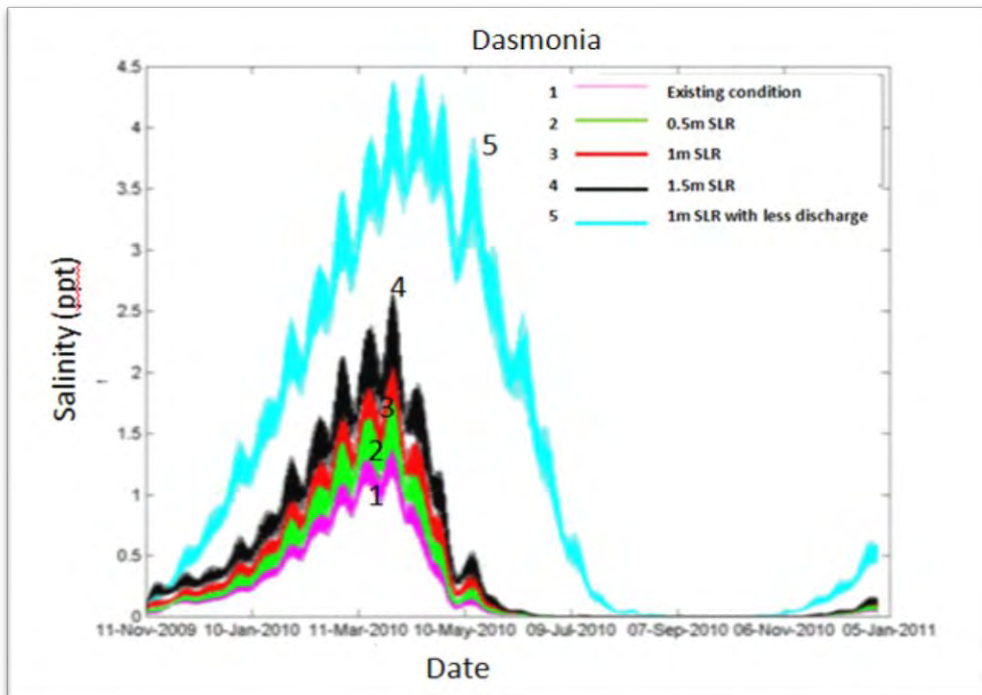


Figure 4.19: Predicted salinity at Dasmonia station for different SLR scenarios

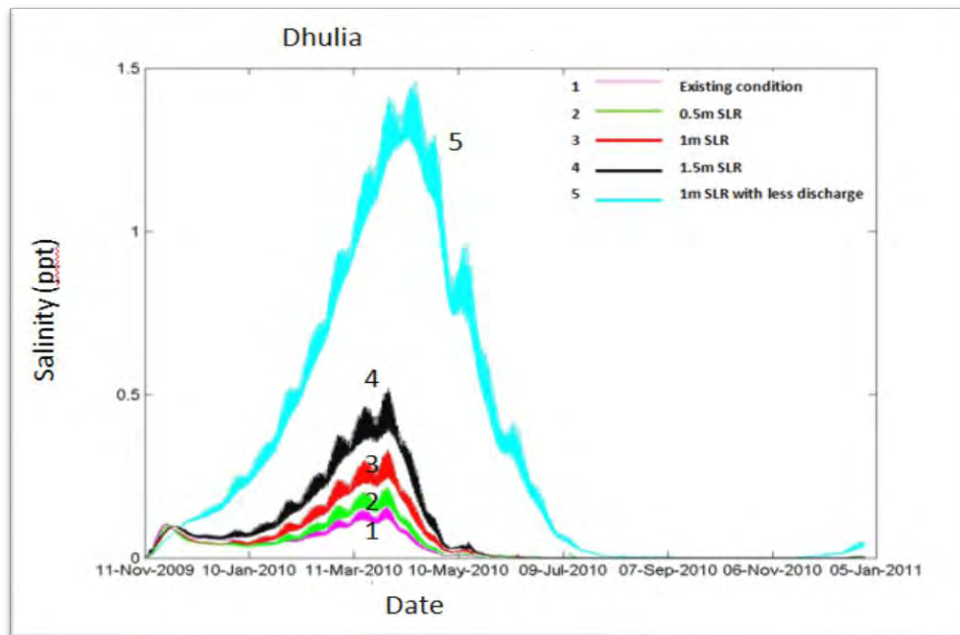


Figure 4.20: Predicted salinity at Dhulia station for different SLR scenarios

It is important to note that Tajimuddin is located in Meghna River, while Dasmonia and Dhulia are located in the Tentulia River. Similar trend has been observed for Char Fession and Daulatkhan, which are located in Meghna River. Thus, for all five location/stations located in Meghna and Tentulia rivers, a similar pattern of salinity is observed in response to sea level rise and reduction in upstream discharge. However, as discussed below, a somewhat different trend has been observed for locations/station located in other smaller rivers.

Figure 4.21, Fig. 4.22 and Fig. 4.23 shows predicted salinity for Patuakhali, Betagi and Chalna, respectively. The predicted salinity trends for these stations (in response to SLR) are different than those found for the five stations/locations discussed above. For these three locations, salinity in fact decreased in response to SLR. For example, at Patuakhali, the peak salinity under existing has been predicted to be 1.9 ppt; the predicted salinity decreased to 1.75 ppt, 1.25 ppt, and 1 ppt, as sea level increased by 0.5 m, 1.0 m and 1.5 m, respectively. However, when upstream flow of Brahmaputra was reduced by 20%, the predicted salinity increased significantly. For example, peak salinity at Patuakhali is predicted to reach 1.25 ppt for a sea level rise of 1.0 m (from a baseline/existing value of 1.9 ppt). If upstream flow is decreased by 20%, then the predicted peak salinity increases significantly to 3.25 ppt. This once again shows the very strong effect of upstream flow on salinity.

A similar trend is also observed for Betagi and Chalna. For Chalna, the peak salinity appear to shift to earlier part of the year as sea level increases. For example, under exiting condition, peak salinity is predicted at Chalna is predicted in April/May; while for the sea level rise of 1.5 m, peak salinity is predicted to reach in March. The peak salinity for existing condition is 4.2 ppt at Betagi and 14.2 ppt at Chalna. For 1m sea level rise peak salinity drop to 2.8 at Betagi and 12.8 ppt at Chalna.

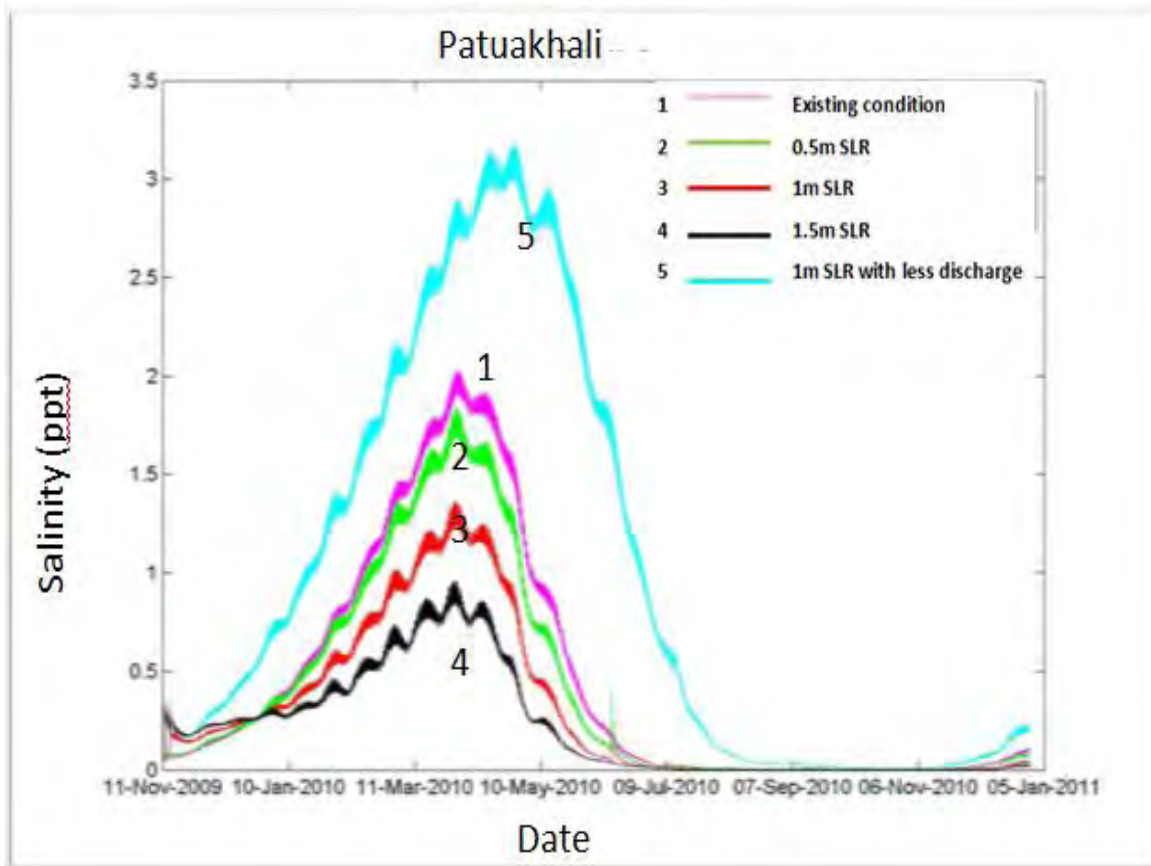


Figure 4.21: Predicted salinity at Patuakhali station for different SLR scenarios

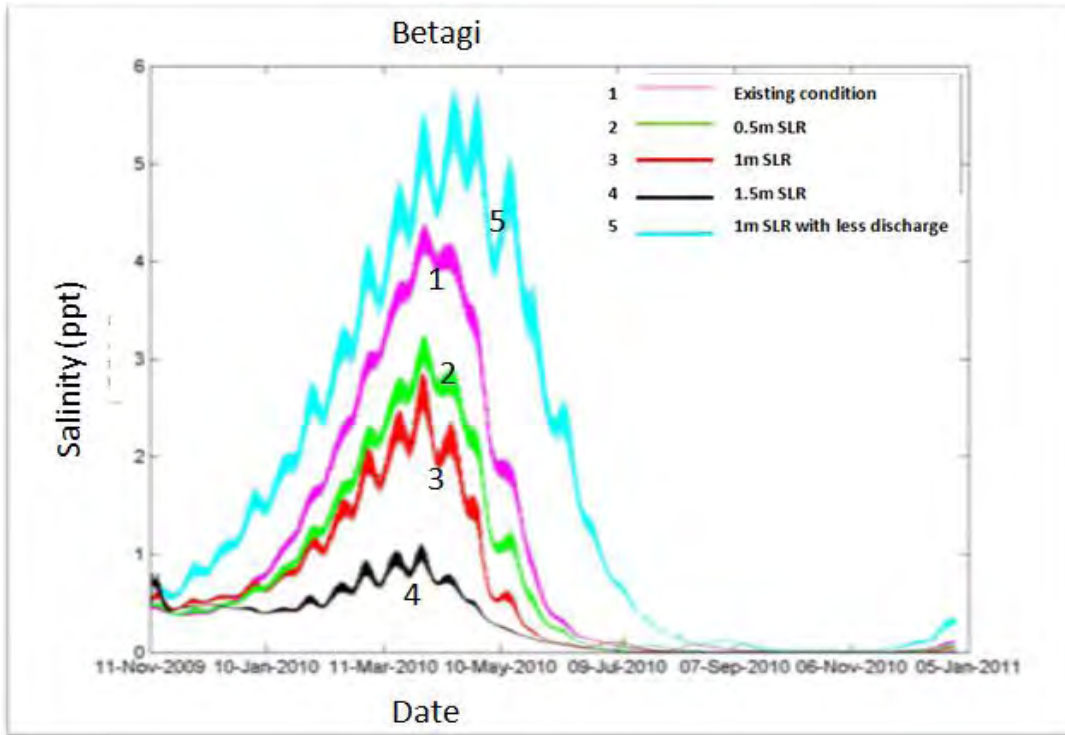


Figure 4.22: Predicted salinity at Betagi station for different SLR scenarios

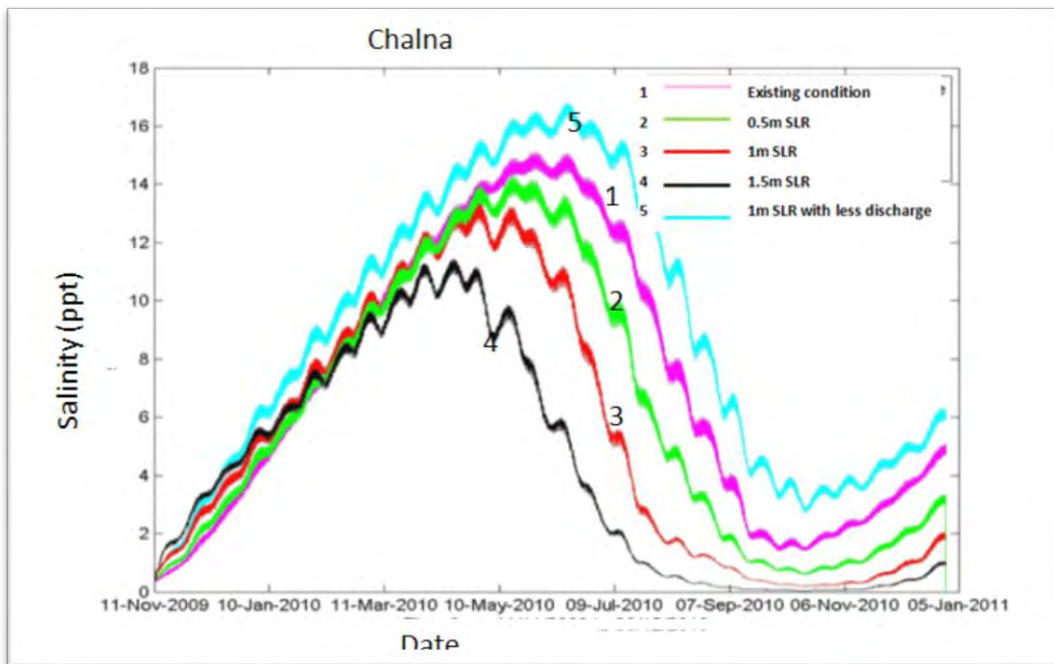


Figure 4.23: Predicted salinity at Chalna station for different SLR scenarios

It should be noted that Patuakhali is located in the Galachipa River, which is a distributory of the river Tentulia. Betagi is located in Bishkhali River, which is a distributory of Tentulia river; while Chalna is fed from Ganges through Gorai river.

A similar trend, that is decreasing salinity with increasing sea level rise, has all been predicted for all the remaining 6 stations/locations considered in this study. All these stations (including the three discussed above) are located to the west and away from the main Meghna River.

Figure 4.24, Fig. 4.25 and Fig. 4.26 shows predicted salinity for Mongla, Khulna and Bamna, respectively. It should be noted that Mongla and Khulna are fed by the Ganges through Gorai river. For Mongla and Khulna, the peak salinity is reached earlier in the year as sea level increases (similar to the trend observed for Chalna). The peak salinity predicted at Mongla and Khulna for existing condition are 14.2 and 9.6 ppt respectively. After 1.5m sea level rise these values reduced to 13.5 ppt for Mongla and 6.2 ppt for Khulna. The Bamna station is located in the Bishkhali river. Bishkhali river is a distributory of Tentulia river. The peak salinity predicted at Bamna for existing condition is 5.7 ppt . After 1.5m sea level rise this value reduced to 2 ppt.

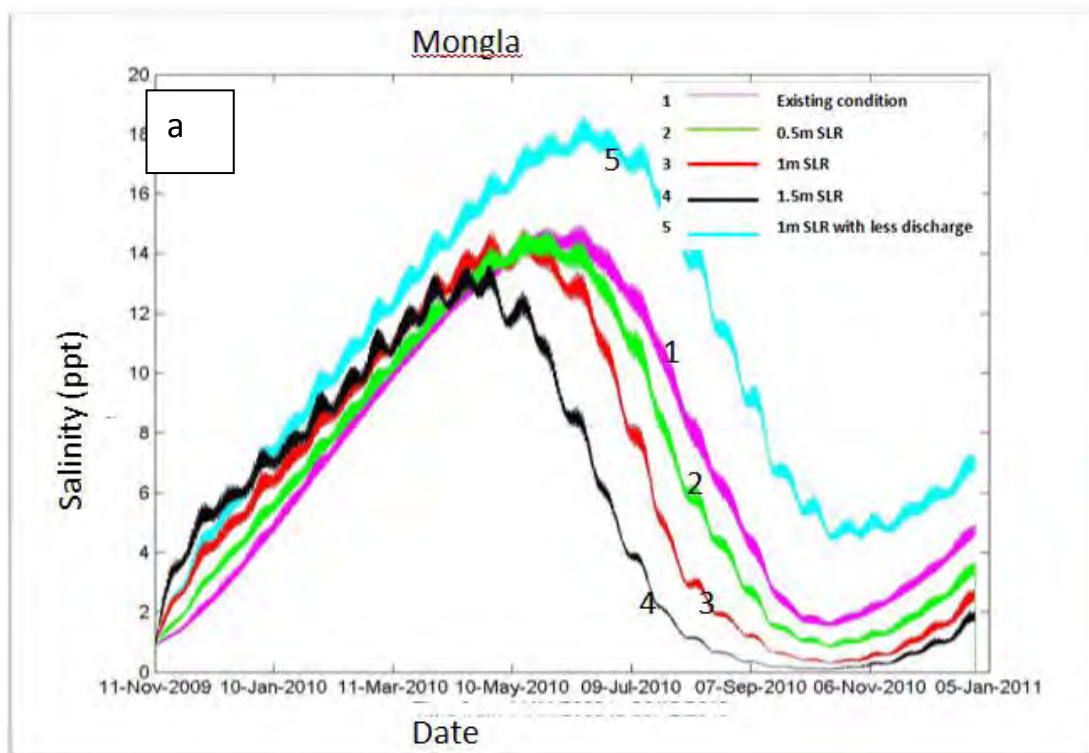


Figure 4.24: Predicted salinity at Mongla station for different SLR scenarios

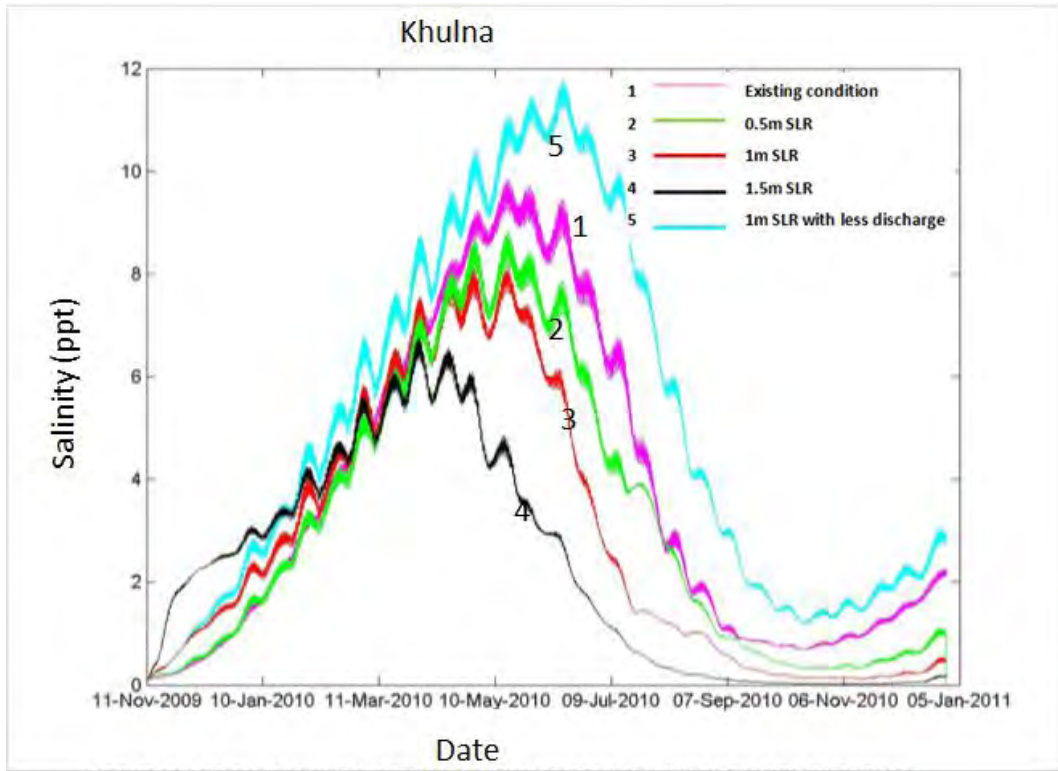


Figure 4.25: Predicted salinity at Khulna station for different SLR scenarios

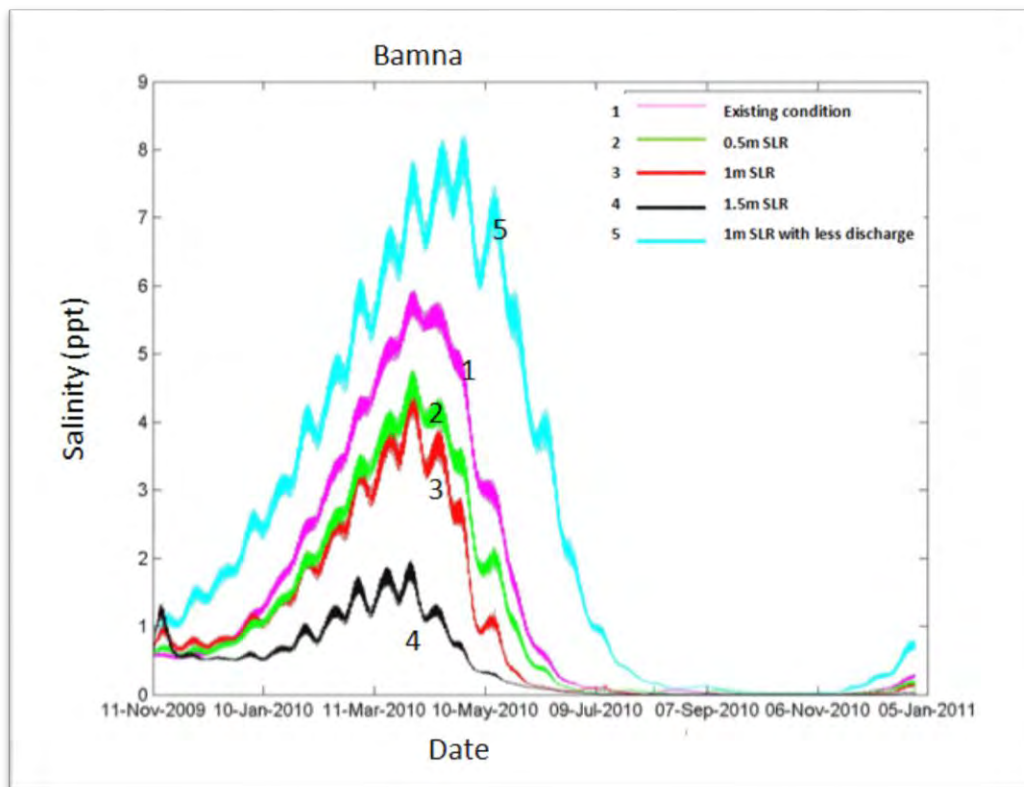


Figure 4.26: Predicted salinity at Bamna station for different SLR scenarios

Figure 4.27, Fig 4.28 and Fig. 4.29 show predicted salinity for Jhalokati, Patharghata and Hiron Point, respectively. It should be noted that Jhalokathi fed from Tentulia by Bishkhali

river. Hironpoint is located at the estuary of Pussur river, which is mainly fed by Ganges through Gorai river; Patharghata is located in Balaswar river, which is fed from Tentulia river. As all other stations in distributory of Meghna or Tentulia Jhalokathi and Patharghata show a similar trend of salinity with sea level rise, salinity decreases with SLR. At existing condition salinity at Jhalokathi and Patharghata are 2.25 and 13.5 ppt, respectively. After 1.5m SLR salinity reduced to 0.5 ppt at Jhalokathi and 9.5 ppt at Patharghata. Hiron Point is an important station as it is located very close to Sundarbans. The Salinity predicted at this location also decreases with sea level rise. At existing condition salinity at this point is around 25 ppt but after 1.5m SLR salinity reduced to 22.5ppt.

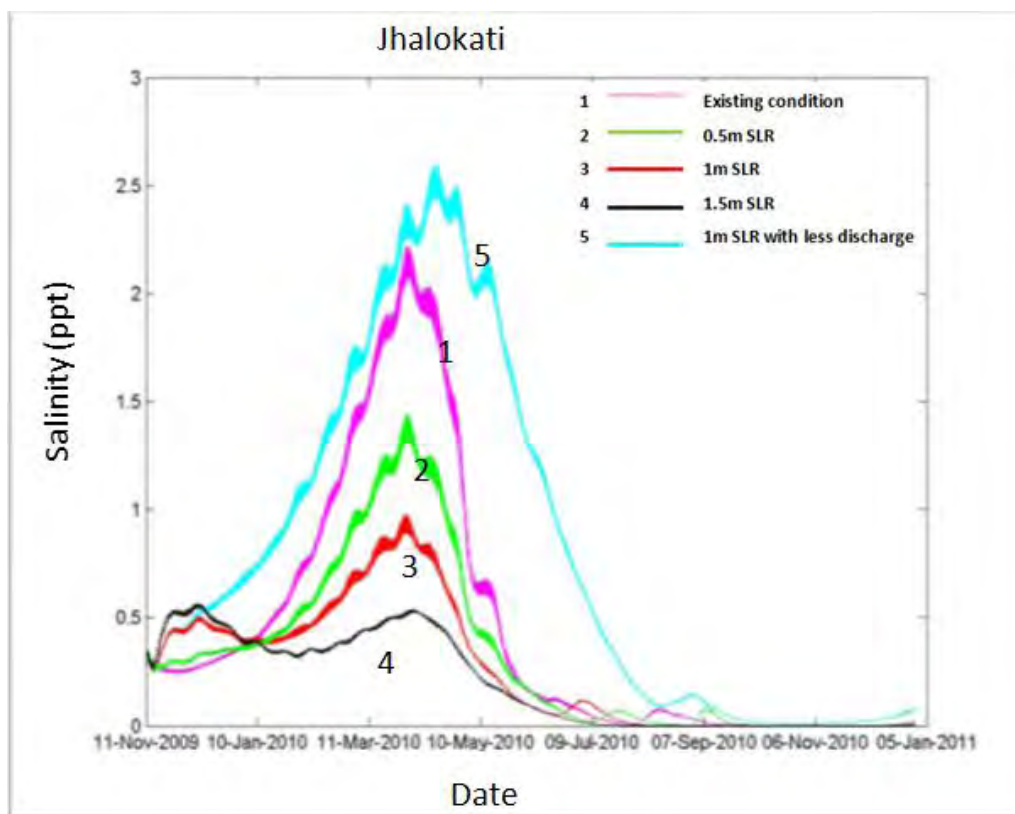


Figure 4.27: Predicted salinity at Jhalokhati station for different SLR scenarios

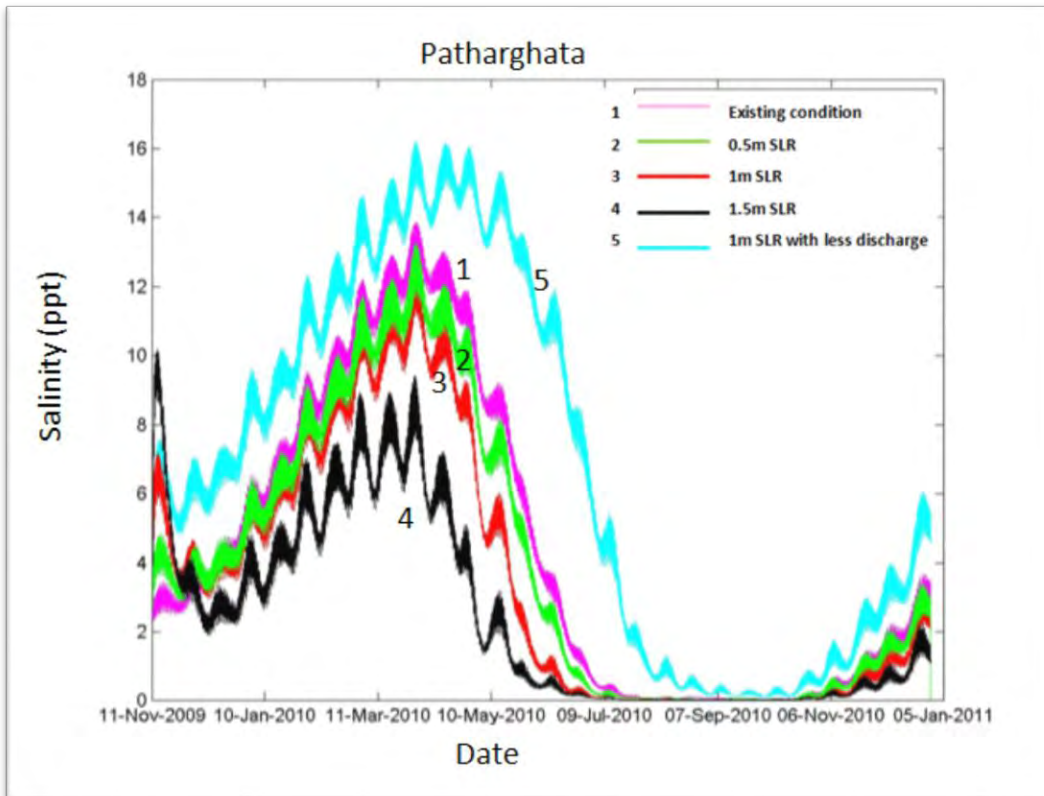


Figure 4.28: Predicted salinity at Patharghata station for different SLR scenarios

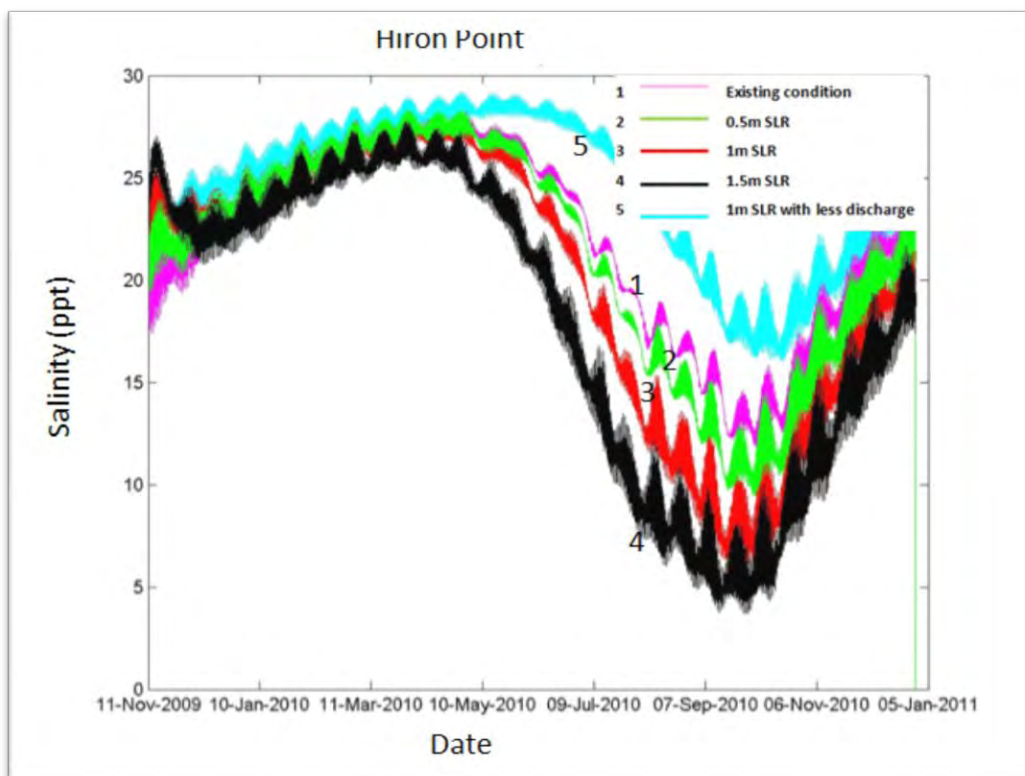


Figure 4.29: Predicted salinity at Hiron Point station for different SLR scenarios

From the analysis of predicted salinity patterns at 17 locations/stations, it has been found that salinity increases with increasing sea level rise for 5 stations (Char Fession, Daulakhan, Tajumuddin, Dasmunia, and Dhulia); these five stations are located on Meghna and Tetulia river. This increasing trend is expected. This increase in salinity will affect particularly the estuary area of Meghna. It includes all island covering Bhola, Hatia, Monpura, Sandwip, Char Kukri Mukri and all other small island in this area. The increase in river water salinity will subsequently cause increase in soil salinity over this area, destroying present characteristics of soil. The cohesiveness and fertility of soil will surely be reduced. This will affect crop production and construction of clay house. It may cause economic loss in terms of crop yield reduction, hampering industrial production, increasing health hazard and reducing productivity of the forest species. Agriculture production is likely to decrease as saline water reduces plant growth through concentrating salt in the root zone of plant and resulting in nutrients imbalance and yield loss. This will also have adverse effect on biodiversity and wild life of this area. Industrial production is reduced when saline water from river is used to cool condenser or to keep turbine running. Saline water causes leakages in equipment and makes production loss and also increases production cost by compelling the producer to import fresh water for avoiding the corrosion and leakage.

However, the predicted salinity patterns show reverse trend, that is decreasing salinity with increasing sea level rise, for the remaining 12 stations. These 12 stations are located in smaller rivers, which are fed from Ganges, Meghna or Tetulia Rivers. It should be noted that salinity has been predicted to increase in all 17 stations in response to decreased upstream flow. Figure 4.30 shows a map identifying stations with increasing and decreasing salinity in response to sea level rise.

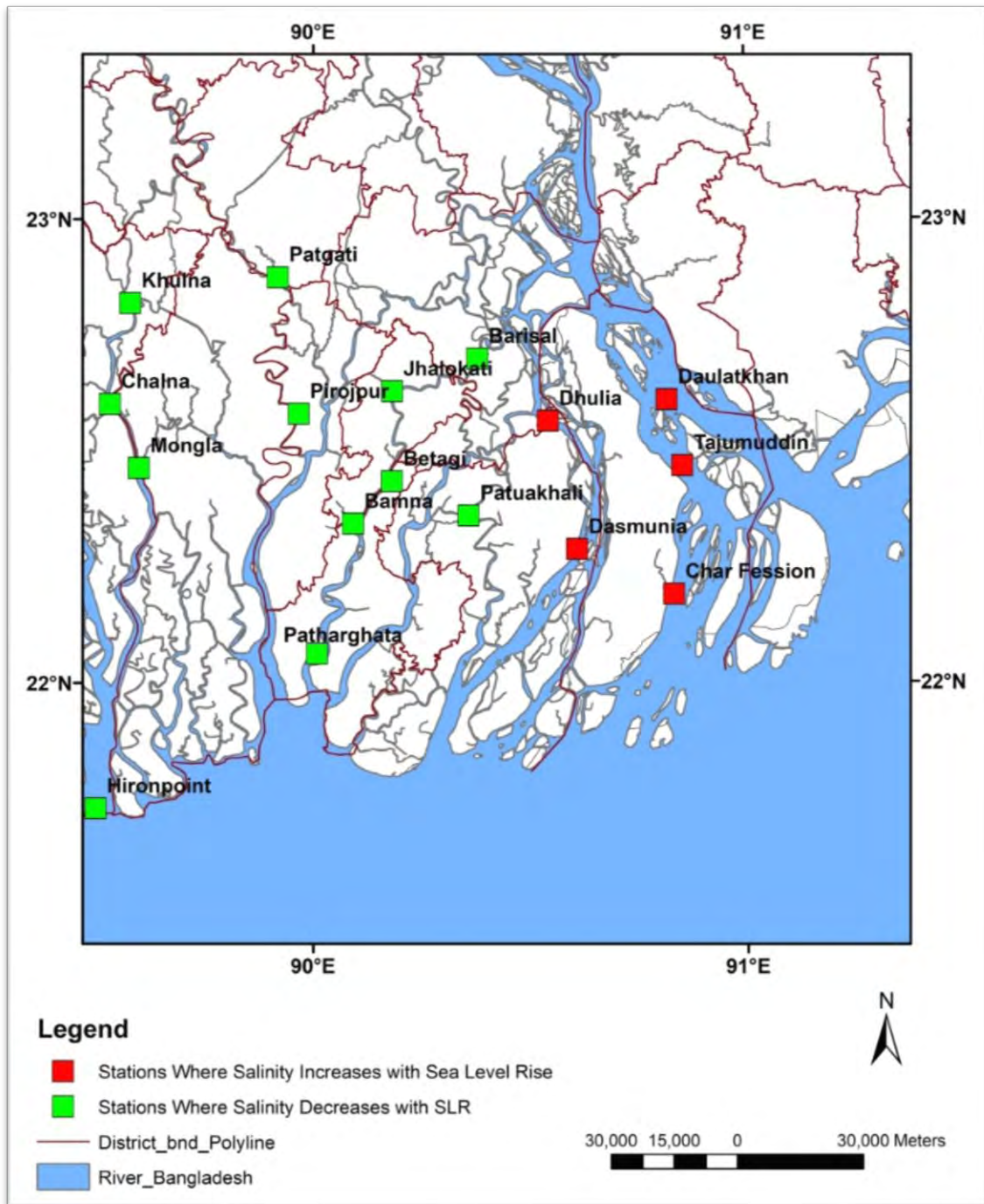


Figure 4.30: Map identifying station with increasing and decreasing salinity in response to sea level rise

This reverse trend (i.e., decreasing salinity with increasing sea level rise in some rivers) predicted by the model was not expected. In order to explain these results, first distribution of freshwater in the rivers were considered. It is possible with rise in sea level, the extra pressure of tide that would develop would hinder the flow of fresh water from upstream. Meghna and Tentulia are two major rivers through which nearly all of fresh water flow into the Bay of Bengal. Under extra pressure of tide from sea (due to sea level rise), the fresh water would

face difficulty to flow downstream through Meghna. So, it is likely that a part of the upstream flow would find their way into the distributories of Ganges, Padma, Meghna and Tentulia. So, fresh water availability in Meghna and Tentulia should decrease, while all other small distributories would get higher fresh water compared to existing condition. So, salinity in Meghna and Tentulia would increase with sea level rise due to lower fresh water flow, and salinity in smaller rivers would decrease due to relatively higher fresh water flow with increase in sea level rise.

To test this hypothesis the availability/flow of fresh water at different stations need to be estimated for different SLR scenarios. However, it is challenging to find out a way to separate fresh water flow from saline water flow for different scenarios at the various stations. The mean water level of a station appears to be a representative parameter for estimating differences in fresh water flow. In this work neither temperature nor arctic snow melting phenomena is included. So, the only reason for seasonal variability of water level at different stations is variation in upstream fresh water flow. So, if the monthly mean of water level for a particular station is calculated and plotted, the curve should represent the variability of fresh water flow. But, for a particular sea level rise, the water level would experience a vertical upward shift. As we are interested in comparing water level that represents only fresh waterflow, this vertical upward shift has been eliminated by subtracting the “minimum value of water level after SLR” from the “minimum value of water level at existing condition”. Then this difference of minimum value is deducted from the mean water level curve after SLR.

Figure 4.31 to 4.35 shows water level at five stations (Char Fession, Daulakhan, Tajumuddin, Dasmunia, and Dhulia) for which the model predicted increasing salinity with increasing sea level rise; these five stations are located in Meghna and Tetulia Rivers. For these five stations, the model predicts decreasing water level (monthly mean) with increasing sea level rise. In other words, it indicates lower freshwater flow with increasing sea level rise. These figures also show that reduction in upstream flow has significant effect on water level.

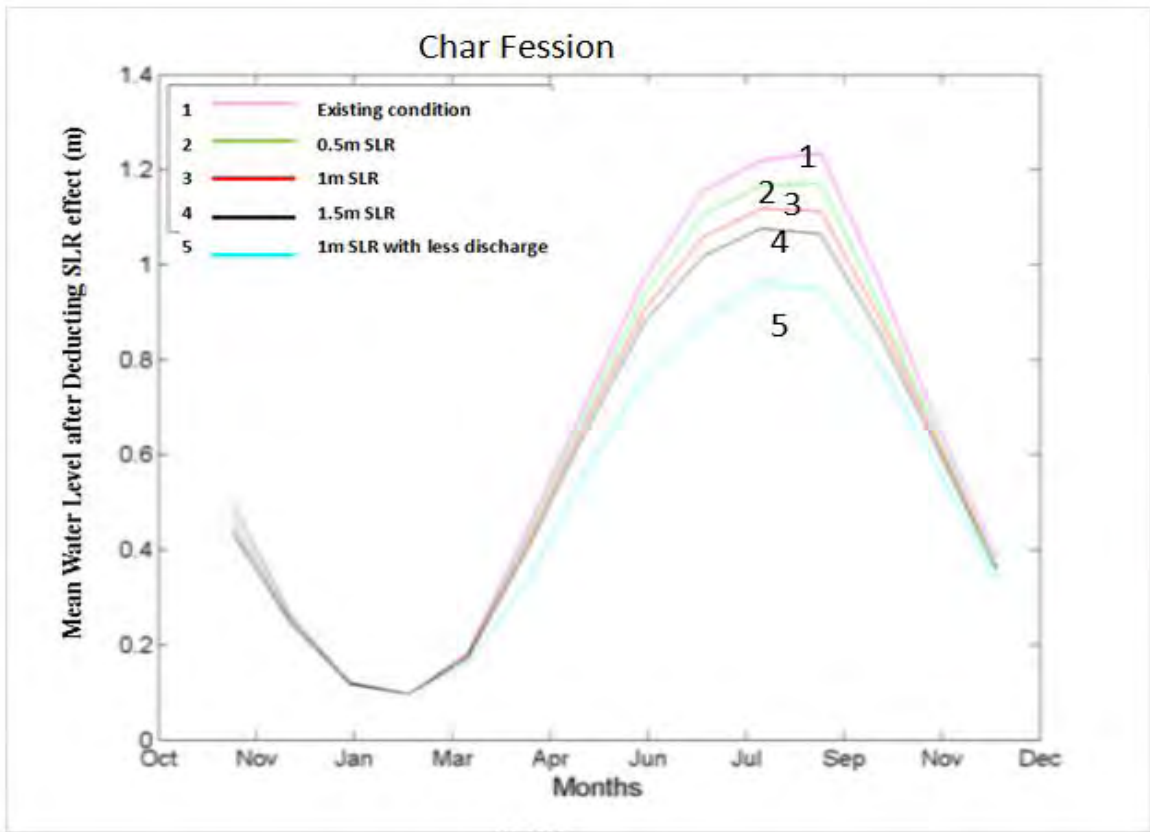


Figure 4.31: Mean water level at Char Fession for different SLR scenario.

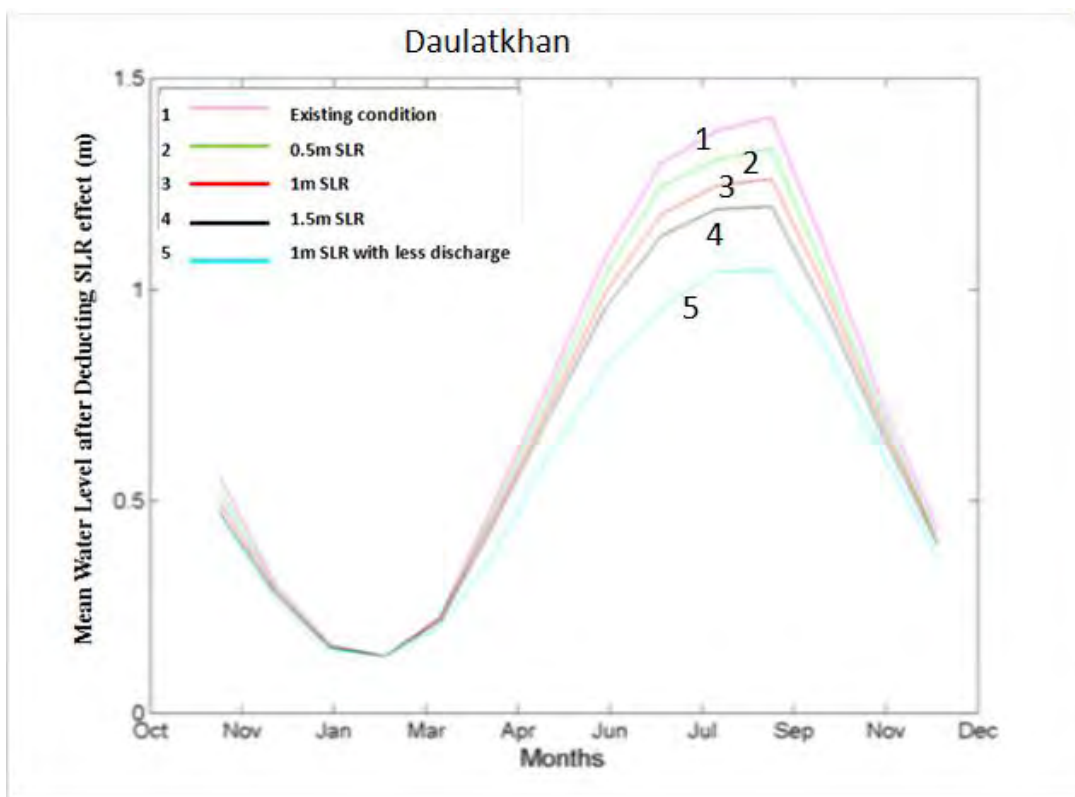


Figure 4.32: Mean water level at Daulatkhan for different SLR scenario.

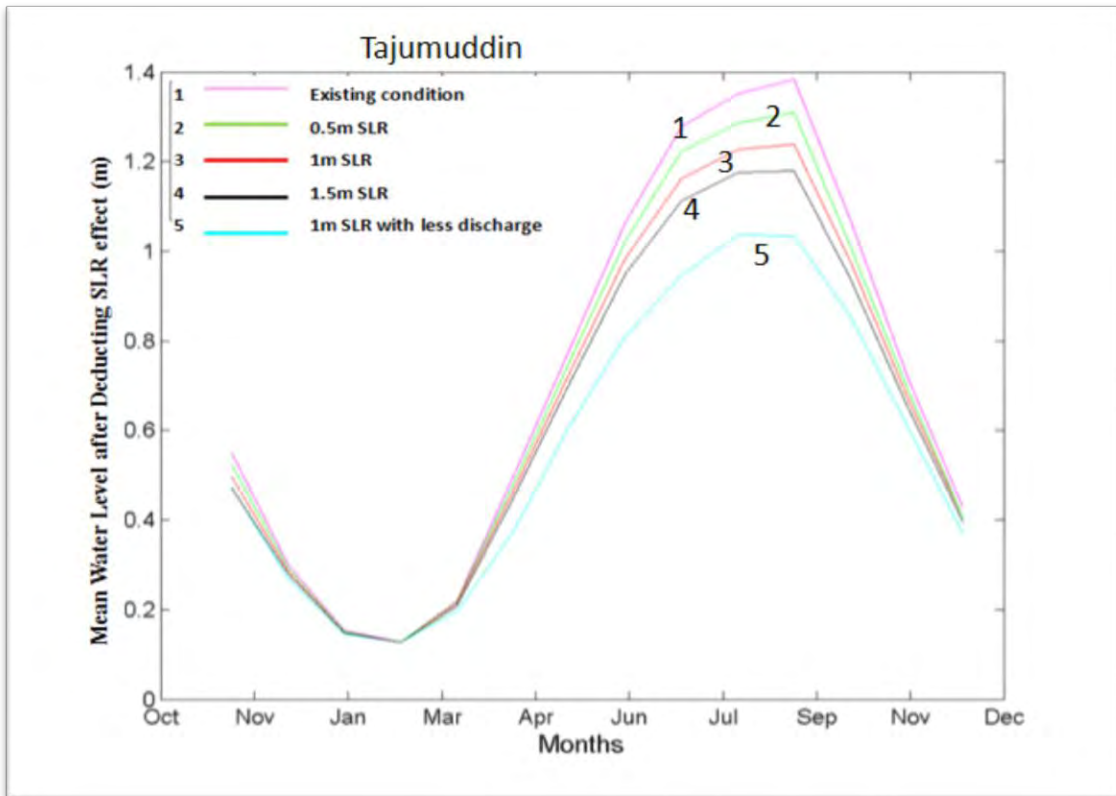


Figure 4.33: Mean water level at Tajumuddin for different SLR scenario.

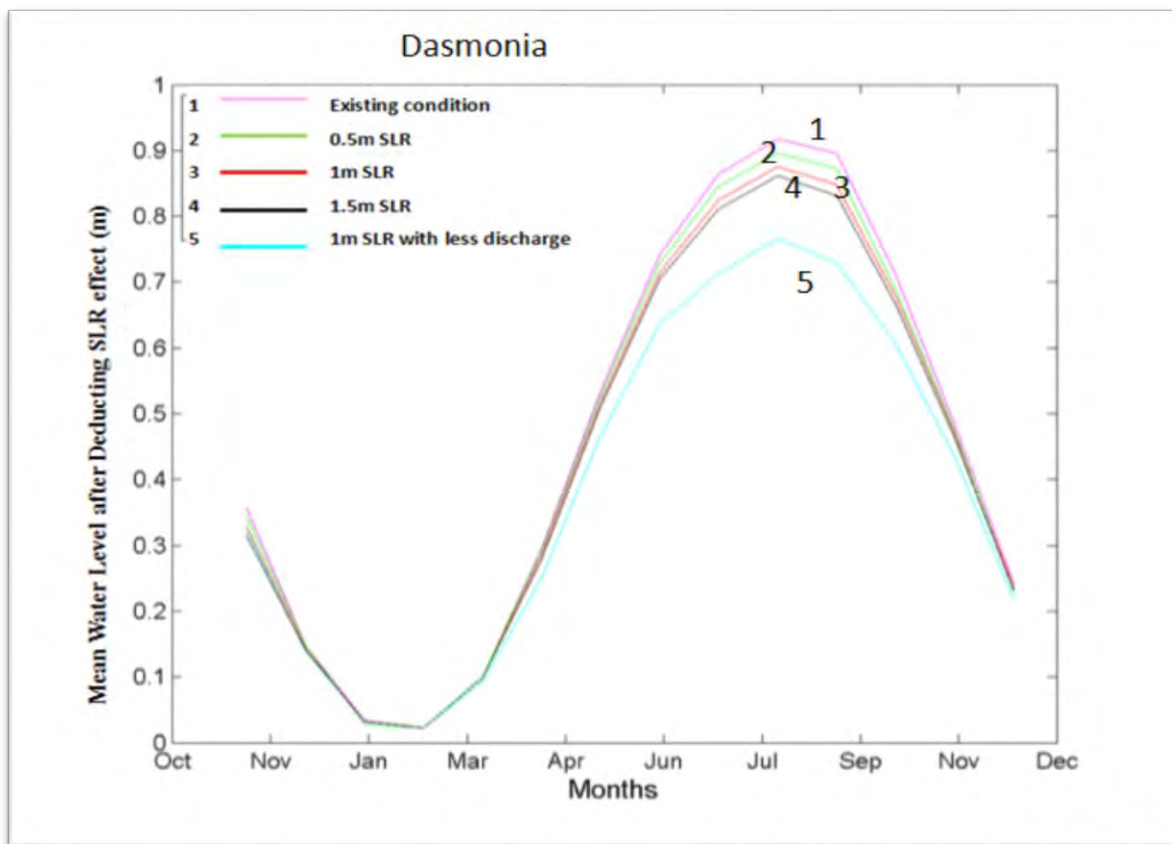


Figure 4.34: Mean water level at Dasmunia for different SLR scenario.

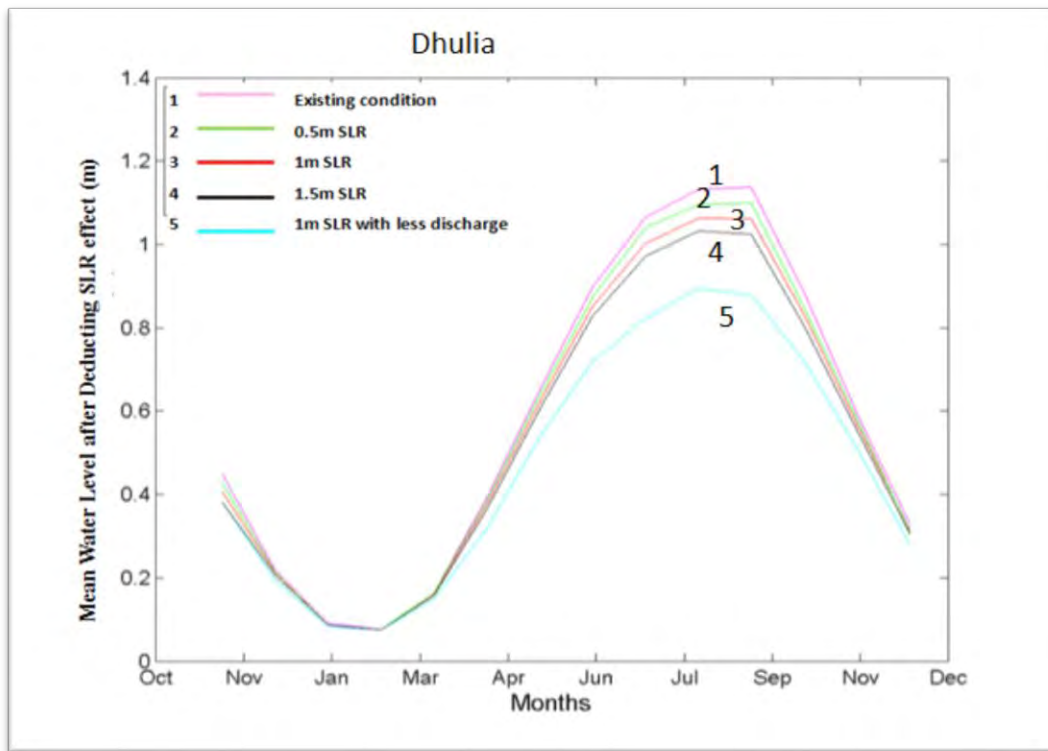


Figure 4.35: Mean water level at Dhulia for different SLR scenario.

Figure 4.36 to Fig. 4.42 show water level at seven stations (Patuakhali, Chalna, Mongla, Bamna, Hiron Point, Patgati, and Pirojpur) for which the model predicted increasing salinity with increasing sea level rise. These stations show increasing water level with increasing sea level rise. Only when the upstream flow is decreased, the water level decreases. This means that as sea level rises, freshwater flow at these stations increases; this in turn results in decreased salinity as sea level rises. This decreasing pattern of salinity in distributory rivers of Ganges, Meghna and Tentulia has profound implication regarding salinity intrusion in south west coastal region of Bangladesh. It implies that the increase in salinity in this region over past few decades has probably not been caused by sea level rise. Reduction of upstream flow is primarily responsible for this increased salinity in this area.

Thus, these model simulations appear to support the hypothesis about the distribution of fresh water flow in the coastal rivers in response to sea level rise (SLR), which in turn determines salinity level in response to sea level rise..

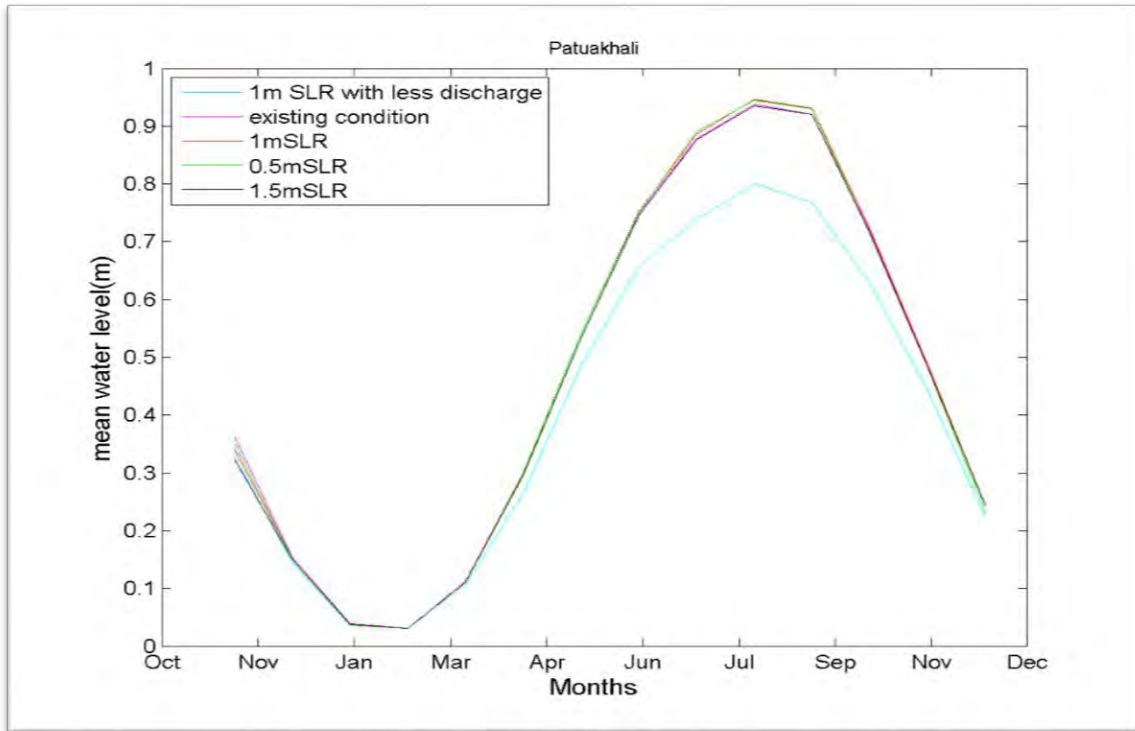


Figure 4.36: Mean water level at Patuakhali for different SLR scenario.

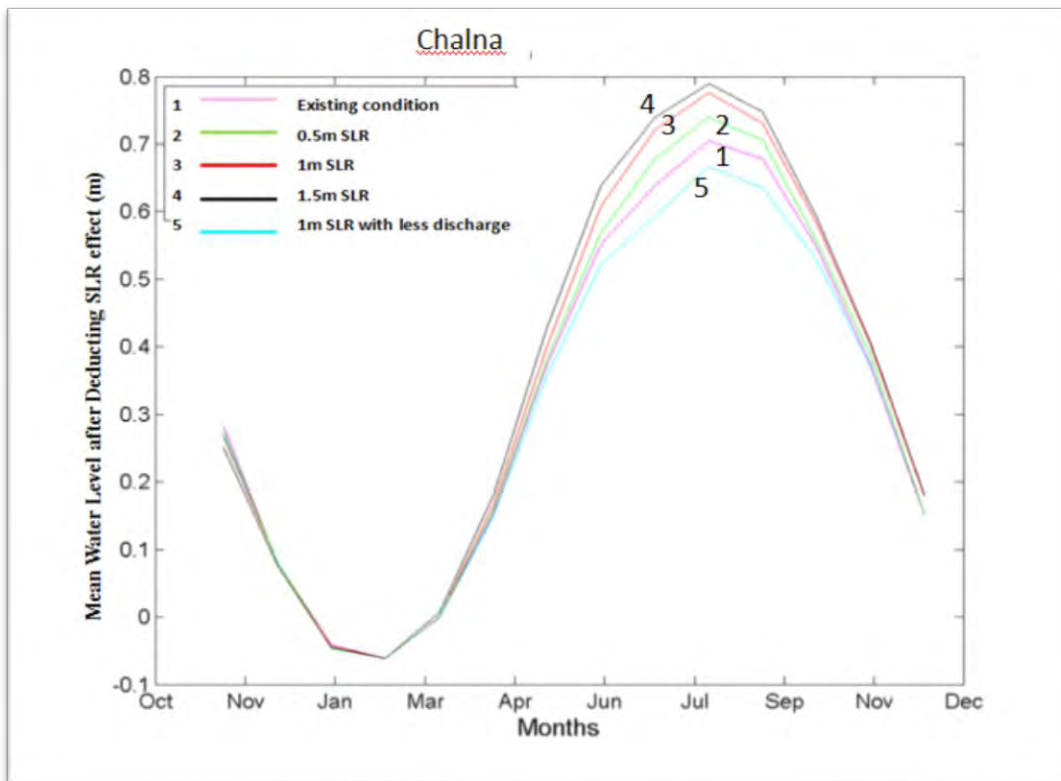


Figure 4.37: Mean water level at Chalna for different SLR scenario.

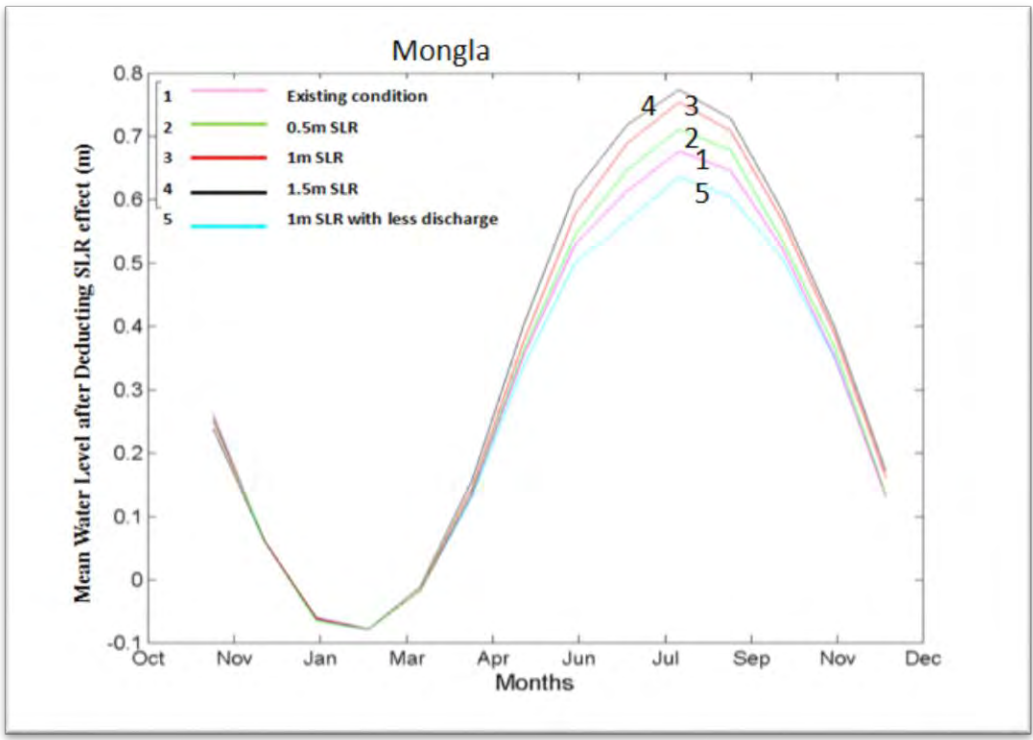


Figure 4.38: Mean water level at Mongla for different SLR scenario.

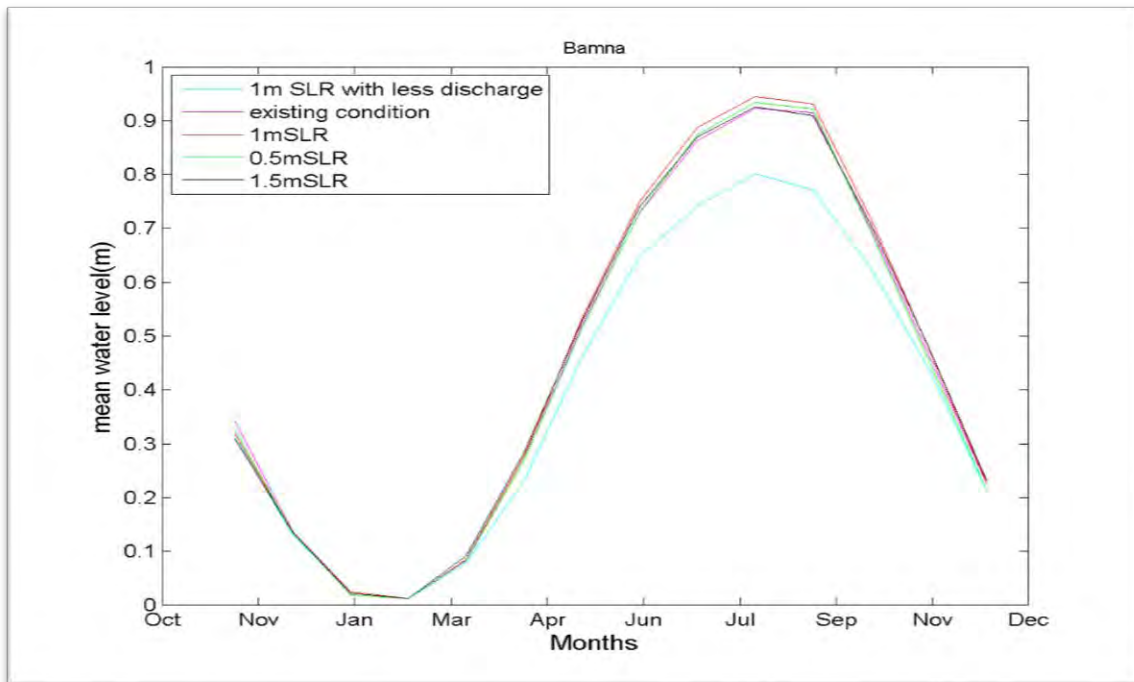


Figure 4.39: Mean water level at Bamna for different SLR scenario.

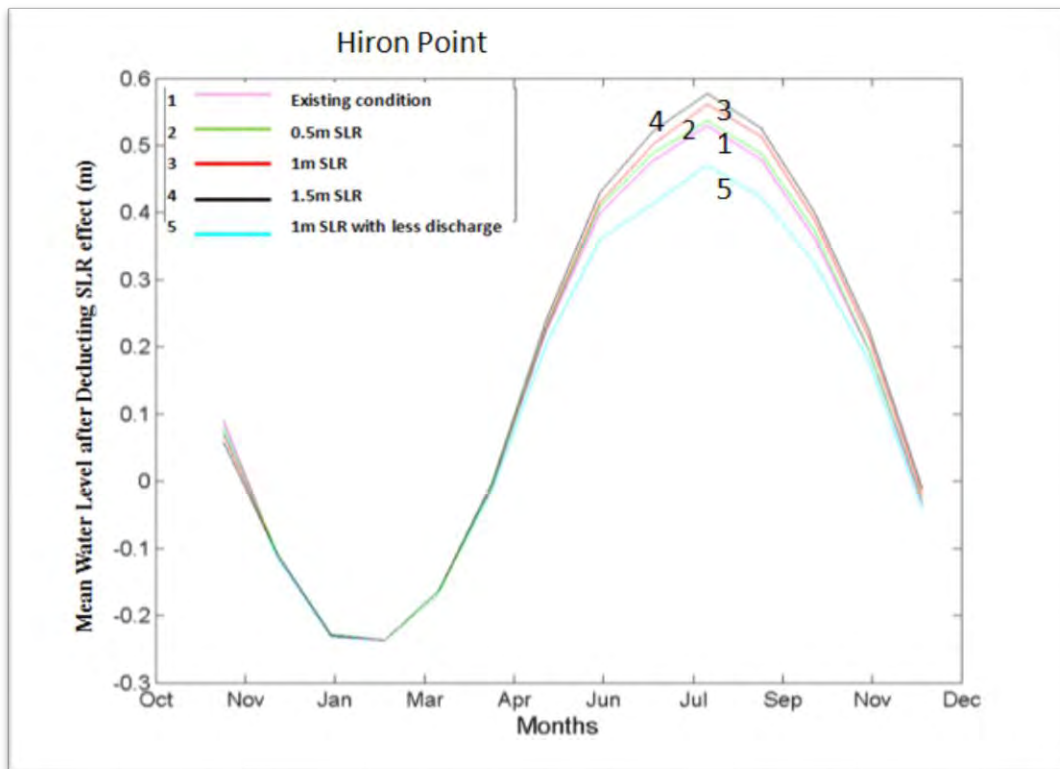


Figure 4.40: Mean water level at Hiron Point for different SLR scenario.

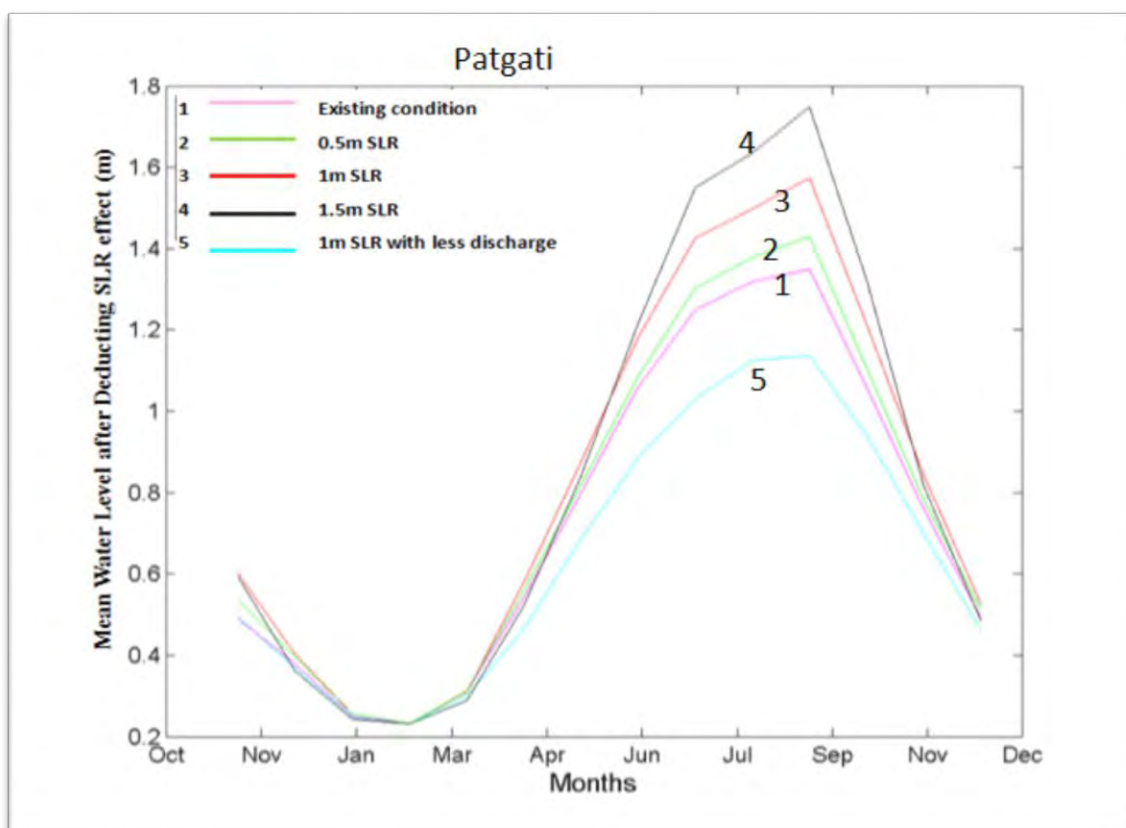


Figure 4.41: Mean water level at Patgati for different SLR scenario.

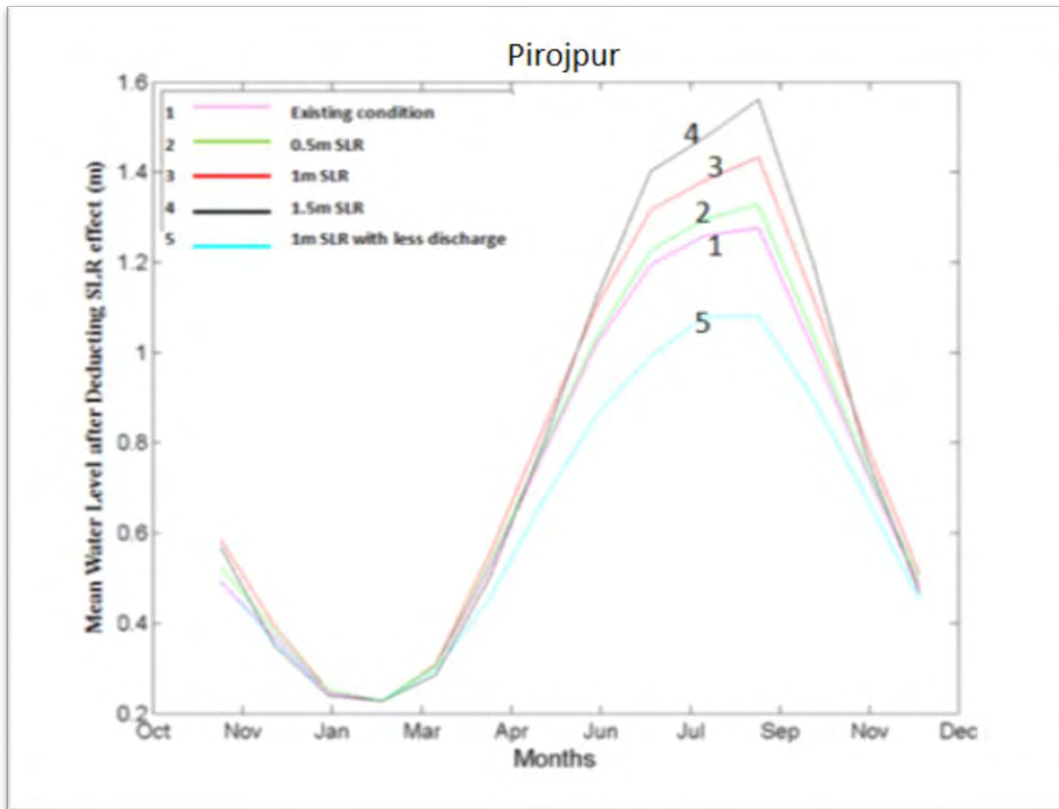


Figure 4.42: Mean water level at Pirojpur for different SLR scenario.

Figure 4.43 to 6.20 presents spatial pattern of salinity in the coastal areas of Bangladesh for different scenario. Figure 4.43 the salinity pattern based on the observed data of BWDB. The salinity observed data used in this map is for the year 2010; the maximum value of salinity of year 2010 has been sorted out for fourteen stations for preparing this map. This figure shows an overall higher salinity in the south-west region of Bangladesh, and decreases gradually as one moves toward north or east. The map does not cover Chittagong region due to unavailability of salinity data for the Chittagong region.

Figure 4.44 is a salinity map of the coastal region of Bangladesh, prepared based on model output for the year 2010. This map shows a pattern that is more or less similar to the pattern shown in Fig. 4.43. Figures 4.45, 4.46 and 4.47 predicted salinity pattern for the 0.5 m, 1.0 m and 1.5 m sea level rise, respectively.

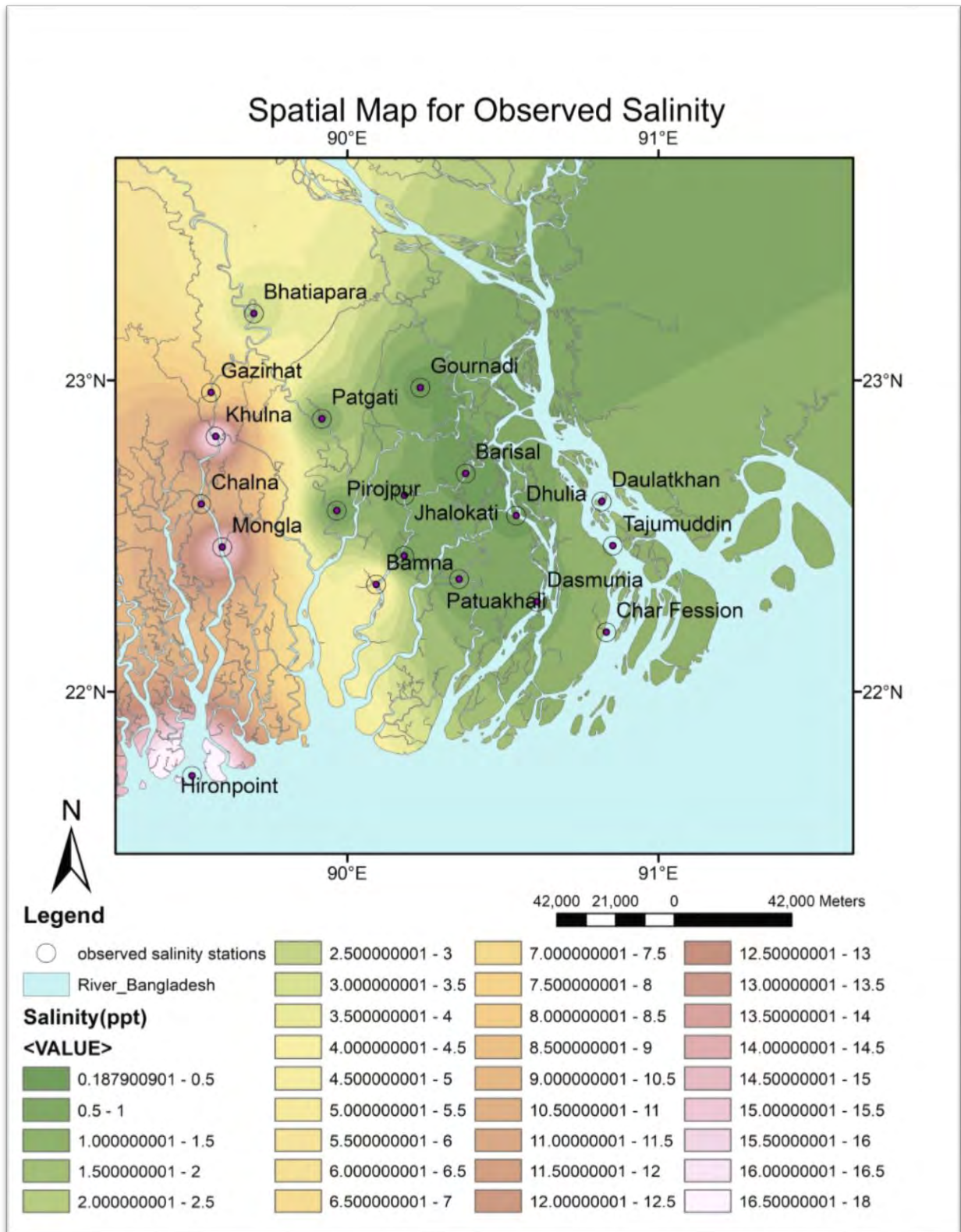


Figure 4.43: Map showing spatial pattern of salinity distribution over Bangladesh coastal zone prepared from observed data

Spatial Map for Salinity of Model Output at Existing Condition

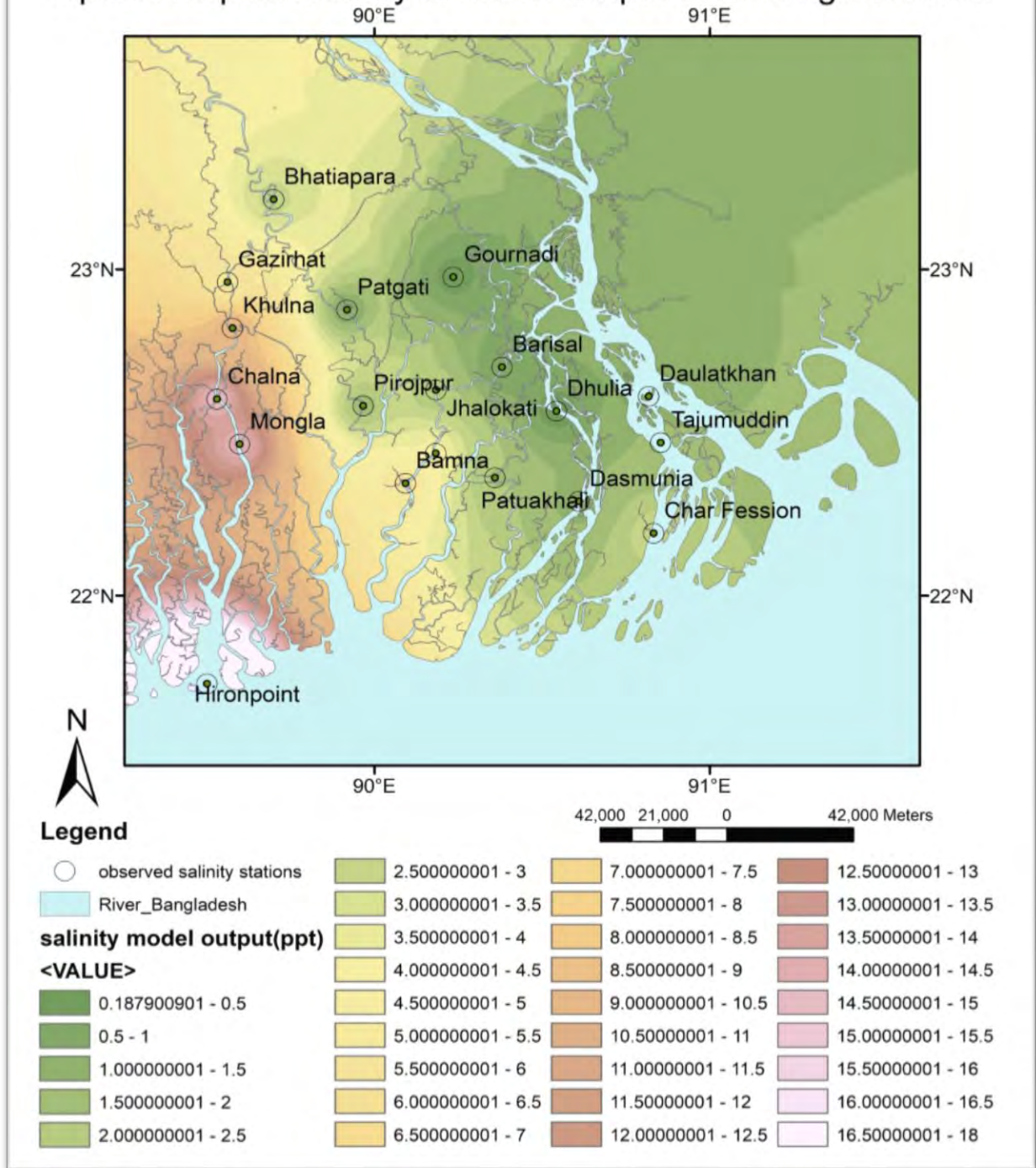


Figure 4.44: Map showing spatial pattern of salinity distribution over Bangladesh coastal zone prepared from model output under existing (2010) condition

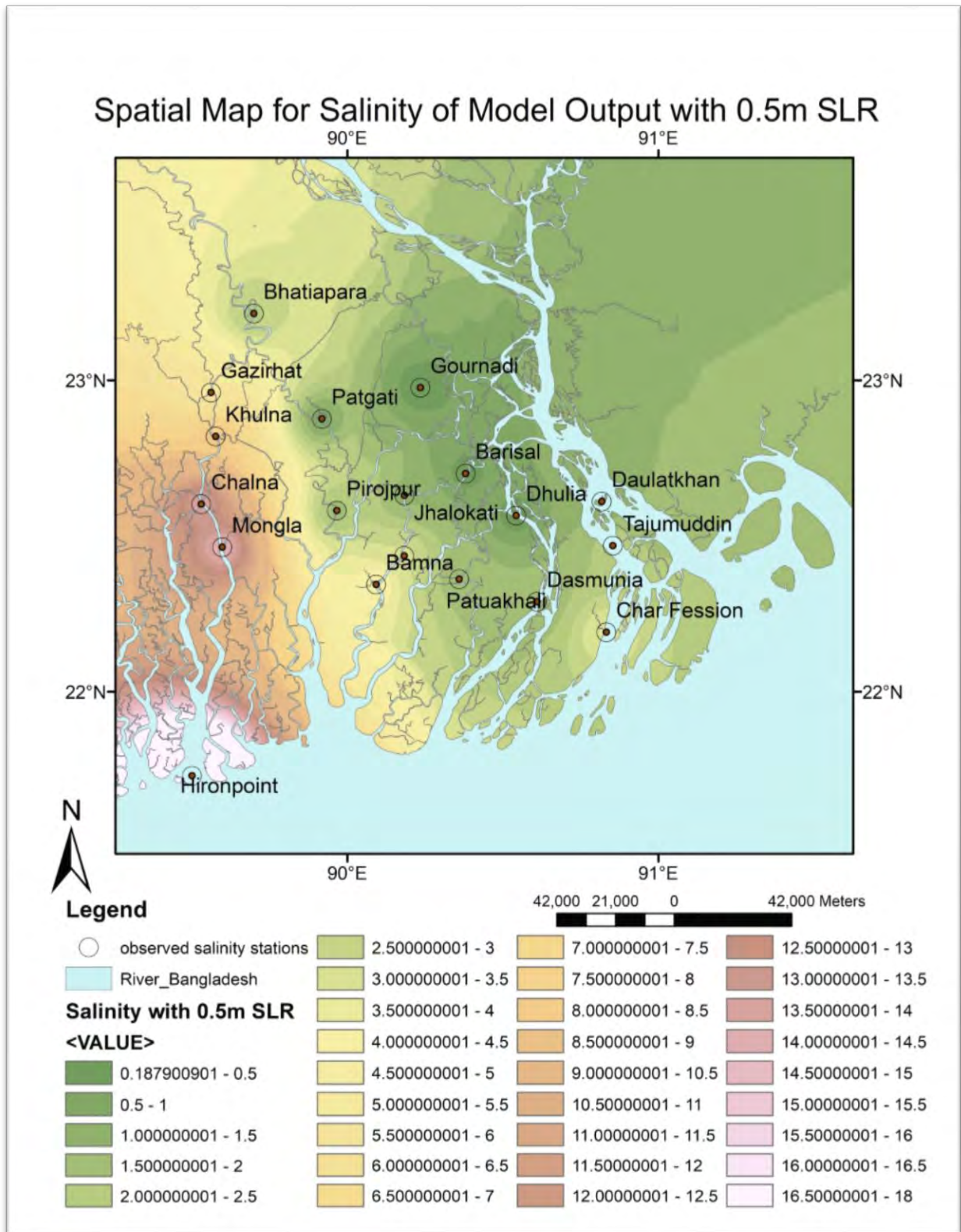


Figure 4.45: Map showing spatial pattern of salinity distribution over Bangladesh coastal zone prepared from model simulation with 0.5m SLR

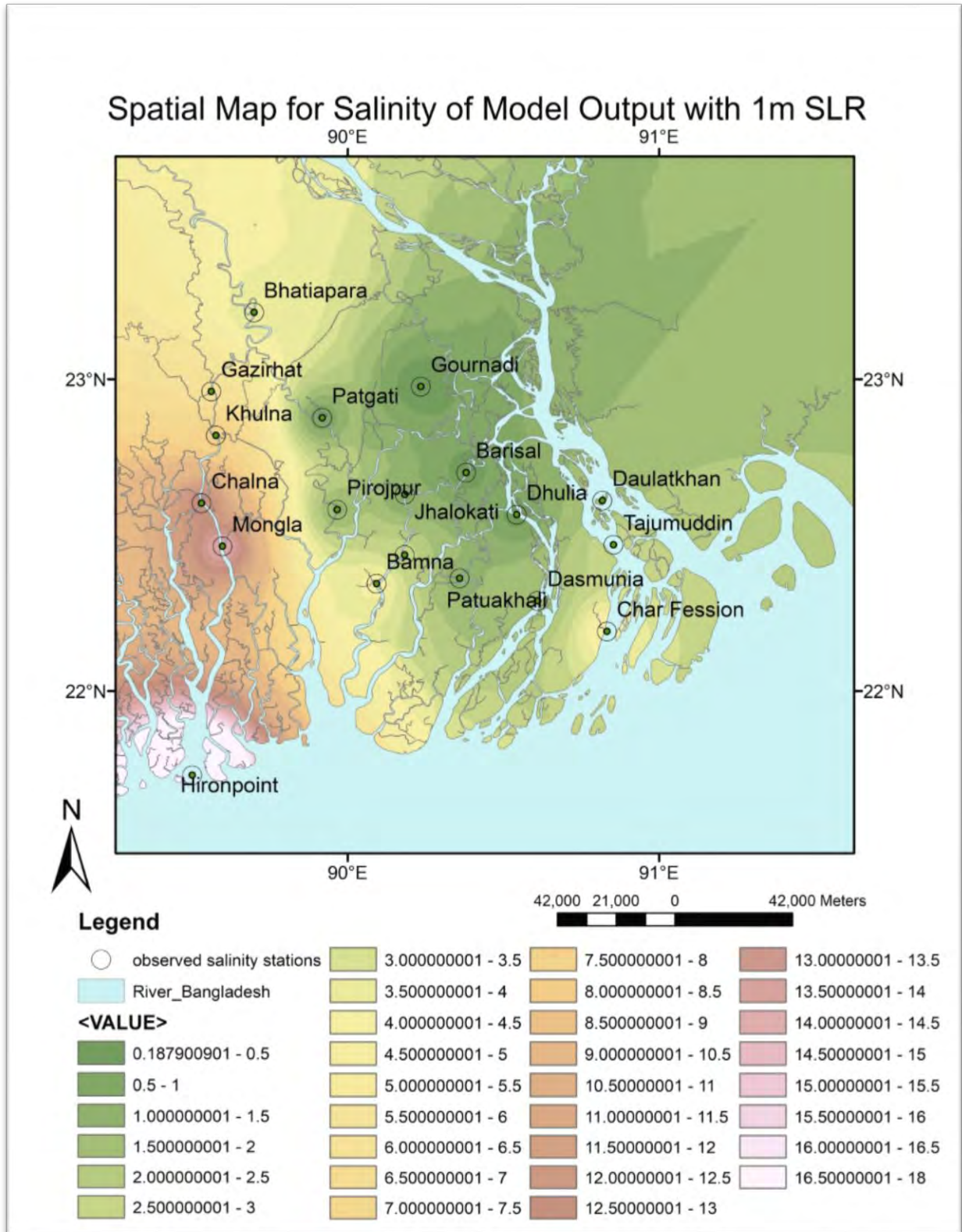


Figure 4.46: Map showing spatial pattern of salinity distribution over Bangladesh coastal zone prepared from model simulation with 1.05m SLR

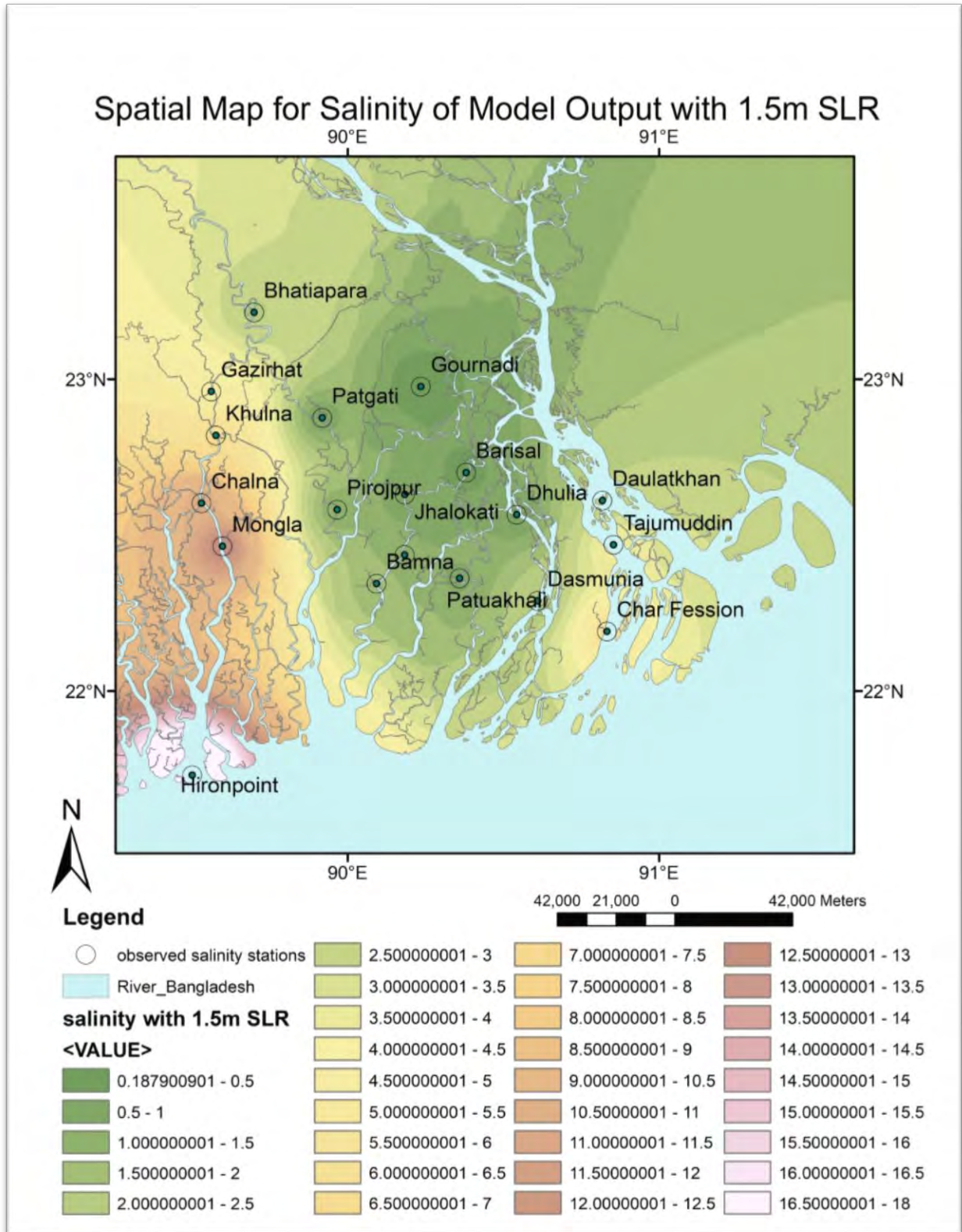


Figure 4.47: Map showing spatial pattern of salinity distribution over Bangladesh coastal zone prepared from model simulation with 1.5m SLR

Spatial Map of Salinity Pattern for 1m SLR along with 20 percent Decreased Brahmaputra Discharge

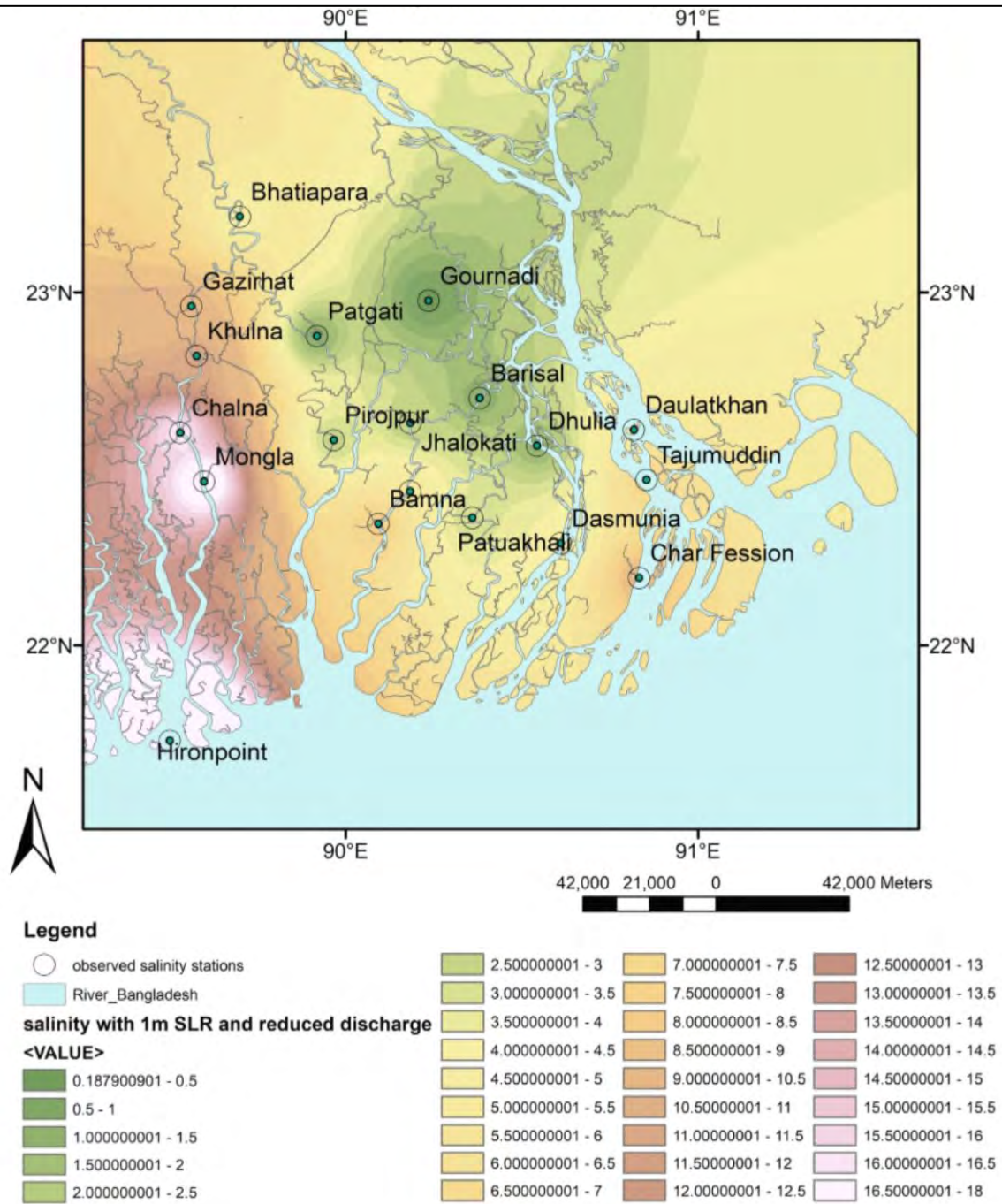


Figure 4.48: Map showing spatial pattern of salinity distribution over coastal zone prepared from model simulation with 1.5m SLR and 20% reduction in upstream flow

CHAPTER 5

CONCLUSIONS AND RECOMMENDATIONS

5.1 Conclusions

The main objective of this research was to assess effect of sea level rise on salinity intrusion in the coastal areas of Bangladesh. This research work involved setting up and validation of Delft3D model for the coastal part of GBM delta; the hydrodynamic module Delft3D-FLOW was used in this study. In this research, evaluation of salinity pattern of Bangladesh coastal zone was assessed for 0.5m, 1m and 1.5m sea level rise (SLR) along with one additional scenario in which 20 percent decrease in Brahmaputra discharge is considered with 1m SLR. The important conclusions from this research are as follows:

- (1) The Delft3D model is able to capture the tidal phenomenon of the complex coastal Bengal Delta with a moderate level of success. Bathymetric data appears to have a significant influence on model performance. Use of improved bathymetric data (in place of previous version of the bathymetry based on the Global GEBCO data sets) improved model output appreciably. The model performance appears to be better than some of the global models (e.g., FES2012, FES2014).
- (2) Comparison of predicted salinity and water level with available data at fourteen stations suggests that the model performance for salinity is comparatively poor than it is for water level. However, salinity data for some of the stations appear to be erratic (with virtually no seasonal variation), and difficult to explain.
- (3) The bathymetry data used in the model has limitations, which appears to be a main reason for poor performance of the model in predicting salinity. It should be kept in mind that the bathymetry of coastal rivers is immensely complex and dynamic, and it is nearly impossible to incorporate this bathymetry accurately.
- (4) Model predictions suggest that stations (or river reaches) located in the Meghna and the main Tentuli river system would experience increase in salinity in response to increase in sea level. But all other stations located in the small distributories of Ganges, Meghna and Tentulia would undergo a decrease in salinity in response to sea level rise.

- (5) It appears that under extra pressure of tide from sea (due to sea level rise), the fresh water would face difficulty to flow downstream through Meghna. So, it is likely that a part of the upstream flow would find their way into the distributories of Ganges, Padma, Meghna and Tentulia. Thus, fresh water availability in Meghna and Tentulia would decrease, while all other small distributories would get higher fresh water compared to existing condition. So, salinity in Meghna and Tentulia would increase with sea level rise due to lower fresh water flow, and salinity in smaller rivers would decrease due to relatively higher fresh water flow with increase in sea level rise.
- (6) This result was explained by model simulation by comparing seasonal variation of mean water level for different scenarios at different stations, with the understanding that the seasonal variation of water level is representative of fresh water availability at different times of a year. The model simulated mean water levels at different scenarios show that fresh water would decrease in estuary of Meghna and Tentulia and increase in all other small distributories with increase in sea level rise; this explains why salinity would increase in estuary of Meghna and Tentulia and decrease in other places. Finally, Spatial pattern of salinity has been prepared based on observed data and model output for different scenarios.

It is important to identify some of the limitations of this work, which include:

- A major limitation of hydrodynamic modeling, considering a huge complex area like Bangladesh coastal zone, is the inability to properly capture the topography. The better the topography data, the better the model output.
- There are many small channels and canals which could not be incorporated in the model input bathymetry.
- The processes considered in this study to calculate salinity is the interaction between fresh water from upstream and the saline water from southern boundary i.e., the Bay of Bengal and the molecular diffusion. But, there are some other factors which also affect salinity. For example, temperature, arctic ice melting, etc cause a seasonal variation in global sea salinity. In this research, these factors have not been considered and the salinity at southern boundary has been considered constant throughout the year.

5.2 Recommendations

This work can be extended by addressing the limitations described above. The following should be considered for future studies:

- 1) Efforts should be made to collect better/updated bathymetry. Bangladesh water development board (BWDB) and Bangladesh Inland Water Transport Authority (BIWTA) conduct bathymetric survey every year for their official purposes (mainly dredging) at many locations of different rivers. If these data could be collected from them and incorporated in the data used in this work, the bathymetry data can be updated for many rivers which will improve model output.
- 2) The number of channels included in the data set used in this bathymetry can be increased by digitizing Google Earth images.
- 3) The 3D version of the model could be run including temperature and other processes that can affect salinity over the whole year.
- 4) The model should run for several years instead of one year to get better results.

References

- Abdullah F. R., Danilo, D., and Bassil, E. (2011) "Response of the Sundarbans coastline to sea level rise and decreased sediment flow." A remote sensing assessment. *Remote Sensing of Environment*, 115(12):3121 – 3128, ISSN0034-4257.
- Allison, M.A.(1998) "Historical changes in the Ganges-Brahmaputra delta front". *Coastal Research*, pages 1269–1275.
- Auerbach, L.W., Goodbred, S.L., Mondal D. R., Wilson C.A, Ahmed K.R., Roy K. (2015) "Flood risk of natural and embanked landscapes on the Ganges-Brahmaputra tidal delta plain". *Nature Climate Change*.
- BBS, (2003) *Statistical Yearbook of Bangladesh*, Bangladesh Bureau of Statistics (BBS), Government of the People's Republic of Bangladesh, Dhaka.
- Birkemeier, W.A., and R.A. Dalrymple (1975) *Nearshore Water Circulation Induced by Wind and Waves*. *Proceedings of Modeling 75*, ASCE, San Francisco.
- Chen, Q., R.A. Dalrymple, J.T. Kirby, A. Kennedy, and M.C. Haller (1999) Boussinesq Modelling of a Rip Current System. *J. Geophys. Res.*, 104, C9, 20,617–20, 638.
- Church, J. A. and White, N. J. (2011) "Sea-level rise from the late 19th to the early 21st century." *Surveys in Geophysics* **32**(4-5): 585-602.
- Clarke, D., Williams, S., Jahiruddin, M., Parks, K., and Salehin, M.(2015) "Projections of on farm salinity in coastal bangladesh." *Environmental Science : Processes & Impacts*, 17(6), 1127-1136..
- CZPo (2005) *Coastal Zone Policy*, Ministry of Water Resources, Government of the People's Republic of Bangladesh, Dhaka.
- Ebersole, B.A., and R.A. Dalrymple (1980) *Numerical Modelling of Nearshore Circulation*. *Proc. 17th Intl. Conf. Coastal Eng.*, ASCE, Sydney.
- Edward B. B. (2012) "A spatial model of coastal ecosystem" *Ecological Economics*, 78:70–79.
- Ericson, J. P., C. J. Vörösmarty, S. L. Dingman, L. G. Ward and M. Meybeck (2006) "Effective sea-level rise and deltas: Causes of change and human dimension implications." *Global and Planetary Change* **50** (1): 63-82.
- Funakoshi Y., Jesse C., Frank A., Lozano C., Tolman H.(2010) "Coupling a Finite Element Storm Surge Model of the North Carolina Sounds with Operational Ocean and Weather Prediction Models", NOAA office of coast survey.
- Gopal, B. and Malavika, C. (2006) "Biodiversity and its conservation in the Sundarbans mangrove ecosystem", *Aquatic Sciences*, 68(3):338–354.
- Grinsted, A., J. C. Moore, and Jevrejeva S., (2010), "Reconstructing sea level from paleo and projected temperatures 2000 to 2100 AD", *Climate Dynamics.*, 34, 461–472, doi:10.1007/s00382-008-0507-2.

Han, W., Meehl, G. A., Rajagopalan, B., Hu A., Lin J., Large W. G., Wang J. and Trenary L. L. (2010). "Patterns of Indian ocean sea-level change in a warming climate", *Nature Geoscience* 3(8): 546-550.

Holthuijsen, L.H., Booij, N., and Ris, R.C. (1993) A Spectral Wave Model for the Coastal Zone, Proc. 2nd Intl. Symp. Ocean Wave Measurement and Analysis, ASCE, NewOrleans, 630–641.

IPCC (2013) *Climate Change 2013: The Physical Science Basis. Contribution of Working Group I to the Fifth Assessment Report of the Intergovernmental Panel on Climate Change* [Stocker, T.F., D. Qin, G.-K. Plattner, M. Tignor, S.K. Allen, J. Boschung, A. Nauels, Y. Xia, V. Bex and P.M. Midgley (eds.)]. Cambridge University Press, Cambridge, United Kingdom and New York, NY, USA, 1535 pp, doi:10.1017/CBO9781107415324.

Islam, M. R. (2004). “Where Land Meets the Sea: A Profile of the Coastal Zone of Bangladesh”, The University Press Ltd., Dhaka.

Islam, M.S., Haque, M., (2004). “The Mangrove-based Coastal and Nearshore Fisheries of Bangladesh”: Ecology, Exploitation and Management, *Reviews in Fish Biology and Fisheries* 14, pp. 153–180.

Jevrejeva, S., A. Grinsted, and J. C. Moore (2009), “Anthropogenic forcing dominates sea level rise since 1850”, *Geophys. Res. Lett.*, 36, L20706, doi:10.1029/2009GL040216.

Jevrejeva, S., Grinsted, A. and Moore, J.C., 2014. “Upper limit for sea level projections by 2100”. *Environmental Research Letters*, 9(10), p.104008.

Jevrejeva, S., Moore J. C., and Grinsted A. (2008), “Relative importance of mass and volume changes to global sea level rise”, *J. Geophysical Research Letter*, 113, D08105, doi:10.1029/2007JD009208

Kawahara, M., and K. Kashiyaama (1984). Selective Lumping Finite Element Model for Nearshore Currents. *Int. J. Numerical Methods Fluids*, 4, 71–97.

Levermann A., Winkelmann R., Nowicki S., Fastook J. L., Frieler K., Greve R., Hellmer H. H., Martin M. A., Meinshausen M., Mengel M., Payne A. J. (2014) “Projecting Antarctic ice discharge using response functions from SeaRISE ice-sheet models”. *Earth System Dynamics*, 5:271-93.

Lin J.L. (2007) The double-ITCZ problem in IPCC AR4 coupled GCMs: Ocean–atmosphere feedback analysis. *Journal of Climate*. Sep;20(18):4497-525.

Madsen, P.A., O.R. Sorensen, and H.A. Schaffer (1997a). Surf Zone Dynamics Simulated by a Boussinesq Type Model. Part I. Model Description and Cross-shore Motion of Regular Waves. *Coastal Eng.*, 32, 255–287.

Madsen, P.A., O.R. Sorensen, and H.A. Schaffer (1997b). Surf Zone Dynamics Simulated by a Boussinesq Type Model. Part II. Surf Beat and Swash Oscillations for Wave Groups and Irregular Waves. *Coastal Eng.*, 32, 287–319.

Moss, R.H. et al. (2010). “The next generation of scenarios for climate change research and assessment”, *Nature* 463: 747-756.

Moss, R.H., et al. (2008), "Towards New Scenarios for Analysis of Emissions, Climate Change, Impacts, and Response Strategies. Intergovernmental Panel on Climate Change", Geneva, 132 pp.

Nicholls R. J., Frank M.J., and Marcel, M. "Increasing flood risk and wetland losses due to global sea-level rise: regional and global analyses". *Global Environmental Change*, 9:S69–S87, 1999.

Putrevu, U., and I.A. Svendsen (1993). Shear Instability of Longshore Currents: A Numerical Study. *J. Geophys. Res.*, 97, C5, 7283–7303.

Rahmstorf, S. (2007) "A semi-empirical approach to projecting future sea-level rise", *Science*, 315, 368–370, doi:10.1126/science.1135456.

SMRC (2003) The vulnerability assessment of the SAARC coastal region due to sea level rise: Bangladesh case, SMRC publication No. 3, SAARC Meteorological Research Centre, Dhaka.

UNCLOS (1982) United Nations Convention on the Law of the Sea (UNCLOS), 10 December 1982, Montego Bay, Jamaica.

Unnikrishnan A. S. (2017) "Long term variability in the tide gauge records along the coasts of the north Indian Ocean climate." *Nature Geoscience*, 3(8): 546-550.

Van Dongeren, A.R., F.E. Sancho, I.A. Svendsen, and U. Putrevu (1994) SHORECIRC: A Quasi 3-D Nearshore Model. Proc. 24th Intl. Conf. Coastal Eng., ASCE, Kobe.

Vemulakonda, S.R., J.R. Houston, and H.L. Butler (1982) Modeling of Longshore Currents for Field Situations. Proc. 18th Intl. Conf. Coastal Eng., ASCE, Cape Town.

Vermeer, M., and Rahmstorf, S. (2010) "Global sea level linked to global temperature", Proc. Natl. Acad. Sci. U. S. A., doi:10.1073/pnas.0907765106, in press

Warrick, R. and J. Oerlemans (1990). "Sea level rise." 257-281

Williams, S.J., Gutierrez, B.T., Titus, J.G., Gill S.K., Cahoon D.R., Thieler E.R., Anderson K.E., Gerald D. F., Burkett V., and Samenow J. (2009) "Sea-level rise and its effects on the coast. In: Coastal Sensitivity to Sea-Level Rise: A Focus on the Mid-Atlantic Region." U.S. Environmental Protection Agency, Washington DC, pp. 11-24.

Wind, H.G., and C.B. Vreugdenhil (1986) Rip-current Generation Near Structures. *J. Fluid Mechanics*, 171, 459–476

Wu, C.-S., and P.L.-F. Liu (1985). Finite Element Modelling of Nonlinear Coastal Currents. *J. Waterway, Port, Coastal and Ocean Eng.*, ASCE, 111, 2, 417–432.